AFFDL-TR-64-160

EMPIRICAL CORRELATION OF EXCITATION ENVIRONMENT AND STRUCTURAL PARAMETERS WITH FLIGHT VEHICLE VIBRATION RESPONSE

TECHNICAL REPORT AFFDL-TR-64-160

December 1964

AF FLIGHT DYNAMICS LABORATORY
RESEARCH AND TECHNOLOGY DIVISION
AIR FORCE SYSTEMS COMMAND
WRIGHT-PATTERSON AIR FORCE BASE, OHIO

Project No. 1370, Task 137005

(Prepared under Contract AF 33(657)-8218
Northrop Corporation, Norair Division
Hawthorne, California
Co-Authors: R.W. White, D.J. Bozich, K.M. Eldred)

NOTICES

When Government drawings, specifications, or other data are used for any purpose other than in connection with a definitely related Government procurement operation, the United States Government thereby incurs no responsibility nor any obligation whatsoever; and the fact that the Government may have formulated, furnished, or in any way supplied the said drawings, specifications, or other data, is not to be regarded by implication or otherwise as in any manner licensing the holder or any other person or corporation, or conveying any rights or permission to manufacture, use, or sell any patented invention that may in any way be related thereto.

Qualified requesters may obtain copies of this report from the Defense Documentation Center (DDC), (formerly ASTIA), Cameron Station, Bldg. 5, 5010 Duke Street, Alexandria, Virginia 22314.

This report has been released to the Office of Technical Services, U.S. Department of Commerce, Washington 25, D.C., for sale to the general public.

Copies of this report should not be returned to the Research and Technology Division unless return is required by security considerations, contractual obligations, or notice on a specific document.

AFFDL-TR-64-160

EMPIRICAL CORRELATION OF EXCITATION ENVIRONMENT AND STRUCTURAL PARAMETERS WITH FLIGHT VEHICLE VIBRATION RESPONSE

TECHNICAL REPORT AFFDL-TR-64-160

December 1964

AF FLIGHT DYNAMICS LABORATORY
RESEARCH AND TECHNOLOGY DIVISION
AIR FORCE SYSTEMS COMMAND
WRIGHT-PATTERSON AIR FORCE BASE, OHIO

Project No. 1370, Task 137005

(Prepared under Contract AF 33(657)-8218
Northrop Corporation, Norair Division
Hawthorne, California
Co-Authors: R.W. White, D.J. Bozich, K.M. Eldred)

FOREWORD

This report was prepared by the Norair Division of Northrop Corporation, Hawthorne, California, in conjunction with the Wyle Laboratories Research Staff, Huntsville, Alabama, for the Aerospace Dynamics Branch, Vehicle Dynamics Division, AF Flight Dynamics Laboratory, Wright-Patterson Air Force Base, Ohio, under Contract No. AF33(657)-8218. This research is part of a continuing effort to obtain accurate and reliable methods of vibration prediction, control and measurement for flight vehicles which is part of the Research & Technology Division, Air Force Systems Command's exploratory development program. The Project No. is 1370, "Dynamic Problems in Flight Vehicles," and Task No. is 137005, "Prediction and Control of Structural Vibration." Mr. R. N. Bingman and Capt. R. M. Berg of the AF Flight Dynamics Laboratory were the Project Engineers. The report covers work from May 1962 to July 1964. Contractors report number is NOR 64-226.

The authors express their appreciation for the contributions of Mr. C. E. Thomas, Dr. O. R. Rogers, and other AFFDL personnel and a number of aerospace companies for reports and data. In addition to the principal authors and Dr. E. Rodine of Wyle Laboratories Research Staff, contributing personnel included Dr. C. M. Wong, P. E. Holligan and A. P. Wang of Northrop; P. S. Veneklasen of Western Electric Acoustic Laboratories; and W. R. Roberts of Martin, Orlando.

This report has been reviewed and is approved.

WALTER J. WHITON
Asst. for Research & Technology
Vehicle Dynamics Division

AF - [illegible]

ABSTRACT

The design of fatigue resistant structures for high speed aircraft and aerospace vehicles depends largely on the prediction of realistic acoustic, fluctuating aerodynamic, and engine vibration environments and on the estimation of the attendant vibration levels of structural components and attached equipment. The practical engineering limitations on the mathematical and numerical analyses required to treat such structures rigorously by classical dynamics necessitate studies of alternate, approximate methods. In this report, a definitive statement is presented of the empirical approach for determining correlations between the excitation environment and the vibration response of typical flight vehicle structures by means of statistical analyses of measured vibration data. The various aspects of the vibration prediction problem and the general philosophy motivating research in the area of empirical correlation are discussed. Specific treatment is given to the effects of bandwidth, modal density, and surface pressure spacecorrelation on the cross-correlation of energy transmitted along various structural transmission paths in complex linear structures. An engineering model for empirical correlation is developed and several examples are given to demonstrate the utility of the equations.

TABLE OF CONTENTS

TABLE OF CONTENTS (Cont'd)

LIST OF ILLUSTRATIONS

LIST OF ILLUSTRATIONS

LIST OF SYMBOLS

A	total surface area over which distributed pressure acts
A_n	n-th surface area segment
$C(f)$	space correlation coefficient
c	damping constant
D	constant proportional to average value of $\overline{\overline{\beta^2}}$
$F(t)$	applied force
f	frequency, cycles per second
$H(f)$	single degree-of-freedom response function
$h(t)$	unit-impulse function
i	$\sqrt{-1}$
k	generalized stiffness or single stiffness
L	length of beam
M	generalized mass or total mass of bay
m	mass density or single mass
N	total number of applied point forces or distributed forces
$P(t)$	applied pressure
Q	dynamic magnification factor = $1/2\zeta$
q	dynamic pressure (freestream)
$q(t)$	generalized coordinate
R	total number of response points in bay
$S(f)$	spectral density or cross-spectral density
T	period = $1/f$
t	time, seconds
$\ddot{W}(t)$	total acceleration response at a point $\tilde{y}$
$\ddot{w}(t)$	single frequency component of $\ddot{W}(t)$
$\tilde{x}$	point of force application
$\tilde{y}$	point of response measurement
$Z(f)$	mechanical velocity impedance
$\alpha(f)$	force - to - acceleration transfer function
$\beta(f)$	acceptance function
$\Gamma(\tau)$	autocorrelation or crosscorrelation
$\gamma(f)$	transmission function

LIST OF SYMBOLS

Δ	absolute value of distance between x and x'
Δf	frequency bandwidth
$\delta(f)$	axial decay function
ζ	damping ratio
$\theta(f)$	transfer function phase angle, radians
σ	damped natural frequency, cycles per second
τ	time delay, seconds
Φ	space average of $\overline{\psi^2}$
$\phi(f)$	applied force phase angle, radians
$\phi(\tilde{x})$	normal mode shape of entire structure
$\psi(f)$	receiver function
ω	frequency, radians per second

Subscripts

k refers to k-th discrete frequency component

L refers to lower frequency band limit

m, n refer to forces applied at points $\tilde{x}_m$, $\tilde{x}_n$ or over area segments A_m, A_n

r, s refer to response measured at points $\tilde{y}_r$, $\tilde{y}_s$

u refers to upper frequency band limit

μ, ν, q, j refer to normal mode shapes or natural frequencies of entire structur

LIST OF SYMBOLS

Other Symbols

$\mathcal{R}(\ )$	real part of --
$\mathcal{I}(\ )$	imaginary part of --
$\overline{(\quad)}$	time average of --, space average of --, or frequency average of --
$(\ )^*$	complex conjugate of --
$\lvert(\ )\rvert$	absolute value of --

SECTION 1

INTRODUCTION

At the present time, adequate methods do not exist for predicting the vibration response levels of the many structural and equipment components of aircraft and aerospace flight vehicles. Methods generally used for these predictions consist of vibration analyses of rather elementary structures, such as uniform beams, plates and shells, and comparati analysis in which measured data from one vehicle are used to estimate response levels of another vehicle by appropriate mass and stiffness scaling. In the search for more powerful prediction techniques and more realistic vibration response estimates, consideration should be given to the method of empirical correlation, in which statistical analysis is used to correlate the measured responses with excitation parameters, overal structural and performance parameters, and detailed local structural parameters.

The purpose of this report is to present the general philosophy which has motivated research in the area of empirical correlations, to discuss the various aspects of the vibration prediction problem, to develop the general equations for predicting vibration responses of complex, linear structures, and to set forth empirical correlation methods and methods for developing vibration prediction tools from these correlations.

Section II contains a general discussion of the engineering problem of flight vehicle structural vibrations and the relationship of this problem to vehicle reliability. The environmental prediction problem, the vibration response prediction problem, and the importance of realistic vibration predictions and the establishment of vibration controls during initial design are also discussed in Section II.

In Section III, the general equations for computing vibration response in any complex, linear structure are developed for point force excitation and distributed pressure excitation, having discrete and continuous frequency spectra. These equations are developed in terms of a force-to-acceleration transfer function which is directly relatabl to transfer impedances.

Manuscript released by the authors July 1964 for publication as an AFFDL Technical Report.

Equations for mean-square response at a point, autocorrelation of response, cross-correlations of responses at two points, response spectral densities and cross-spectral densities are presented. Several examples are given to clarify the meanings of the transfer functions and to demonstrate the utility of the equations.

Some essential background material on the development of empirical correlation techniques is presented in Section IV. Several methods for obtaining correlations between excitation and response using statistical techniques are developed and methods for using these computed correlations as vibration prediction tools are discussed.

SECTION II

GENERAL DISCUSSION

Among the many technological problems which confront the aircraft and aerospace industries, the problems associated with structural and equipment vibrations are of paramount importance. Fatigue of structural components, and malfunction and breakage of equipment in flight vehicles often accompany high vibration levels; such phenomena can lead to losses of mission capability and even to catastrophic failures. Past and present generation vehicles have experienced severe and damaging vibration response to engine exhaust noise, engine vibrations, boundary layer turbulence, and oscillating shocks. In several instances, time consuming engineering studies and costly test programs were required to reduce the levels of response to within tolerable limits. With the ever increasing sizes of vehicles and powerplants, and with increasing flight speeds, the vibration excitation environment imposed on the structure may become more severe. As a result, the vibration response problem for future generation flight vehicles is expected to become increasingly important and will require considerably greater attention than has been devoted to this problem heretofore.

VIBRATION CONTROL THROUGH INITIAL DESIGN

The operations of flight vehicles within the atmosphere and under any thrust conditions are always accompanied by sources of vibration excitation. Because of the flexibility and general dynamic nature of the vehicle structure, a portion of the oscillatory energy supplied by the excitation sources is accepted by the structure and transmitted throughout the vehicle. Thus, under such operational conditions, every structural and equipment component is placed in a state of vibration and must function properly in that state. Clearly, vibrations cannot be eliminated completely; hence, any positive approach towards solving the vibration problem must be one of vibration control instituted for the purpose of minimizing failure and malfunction potentials and thereby maximizing the overall vehicle reliability.

Controlling vibration response levels by controlling the environmental excitation levels is impractical since the environments are dependent upon such major design and performance parameters as engine thrust, engine location, vehicle surface contours, trajectories and flight speeds. Rather, vibration controls lie in the design of fatigue resistant structure, the design of equipment to withstand operational vibration levels without damage and malfunction, the positioning and mounting of equipment to minimize response to structurally transmitted vibratory energy, optimum design of structural components, the reduction of stress concentration factors, the development of maximum damping through joint design, and the use of damping compounds. As such, many built-in vibration control measures can be incorporated during the initial planning and design phases. Other detailed vibration control measures can be used during the advanced design and qualification testing phases; while still other limited controls can be supplied after vehicle construction from a knowledge of vibration response levels measured during operation.

Although the need for vibration control and the extent and degree of the control cannot be predetermined for all key structural and equipment components, the most effective and the most economic controls are those incorporated in the initial design of both the structure and the equipment. Altering the structure after fabrication begins is difficult and in many instances it is hard to justify on the basis of the value gained when weighed against the time and expense required for changing drawings, tooling, and construction procedures. The usual result is a compromise in which the full effect of the newly instituted control measure cannot be realized. This is generally less true of equipment packages which are not integral parts of the structure and which can be easily removed; however, here again, valuable time may be required for evaluation of the vibration problem, redesign, and retesting for qualification. Consideration of the vibration response problem must therefore begin during preliminary design.

Ideally, these considerations should begin with the estimations of environments, at

the vehicle surface, caused by such fluctuating pressure sources as engine exhaust noise, boundary layer turbulence, separated flow, base pressure fluctuations, jet wake noise and oscillating shock waves. The various characteristics of interest for these environments are distributions of pressure levels over the vehicle surface, frequency distributions, propagation speeds, impingement angles and spatial correlations. Estimates should also be made of the direct vibratory input to the structure due to engine burning, vibrations of propellant piping systems, and other on-board mechanical sources of excitation. From the knowledge of the estimated environmental levels and other environmental characteristics, vibration response levels would be predicted for vibration sensitive structural components in regions of high level excitation and for all key structural and equipment components such as skin panels, skin stiffeners, brackets, piping systems, equipment mounting structure and equipment components. Specific requirements for vibration control could then be defined from the estimated response levels, structural fatigue criteria, and equipment malfunction criteria. Finally, detailed design techniques could be developed in order to obtain sufficient vibration control to reduce the severity of potentially damaging vibrations; and, realistic qualification test specifications could be established for critical structural and equipment components. Such an effort should result in the maximum, practical built-in vibration control. Continuing this effort through the various refinement phases of advanced design, qualification testing and flight testing should result in the maximum vehicle reliability within the limits that vibration induced failures influence overall vehicle reliability.

The three principal tools required for attaining vibration control through initial design are methods for predicting the environmental levels and other environmental parameters, methods for predicting vibration response levels and transmission characteristics of vehicle structures, and design techniques for minimizing structural response levels and safeguarding equipment against damage and malfunction. During the past ten years, in which significant advances have been made in the development of large turbojet and rocket engines and in attaining higher flight speeds, a consider-

able engineering effort has been devoted to the measurement and analysis of exhaust noise, boundary layer turbulence, and other fluctuating pressure phenomena. From this effort have come empirical prediction methods which allow for reasonably accurate estimates of the environmental levels, distribution over the structure, frequency distributions, propagation characteristics, and in some cases, spatial correlation properties.

In contrast, practical engineering methods for predicting vibration response levels in typical flight vehicle structure have not been developed primarily because of the complexities of the structural acceptance and transmission properties. The few limited attempts to develop empirical vibration prediction methods, based on measured data, show several orders of magnitude of scatter in the data even when normalized against typical weight, stiffness, and excitation parameters. A typical scatter in the vibration data may be 20 decibels whereas a typical scatter in appropriately normalized environmental data may be 2 to 3 decibels. The sensitivity of the vibration levels to local structural parameters, which can have wide variations throughout a structure, and to the highly resonant character of a structure, is considered to be a major factor in causing such a broad scatter. Generally, response predictions are made by idealizing complex structural components to mathematically tractable systems and analyzing such systems by either lumped parameter methods or by generalized harmonic analysis methods. Except for the use of damping compounds and the design of joints for high damping, most design techniques for vibration control are dependent upon a knowledge of the dynamic characteristics of the structure. A major effort must therefore be made to develop vibration response prediction methods which will account for necessary excitation parameters and major and local structural parameters.

THE MAJOR FREQUENCY REGIMES OF STRUCTURAL RESPONSE

The Low Frequency Regime - Overall Fundamental Vehicle Modes

The fundamental principles of elasticity and mechanics provide all of the analytical relations that are required to mathematically describe the dynamic response of any structure, simple or complex, by means of differential equations of motion. However, since the dynamical complexity of the structure has a definite bearing on the complexity

of the equations of motion and their solutions, a direct mathematical approach to the vibration prediction problem is limited to those systems which display more or less elementary resonance characteristics. In the sense used here, elementary resonance characteristics refer to resonant deflection shapes, or mode shapes, which can be expressed mathematically in closed form or which can be obtained with reasonable accuracy by numerical techniques, such as finite difference methods, or by lumped parameter techniques. Examples of such systems for which the mode shapes can generally be expressed in closed form are uniform rods with longitudinal resonances, uniform beams and plates with bending resonances, and uniform shells with uncoupled extensional and bending resonances.

Other systems which are complex in geometry, mass distribution or stiffness distribution can have elementary resonance characteristics for the first few resonant modes. Although the mode shapes will seldom admit to simple mathematical representation, numerical techniques and lumped parameter methods can be used to easily define the mode shapes and compute the resonant frequencies. Examples of such systems are overall vehicles vibrating in the fundamental bending mode or fundamental longitudinal mode, and stiffened panel configurations vibrating in overall configuration modes whose resonant frequencies are well below those of the individual subpanels. The significant feature to be observed in the latter two examples is that the elastic wave lengths at resonance are long relative to the dimensions and, hence, to the resonant elastic wave lengths of the individual structural components. Consequently, the complex local variations in mass and stiffness are averaged out so that much of this fine detail can be neglected. Thus, for example, a panel having a large number of closely spaced orthogonal stiffeners can be treated as an equivalent uniform panel in the fundamental mode. Higher modes of the panel may be similarly approximated with the restri that the overall stiffened panel wave lengths are much longer than the distances between stiffeners.

The Medium Frequency Range - Fundamental Resonances of Structural Elements

When built-up structures are excited at frequencies above those of the overall resonant modes, the elastic bending and torsional wave lengths are of the same order as the

dimensions of individual structural components. At these wave lengths the local variations in stiffness and mass distribution significantly affect the local character of the vibration response. As a result, the higher order resonances of the vehicle tend to break up into resonances of individual structural components, or small groups of such components, so that the overall modal pattern becomes exceedingly complex. It is impractical at these frequencies to consider the local resonant modes as being an integral part of some higher order resonant modes of the overall vehicle. In fact, two structural components which are widely separated may be essentially uncoupled so that their responses are nearly independent. Present methods for predicting vibration response in this frequency range generally consist of the analysis of the response of single components to the local environment acting on the components. Typically, the structural components are treated as uniform beams, plates and shells for which mathematical solutions of the response to fluctuating surface pressures or to other fluctuating excitations are known.

The accuracy of such methods depends upon the accuracy with which the excitation can be mathematically simulated, the degree of accuracy in approximating the true natural boundary conditions of the component, and the degree of dynamical independence of the component with respect to neighboring components. Structural components such as skin panels excited by fluctuating surface pressures are sensitive to the ratios of elastic wave length to pressure wave lengths, pressure propagation speeds, angles of impingement and spatial correlation lengths. These excitation parameters must, therefore, be known in order to have reasonably accurate response predictions.

The resonant frequencies, deflection amplitudes, and strain levels of panels are also dependent upon the boundary conditions at the edges of the panel. The bending and torsional stiffnesses of the edge members which support the panel determine the degree of translational and rotational fixity of the panel, and the edge deflections associated with these flexibilities have a marked effect upon strain amplitudes at the

edge. The dynamical properties of these edge members also control the flow of vibratory energy from the panel to neighboring structural components and from the neighboring components to the panel. When the fundamental bending and torsional frequencies of these edge stiffeners are much higher than the fundamental panel frequency, response of the first few modes of the panel can be predicted fairly accurately by treating the panel as an individual component which is essentially uncoupled from the surrounding structure. However, if the flexibilities of the edge members are significant, a group of several panels may have to be analyzed simultaneously. This is particularly true in the case of regular structure in which several connected panels have nearly the same resonant frequencies -- the individual structural components do not respond independently but are highly coupled with adjacent components.

These considerations are not confined to skin panels but are valid for any single structural component or group of components within the vehicle. In general terms, if the support structure and structural components adjacent to a certain structural component exhibit a high impedance relative to the impedance of the component, then the response of the component will be essentially independent of the neighboring structure. When these impedances are of the same order of magnitude, dynamic coupling can be expected.

Although many vibration analyses in the medium frequency range are based on such idealizations as uniform beams and plates having pinned and clamped edges, serious efforts are being made to develop more general methods which account for the effects of local parameters and thus allow for better approximations of the natural boundary conditions and the dynamic coupling of adjacent structural components. It is difficult to predict how far the state of the art of vibration analysis of complex structures can be extended by means of such generalizations. The increasing storage capacity and computing speeds of digital computers allows the dynamicist to include an ever larger number of structural mass, stiffness and geometry parameters and, in time, quite

complex systems may be analyzable. Two dimensional stiffened panel and shell configurations will certainly be amendable to numerical computation in reasonable computing times with future generation computers. Bulkhead and some internal structure will probably also be included at allowable computing costs.

Unfortunately, the number of parameters and the general size of the computing task increases very rapidly with the number of individual structural components being considered and with the order of the response mode being analyzed. There will be at least five parameters required to determine the dynamics of each structural element included in the analysis, and several resonant frequencies will be required for each such element. As the order of the resonance increases, the amount of computing required to locate system resonant frequencies increases because of the nature of the numerical methods used for finding these resonances. In addition, the modal density increases with frequency so that the resonant frequencies become closely spaced and modal deflection patterns become increasingly hard to display. Complexity in the modal patterns of the skin panels implies difficult and lengthy computations of the generalized or effective force caused by random fluctuating surface pressures. Thus, although the computer techniques are expected to provide a bright future for the analyst, it is clear that there exists a definite upper limit on the degree of complexity that can be included in vibration analyses for the medium frequency range.

The High Frequency Regime - Modal Response in Smaller Structural Elements

At frequencies higher than the first few resonant modes of individual structural components, the modal density at all points in a complex vehicle structure is so high as to warrant any exact analysis as impractical. In this frequency range, complex coupled resonances will occur in skin panels, panel stiffeners, stiffener flanges and webs, bracketry, equipment, bulkheads, piping, etc. As such, the structural response is similar to a reverberant acoustic field in that vibratory energy can be easily transmitted in all directions throughout the structure. In part, the difference between the transmission properties in the high frequency region and those in the medium frequency range is due to the fact that the natural stiffness barriers which tend to confine the vibratory energy to a single component, such as a skin panel, or a group of structural components, no longer are effective. Those members which

provided the stiffness barriers are themselves in resonance and can thus easily transmit energy at these frequencies. Predicting vibratory response levels in such a frequency range might more readily be accomplished by considering the structure as a transmission line and treating the vibration response as a random process to be described in terms of statistical parameters.

CONSPECTUS OF THE STATISTICAL APPROACH TO VIBRATION PREDICTION

Analytical techniques involving the solutions of equations of motion of a structural system provide the necessary vibration prediction tools for the low frequency regime of the structure and for certain mathematically tractable structural configurations in the medium frequency regime. For highly coupled, complex configurations in the medium frequency regime and for high frequency excitation of the structure, other less exact methods must be developed for vibration prediction. The use of statistical techniques and the development of statistical relations between vibration response levels and the significant parameters which describe the excitation and the structure appears to be the only reasonable approach to so complex a problem. Such relationships should be developable in terms of correlation coefficients and other statistical averages from a knowledge of measured vibration data, measured or estimated environmental data, and from a knowledge of the structural configuration on which the responses were obtained. Once these relationships are developed and the necessary numerical evaluations are made for representative flight vehicle structure, a practical engineering method should result for vibration response prediction during initial design.

In order to develop the appropriate statistical relations it is necessary first to identify all of the significant excitation and structural parameters that might significantly influence vibration response. These parameters might include engine thrust, flight speed, altitude, mass of vehicle, vehicle surface area, average size of skin panels, distance from engines, distance from projections and aerodynamic discontinuities, frequency, pressure wave lengths, length of vehicle, skin panel thickness, component mass, component stiffness, distances between stiffeners, etc. The actual relations between these parameters and response amplitudes can then be estimated by

several different methods, once a representative sampling of measured vibration data is available. Using linear regression analysis techniques, linear relationships can be computed, on a statistical basis, between response amplitude and each of the above excitation and structural parameters taken singly or as a group. Or, definite mathematical relations could be established between the response amplitude and these parameters, and a statistical analysis can be conducted to determine how well the measured data fits the mathematical model. In the latter case the closer the mathematical model describes the vibration phenomena, the closer will be the fit. As another alternative, very general but realistic mathematical relations could be established containing unknown constants which can be determined so as to obtain a best fit between the relationships and the major body of the measured data. If a broad and representative sampling of measured vibration data could be accumulated, and if these three methods could be used for various types of structures (such as fighter aircraft, bombers, small missiles, large rocket boosters) and for various flight regimes, statistical relationships could be developed which would be of significant value as vibration prediction tools.

SECTION III

STRUCTURAL VIBRATION RESPONSE THEORY

In developing empirical correlation techniques for analyzing the vibration responses of complex structures, it is necessary to obtain expressions for the response amplitudes of the structure in terms of the various structural and excitation parameters that influence vibration response. For example, it is necessary to have functional relationships between the amplitude of acceleration response at a point within the structure and the frequency of excitation, amplitudes of fluctuating acoustic and aerodynamic pressures, distributions and spatial crosscorrelations of these pressures on the surface of the structure, input impedances over the areas of excitation, and transfer impedances between the excitation and the point within the structure where response occurs.

Such equations can be obtained by several different methods and can be written in several different forms. Partial differential equations that express the exact balance of elastic, inertial, and applied forces can be set up for each structural element and the response of any element can be treated as a boundary value problem With this method it is necessary to equate deflections, slopes, bending moments and shears of adjacent structural elements along the lines of attachment. Alternatively, the structural response can be expanded in terms of the normal modes of the structu and ordinary differential equations can be solved for the amplitude of response of each mode. In this method, it is necessary to determine the individual mode shapes the generalized mass, generalized damping, and generalized force for each mode. However, in the analysis of complex structures having complex random forcing func it is necessary that the final equations to be used contain only quantities that are known, that can be estimated with reasonable accuracy, that can be measured on a practical engineering basis, or that can be determined statistically from measure vibration and excitation data. Since the numerous local structural details and the exact transmission characteristics of a complex structure are generally unknown, i appears that the equations of interest must be expressed in terms of input and trans

impedances or other similar quantities which account for the collective effect of mass, stiffness, and damping distributions between points in the structure. For the problem at hand, equations of this kind are more appropriate than those involving the exact balance of elastic, inertial, and applied forces in the structure, or those which require a knowledge of the very complex mode shapes of the vehicle in the medium to high frequency range.

In this section, the acceleration response of an arbitrary, linear, deterministic structure is analyzed for various types of loading. Expressions are derived for the autocorrelation, spectral density, and mean-square acceleration response at a point on the structure. Expressions are also derived for the crosscorrelations of applied force and response and for the crosscorrelations of the acceleration responses between points on the structure. These expressions are developed for both multiple point force loadings and distributed pressure loadings. In each case, discrete and continuous frequency spectra are considered.

The structure is assumed to be linear in order to take advantage of the principle of superposition of responses at a point due to several vibratory inputs acting over different parts of the structure. In the case of nonlinear structures, the linear superposition principle is invalid and special methods must be used to treat each different type of nonlinearity. Nonlinearities are expected to occur in certain limited regions of the structure; however, on the average over the whole structure, linearity is expected to dominate. The structure is deterministic in the sense that all input impedances, transfer impedances, and other quantities appearing in the response expressions are assumed to be known. In this sense, the expressions to be developed are exact for linear systems. A discussion of the necessary simplifications and approximations required to statistically analyze vibration response of complex structures is reserved for Section IV.

POINT FORCE EXCITATION AT DISCRETE FREQUENCIES

Force-to-Acceleration Transfer Function

The net vibration response at any point in a structure is the cumulative effect of all of the oscillatory forces acting on the structure. Forces applied at distinct points induce local vibrations at the points of application; and these local vibrations are transmitted along common structural paths and add to give net responses in accordance with their relative phases. When the response amplitudes are linearly dependent upon the amplitudes of the applied forces, the response amplitude at a point is the linear summation of the responses at that point which result from excitations at each point on the structure.

Consider for example the structural system shown in Figure 1 which has forces $F_n(t)$ applied at points $\vec{x}_n$, and which has a structural element at $\vec{y}_r$ whose net acceleration response is $\ddot{W}_r(t)$. It is assumed that each of the point forces, $F_n(t)$, is a steady-state force having several discrete frequency components, $F_{nk}(t)$, at the frequencies f_k, so that

$$F_n(t) \quad \sum_k \quad F_{nk}(t) \tag{1}$$

If $\ddot{w}_{nrk}$ denotes the component of $\ddot{W}_r(t)$ resulting from the force component $F_{nk}(t)$, then for a linear structure, the net acceleration response of the element at $\vec{y}_r$ is given by the expression

$$\ddot{W}_r(t) \quad \sum_k \sum_n \quad \ddot{w}_{nrk}(t) \tag{2}$$

where the summation index n extends over all applied forces and where the summation index k extends over all discrete frequencies, f_k.

The relationship between the applied force and the vibration response caused by this force involves the acceptance and transmission characteristics of the structure between the points of load application and response. Because of the sensitivity of the structure to excitation frequencies, the structure acts as a complex filter which accepts and transmits certain frequencies more readily than others; and hence the relationships between the applied forces and the responses are dependent upon the excitation frequency. Once these relationships are known for each frequency component of each of the applied forces, the net acceleration response at a given point $\vec{y}_r$ can be expressed in terms of the amplitudes and relative phases of the individual forces and in terms of the structural acceptances and transmission characteristics from each input point, $\vec{x}_n$, to the given response point $\vec{y}_r$. The steady-state excitation, $F_{nk}(t)$ and the steady-state response $\ddot{w}_{nrk}(t)$ can be related by introducing a force-to-acceleration transfer function, $a_{nr}(f_k)$ which accounts for the input and transfer impedance properties of the structure at frequency f_k. In terms of $a_{nr}(f_k)$, the excitation and response are related by the equation

$$\ddot{w}_{nrk}(t) \quad a_{nr}(f_k) \; F_{nk}(t) \tag{3}$$

The net acceleration, $\ddot{W}_r(t)$, of the structural element at $\vec{y}_r$ is obtained by substituting Equation (3) into Equation (2) giving

$$\ddot{W}_r(t) \quad \sum_k \sum_n a_{nr}(f_k) \; F_{nk}(t) \tag{4}$$

The quantity $a_{nr}(f_k)$, which has the units of inverse mass, is related to the structural transfer impedance, $Z_{nr}(f_k)$, by the expression

$$a_{nr}(f_k) \quad 2\pi \, i \, f_k \; / \; Z_{nr}(f_k) \tag{5}$$

where the transfer impedance at frequency f_k is defined by the equation

$$F_{nk}(t) \quad Z_{nr}(f_k)\ \dot{w}_{nrk}(t) \tag{6}$$

Like the transfer impedance, the quantity $a_{nr}(f_k)$ is complex and can be written in the form

$$a_{nr}(f_k) \quad \left|a_{nr}(f_k)\right| e^{i\theta_{nr}(f_k)} \tag{7}$$

where $\left|a_{nr}(f_k)\right|$ is the modulus and $\theta_{nr}(f_k)$ is the phase angle of $a_{nr}(f_k)$.

To illustrate the functional form of $a_{nr}(f_k)$ for simple systems, consider the one-degree-of-freedom spring-mass system shown in Figure 2. Let the applied force, F(t), be steady-state and harmonic at the single frequency f. Then as shown on page 1-7 of Reference 1, the steady-state deflection response W(t) of the mass is given by the Equation

$$W(t) \quad \frac{F(t)/k}{1-\left(\frac{f}{f_0}\right)^2 + \frac{i}{Q}\left(\frac{f}{f_0}\right)}$$

where

$$Q \quad \sqrt{km}/c \quad \text{and} \quad f_0 \quad (1/2\pi)\sqrt{k/m} \quad .$$

Thus the acceleration response $\ddot{W}(t)$ can be written in the form

$$\ddot{W}(t) \quad \frac{-(2\pi f)^2 F(t)/k}{1-\left(\frac{f}{f_0}\right)^2 + \frac{i}{Q}\left(\frac{f}{f_0}\right)} \tag{3}$$

Comparing Equation (8) with Equation (4) shows that the transfer function a(f) for the simple spring-mass system is

$$a(f) = -(2\pi f)^2 H(f) / k \tag{9}$$

where the single degree-of-freedom response function H(f) is

$$H(f) = \frac{1}{1 - \left(\frac{f}{f_0}\right)^2 + \frac{i}{Q}\left(\frac{f}{f_0}\right)} \tag{10}$$

The modulus $|a(f)|$ and the phase angle $\theta(f)$ of a(f) are

$$|a(f)| = (2\pi f)^2 |H(f)| / k$$

$$|H(f)| = \frac{1}{\sqrt{\left[1 - \left(\frac{f}{f_0}\right)^2\right]^2 + \frac{1}{Q^2}\left(\frac{f}{f_0}\right)^2}} \tag{11}$$

$$\theta(f) = -\tan^{-1}\left\{\frac{\frac{1}{Q}\left(\frac{f}{f_0}\right)}{1 - \left(\frac{f}{f_0}\right)^2}\right\}$$

The quantity $|H(f)|$ in Equation (11) is the dynamic magnification factor for the single degree-of-freedom system, and this function has a maximum value of Q at resonance. As shown in Reference 1, page 1-20, the function H(f) is the Fourier transform of the unit impulse function h(t), that is

$$H(f) = k \int_{-\infty}^{\infty} h(t) \cdot e^{-2\pi i f t} \, dt \tag{12}$$

where the unit impulse function for the single degree-of-freedom system is

$$h(t) = \frac{1}{m\sigma} e^{-\zeta\omega_0 t} \sin\sigma t \qquad t \geq 0 \qquad (13)$$

$$= 0 \qquad t \leq 0$$

The quantity ζ is the damping ratio, σ is the damped natural frequency, and ω_0 is the undamped natural frequency, where

$$\zeta = 1/2Q, \qquad \omega_0 = 2\pi f_0, \qquad \sigma = \omega_0 \sqrt{1 - \zeta^2}$$

Thus from Equations (9) and (12) it is seen that the transfer function $a(f)$ can be written in terms of the Fourier transform of the unit impulse function

$$a(f) = -(2\pi f)^2 \int_{-\infty}^{\infty} h(t)\, e^{-2\pi i f t}\, dt$$

To illustrate the functional form of $a_{nr}(f_k)$ for a second example, consider the uniform beam shown in Figure 3 which has a single harmonic force $F(t)$, of frequency f, acting at point x. The deflection response $W(t)$ at point y on the beam can be found from the normal mode expansion

$$W(t) = \sum_{\nu} q_\nu(t)\, \phi_\nu(y) \qquad (14)$$

where $\phi_\nu(y)$ is the ν-th mode shape, normalized to unity, and $q_\nu(t)$ is the deflection amplitude of the ν-th mode. When the modes respond independently, the generalized coordinate $q_\nu(t)$ of the beam satisfies the single degree-of freedom equation

$$\ddot{q}_\nu(t) + \frac{\omega_\nu}{Q} \dot{q}_\nu(t) + \omega_\nu^2 q_\nu(t) = \frac{\phi_\nu(x)\, F(t)}{M_\nu} \qquad (15)$$

where M_ν is the generalized mass and ω_ν ($= 2\pi f_\nu$) the natural frequency of the ν-th mode. The steady-state solution of Equation (15) when $F(t)$ is harmonic of frequency f ($= \omega/2\pi$) is

$$q_\nu(t) = \frac{\phi_\nu(x)\, F(t)/ M_\nu}{\omega_\nu^2 - \omega^2 + i\,\frac{\omega\,\omega_\nu}{Q}}$$

$$= \frac{1}{k_\nu}\,\phi_\nu(x)\; H_\nu(f)\, F(t) \qquad (16)$$

where k_ν ($\omega_\nu^2 M_\nu$) is the generalized stiffness of the ν-th mode and where

$$H_\nu(f) = \frac{1}{1 - \left(\frac{f}{f_\nu}\right)^2 + \frac{i}{Q}\left(\frac{f}{f_\nu}\right)}$$

To obtain the modal acceleration response, replace $q_\nu(t)$ by $-\ddot{q}_\nu(t)/\omega^2$ in Equation (16) giving

$$\ddot{q}_\nu(t) \quad \frac{-(2\pi f)^2}{k_\nu}\;\phi_\nu(x)\; H_\nu(f) \cdot F(t) \qquad (17)$$

The total acceleration $\ddot{W}(t)$ of the beam at y can be found by substituting Equation (17) into Equation (14) giving

$$\ddot{W}(t) \quad a(f)\; F(t)$$

where the beam transfer function $a(f)$ is

$$a(f) = -(2\pi f)^2 \sum_\nu \frac{H_\nu(f)}{k_\nu}\;\phi_\nu(x)\;\phi_\nu(y) \qquad (18)$$

Thus it is seen that the force-to-acceleration beam transfer function can be expressed as an infinite series of normal mode functions for the beam.

Mean Square Acceleration Response

Returning now to the general expression for the net acceleration response $\ddot{W}_r(t)$ in Equation (4), it is instructive to write this equation in terms of the absolute values of $a_{nr}(f_k)$ and $F_{nk}(t)$, the phase angles $\theta_{nr}(f_k)$ introduced by the structural transmission paths, and the relative phase angles of the applied forces. The applied force component $F_{nk}(t)$ is harmonic of frequency f_k and can therefore be written in the complex form

$$F_{nk}(t) = \left|F_{nk}\right| e^{i\phi_{nk}} e^{2\pi i f_k t} \tag{19}$$

where $\left|F_{nk}\right|$ denotes the amplitude and ϕ_{nk} the phase of $F_{nk}(t)$. Substituting Equation (7) for $a_{nr}(f_k)$ and Equation (19) for $F_{nk}(t)$ into Equation (4) gives the following expression for $\ddot{W}_r(t)$

$$\ddot{W}_r(t) = \sum_k \sum_n \left|a_{nr}(f_k)\right| \cdot \left|F_{nk}\right| \cdot e^{i\left[\theta_{nr}(f_k) + \phi_{nk}\right]} \cdot e^{2\pi i f_k t}$$

Equation (20) shows that the net acceleration depends upon both the phase angle changes which take place along the structural transmission paths and the relative phase angles of the applied forces. When the mean-square value $\overline{\ddot{W}_r^2(t)}$ of the net acceleration is to be determined, it is necessary to take the time average of the square of the real value of $\ddot{W}_r(t)$, that is

$$\overline{\ddot{W}_r^2(t)} = \lim_{T \to \infty} \frac{1}{2T} \int_{-T}^{T} \left[\mathcal{R}\left\{\ddot{W}_r(t)\right\}^2\right]^2 dt \tag{21}$$

where $\mathcal{R}\left\{\ddot{W}_r(t)\right\}$ denotes the real part of $\ddot{W}_r(t)$

Substituting Equation (20) into Equation (21), and noting that response components of different frequencies are uncorrelated, gives the following expression for the mean-square value of $\ddot{W}_r(t)$,

$$\overline{\ddot{W}_r^2(t)} = \frac{1}{2} \sum_k \sum_n \left|a_{nr}(f_k)\right|^2 \left|F_{nk}\right|^2 + \frac{1}{2} \sum_k \sum_n \sum_{m \atop (n \neq m)} \left|a_{nr}(f_k)\right| \cdot \left|a_{mr}(f_k)\right| \cdot \left|F_{nk}\right| \cdot \left|F_{mk}\right| \cdot \cos\left[\theta_{nr}(f_k) - \theta_{mr}(f_k) + \phi_{nk} - \phi_{mk}\right] \tag{22}$$

Equation (22) shows that the mean-square value of the net acceleration response is equal to the summation of mean-square response components and crosscorrelations of response components. The quantity

$\frac{1}{2} \left|a_{nr}(f_k)\right|^2 \cdot \left|F_{nk}\right|^2$ is the mean-square response at $\vec{y}_r$ due to an input force at $\vec{x}_n$ which is harmonic at frequency f_k and which has an amplitude of $\left|F_{nk}\right|$. The terms within the second set of summations in Equation (22) are the crosscorrelations of responses at $\vec{y}_r$, for the same frequency f_k, but for excitations at points $\vec{x}_n$ and $\vec{x}_m$.

It is seen that the magnitudes of the crosscorrelation terms are dependent upon the phase angle differences $\left[\theta_{nr}(f_k) - \theta_{mr}(f_k)\right]$ which occur for different structural paths and upon the phase angle differences $\left[\phi_{nk} - \phi_{mk}\right]$ between the forces applied at $\vec{x}_n$ and $\vec{x}_m$. Clearly the crosscorrelation terms in Equation (22) are exactly equal to zero only for the two special cases in which either there is only one applied force or the phase angles are such that the argument of the cosine term in Equation (22) is equal to $\pi/2$, or an odd multiple thereof. In the special case

when all of the forces are in phase and all transmission paths cause the same phase angle, the argument of the cosine in Equation (22) is equal to zero, and the mean-square response expression reduces to the form

$$\overline{\ddot{W}_r^2(t)} = \frac{1}{2} \sum_k \left[\sum_n \left| a_{nr}(f_k) \right| \cdot \left| F_{nk} \right| \right]^2 \qquad (23)$$

Further, it is to be noted in Equation (22) that the mean-square terms are positive and thus each mean-square response component adds to the value of $\overline{\ddot{W}_r^2(t)}$. The presence of the cosine factor in the crosscorrelation terms can lead to negative valued cross-correlation terms, so that in some instances, crosscorrelation terms tend to reduce the magnitude of $\overline{\ddot{W}_r^2(t)}$. In fact, it is possible for the crosscorrrelation terms to be of such a magnitude and sign that the total mean-square response is equal to zero. This can be demonstrated for the following elementary example. Consider the rigid bar, shown in Figure 4, which has a large number of applied forces $F_n(t)$, all of which are harmonic at the same frequency, and have the same amplitude $|F|$. The bar is assumed to be free to translate but constrained in pitch. The transfer functions $a_{nr}(f_k)$ for this case are equal to $1/M$ where M is the mass of the beam; the structural phase angles $\theta_{nr}(f_k)$ can be set equal to zero; and the force amplitudes $|F_{nk}|$ can be replaced by $|F|$. Thus if there are N such forces, the mean-square acceleration response $\overline{\ddot{W}^2(t)}$ in Equation (12) can be written in the form

$$\overline{\ddot{W}^2(t)} = \frac{|F|^2}{2M^2} \left[N + \sum_{\substack{n=1 \\ (n \neq m)}}^{N} \sum_{m=1}^{N} \cos(\phi_n - \phi_m) \right] \qquad (24)$$

where ϕ_n and ϕ_m denote phase angles of the applied forces. If the phase angles ϕ_n have a uniform probability of occurrence in the range from 0 to 2π, then the double summation in Equation (24) is approximately equal to -N; and it is easily shown that when the phase angles are uniformly distributed between 0 and 2π, this double

summation is exactly equal to -N when N is an even integer. Thus, in this case the summation of all of the crosscorrelation terms is equal in magnitude to the summation of all of the mean-square terms in Equation (22) and there is no net response.

Crosscorrelation of Acceleration Response

In analyzing vibration responses of structural systems, it is often of interest to determine the crosscorrelation of the responses at two different points of the structure for a given loading. Consider once again that point forces $F_n(t)$ are applied to the structure at $\vec{x}_n$, and consider the net acceleration responses $\ddot{W}_r(t)$ at $\vec{y}_r$ and $\ddot{W}_s(t)$ at $\vec{y}_s$. The expression for $\ddot{W}_r(t)$ is given by Equation (4) and the comparable equation for $\ddot{W}_s(t)$ is

$$\ddot{W}_s(t) = \sum_k \sum_m a_{ms}(f_k)\, F_{mk}(t) \tag{25}$$

The crosscorrelation of these two acceleration responses is denoted by $\Gamma_{rs}(\tau)$ and can be defined as follows

$$\Gamma_{rs}(\tau) = \lim_{T\to\infty} \frac{1}{2T}\int_{-T}^{T} \mathcal{R}\left[\ddot{W}_r(t)\right]\mathcal{R}\left[\ddot{W}_s(t+\tau)\right]\, dt \tag{26}$$

where $\mathcal{R}[\ ]$ denotes the real part. It is clear from the form of $\ddot{W}_r(t)$ in Equation (20) that the real part of $\ddot{W}_r(t)$ is

$$\mathcal{R}\left[\ddot{W}_r(t)\right] = \sum_k \sum_n \left|a_{nr}(f_k)\right| \cdot \left|F_{nk}\right| \cos\left[2\pi f_k t + \theta_{nr}(f_k) + \phi_{nk}\right] \tag{27}$$

Similarly for the real part of $\ddot{W}_s(t)$

$$\mathcal{R}\left[\ddot{W}_s(t+\tau)\right] \sum_k \sum_m \left|a_{ms}(f_k)\right| \cdot \left|F_{mk}\right| \cos\left[2\pi f_k(t+\tau) + \theta_{ns}(f_k) + \phi_{mk}\right] \quad (28)$$

Substituting Equations (27) and (28) into Equation (26), performing the necessary integrations, and noting that the response components of different frequencies are uncorrelated, gives the following expression for the crosscorrelation function $\Gamma_{rs}(\tau)$

$$\Gamma_{rs}(\tau) = \frac{1}{2}\sum_k \sum_n \sum_m \left|a_{nl}(f_k)\right| \cdot \left|a_{ms}(f_k)\right| \cdot \left|F_{nk}\right| \cdot \left|F_{mk}\right| \cdot \cos\left[2\pi f_k \tau + \theta_{ms}(f_k) - \theta_{nl}(f_k) + \phi_{mk} - \phi_{nk}\right] \quad (29)$$

It is seen that Equation (29) reduces to the mean-square response given by Equation (22) when $\vec{y}_s$, $\vec{y}_l$ and $\tau = 0$.

POINT FORCE RANDOM EXCITATION

Definitions and Approach

The acceleration response $\ddot{W}_r(t)$ at the point $\vec{y}_r$ on a structure subjected to randomly varying forces $F_n(t)$ applied at the points $\vec{x}_n$ can be described by the methods of harmonic analysis.

Consider the excitation forces $F_n(t)$ and the response $\ddot{W}_r(t)$ to be stationary random processes, and assume that they began at $t = -\infty$. In a strict sense, the Fourier transform of $\ddot{W}_r(t)$ cannot be defined over an infinite time interval for a stationary process. However, the Fourier transform of $\ddot{W}_r(t)$ can be defined for that part of $\ddot{W}_r(t)$ over the interval $-T/2 < t < T/2$, assuming, of course, that

$\ddot{W}_r(t)$ is zero for all other times. Hence, letting $\ddot{W}_{rT}(t)$ represent the response in the above time interval, the mean-square value $\overline{\ddot{W}^2_{rT}(t)}$ of $\ddot{W}_{rT}(t)$ can be expressed in terms of its Fourier transform $A_{rT}(f)$ as follows

$$\overline{\ddot{W}^2_{rT}(t)} \quad \frac{1}{T} \int_{-T/2}^{T/2} \ddot{W}^2_{rT}(t)\, dt$$

$$\frac{1}{T} \int_{-\infty}^{\infty} \ddot{W}^2_{rT}(t)\, dt$$

$$\frac{1}{T} \int_{-\infty}^{\infty} \ddot{W}_{rT}(t)\, \ddot{W}_{rT}(t)\, dt$$

$$\frac{1}{T} \int_{-\infty}^{\infty} \ddot{W}_{rT}(t) \int_{-\infty}^{\infty} A_{rT}(f)\, e^{i2\pi ft}\, df\, dt$$

Integrating first with respect to time gives

$$\overline{\ddot{W}^2_{rT}(t)} \quad \frac{1}{T} \int_{-\infty}^{\infty} A_{rT}(f) \int_{-\infty}^{\infty} \ddot{W}_{rT}(t)\, e^{i2\pi ft}\, dt\, df$$

$$\frac{1}{T} \int_{-\infty}^{\infty} A_{rT}(f)\, A^*_{rT}(f)\, df$$

where $A^*_{rT}(f)$ is the complex conjugate of $A_{rT}(f)$, so that

$$\overline{\ddot{W}^2_{rT}(t)} \quad \frac{2}{T} \int_{0}^{\infty} \left|A_{rT}(f)\right|^2 df$$

Let $T \to \infty$, and an expression for the mean square value of $\ddot{W}_r(t)$ results

$$\overline{\ddot{W}_r^2(t)} = \int_0^\infty \lim_{T\to\infty} \left[\frac{2}{T} \left|A_{rT}(f)\right|^2\right] df$$

$$\overline{\ddot{W}_r^2(t)} = \int_0^\infty S_r(f)\, df \tag{30}$$

where $S_r(f)$ is defined as the spectral density (S.D.) of the response $\ddot{W}_r(t)$. Therefore, in computing the mean-square value $\overline{\ddot{W}_r^2(t)}$ of the response $\ddot{W}_r(t)$ it is seen that the spectral density $S_r(f)$ must be determined. The spectral density $S_r(f)$ indicates the distribution of the harmonic content of $W_r(t)$.

The S.D. $S_r(f)$, however, can be determined from a knowledge of the autocorrelation function $\Gamma_r(\tau)$ of the response $\ddot{W}_r(t)$ and the use of the Wiener - Khinchin relations. The autocorrelation function $\Gamma_r(\tau)$ is defined in terms of the response $\dot{W}_r(t)$ as

$$\Gamma_r(t) = \lim_{T\to\infty} \frac{1}{2T} \int_{-T}^{T} \ddot{W}_r(t)\, \ddot{W}_r(t+\tau)\, dt. \tag{31}$$

In general, the notation for time average will be simplified as follows

$$\Gamma_r(\tau) = \overline{\ddot{W}_r(t)\, \ddot{W}_r(t+\tau)}\ . \tag{32}$$

The autocorrelation $\Gamma_r(\tau)$ and the spectral density $S_r(f)$ of the response $\ddot{W}_r(t)$ are Fourier transform pairs, so that

$$\left.\begin{aligned} S_r(f) &= 2\int_{-\infty}^{\infty} \Gamma_r(\tau)\, e^{-i2\pi f\tau}\, d\tau\,, \\ \Gamma_r(\tau) &= \frac{1}{2}\int_{-\infty}^{\infty} S_r(f)\, e^{i2\pi f\tau}\, df, \end{aligned}\right\} \qquad (33)$$

and these expressions are known as the Wiener-Khinchin relations.

In order to develop further these expressions for response, it is necessary to relate the response to the excitation forces using the transfer characteristics of the structure. The force-to-acceleration transfer function $a_{nr}(f)$ and the unit impulse response function $h_{nr}(t)$ completely describe the dynamical properties of the structural paths between the points $\vec{x}_n$, where the forces $F_n(t)$ are applied, and the points $\vec{y}_r$, where the responses are being considered. The response $\ddot{W}_r(t)$ can be defined in terms of the unit-impulse response function $h_{nr}(t)$ and the applied forces $F_n(t)$ by use of the convolution integral

$$\ddot{W}_r(t) = \sum_n (2\pi f)^2 \int_0^{\infty} h_{nr}(\tau)\, F_n(t-\tau)\, d\tau\,. \qquad (34)$$

Further, the transfer function $a_{nr}(f)$ is defined in terms of the Fourier transform of the unit-impulse response function $h_{nr}(t)$,

$$a_{nr}(f) = -(2\pi f)^2 \int_0^{\infty} h_{nr}(\tau)\, e^{-i2\pi f\tau}\, d\tau\,. \qquad (35)$$

Substituting the inverse Fourier transform

$$h_{nr}(\tau) = \int_0^\infty \frac{a_{nr}(f) e^{i2\pi f\tau}}{(2\pi f)^2}\, df \qquad (36)$$

into equation (34), the expression for the acceleration response becomes

$$\ddot{W}_r(t) = \sum_n (2\pi f)^2 \int_0^\infty \int_0^\infty \frac{a_{nr}(f)\, e^{i2\pi f\tau}}{(2\pi f)^2} F(t-\tau)\, df\, d\tau \,. \qquad (37$$

However, a more convenient approach would involve the development of an expression for the autocorrelation $\Gamma_r(\tau)$ of $\ddot{W}_r(t)$ in terms of the autocorrelations $\Gamma_m(\tau)$, $\Gamma_n(\tau)$, the crosscorrelations $\Gamma_{mn}(\tau)$ of the applied forces $F_m(t)$, $F_n(t)$ and the unit-impulse transfer functions $h_{mr}(t)$ and $h_{nr}(t)$. The crosscorrelation $\Gamma_{mn}(\tau)$ of the forces $F_m(t)$ and $F_n(t)$ is defined as

$$\Gamma_{mn}(\tau) = \overline{F_m(t)\, F_n(t+\tau)} \,. \qquad (38)$$

The spectral density $S_r(f)$ of $\ddot{W}_r(t)$ can then be related to the spectral densities $S_m(f)$, $S_n(f)$, the cross-spectral densities $S_{mn}(f)$ of the forces $F_m(t)$, $F_n(t)$, and the transfer functions $a_{mr}(f)$, $a_{nr}(f)$ and their complex conjugates. The relation between crosscorrelation and C.S.D. is

$$S_{mn}(f) = 2 \int_{-\infty}^{\infty} \Gamma_{mn}(\tau)\, e^{-i2\pi f\tau}\, d\tau \qquad (39)$$

In analyzing the vibrations of complex structure it is often of interest to determine the crosscorrelation $\Gamma_{rs}(\tau)$ and cross-spectral densities $S_{rs}(f)$ of the acceleration responses $\ddot{W}_r(t)$ and $\ddot{W}_s(t)$ at the two points $\vec{y}_r$ and $\vec{y}_s$. These crosscorrelations are defined as

$$\Gamma_{rs}(\tau) = \overline{\ddot{W}_r(t)\ \ddot{W}_s(t+\tau)} \quad . \tag{40}$$

and the C.S.D. of the two responses is defined as

$$S_{rs}(f) = 2\int_0^\infty \Gamma_{rs}(\tau)\, e^{-i2\pi f\tau}\, d\tau \quad . \tag{41}$$

For example, knowledge of the above relations allows a complete description of the responses at various points within a structural compartment of a vehicle excited by multiple external forces. Also, a particular structural path may be traced by use of cross-correlations $\Gamma_{(r-s)}(\tau)$ or cross-spectral densities $S_{(r-s)}(f)$ of the difference of the responses $\ddot{W}_r(t)$ and $\ddot{W}_s(t)$ at two different points $\vec{y}_r$ and $\vec{y}_s$. Such cross-correlations and cross-spectral densities are defined by the equations

$$\Gamma_{(r-s)}(\tau) = \overline{\left[\ddot{W}_r(t) - \ddot{W}_s(t)\right]\left[\ddot{W}_r(t+\tau) - \ddot{W}_s(t+\tau)\right]} \tag{42}$$

$$S_{(r-s)}(f) = 2\int_0^\infty \Gamma_{(r-s)}(\tau)\, e^{-i2\pi f\tau}\, d\tau \quad . \tag{43}$$

The various expressions given above are developed in detail in the discussions to follow.

Response at a Single Point Due to a Single Loading

A. Autocorrelation and Spectral Density of Excitation and Response

The autocorrelation $\Gamma_r(\tau)$ of the acceleration response $\ddot{W}_r(t)$ at a single point $\vec{y}_r$ due to a single force $F_n(t)$ at a point $\vec{x}_n$ is obtained by substituting Equation (34) into Equation (32) and rearranging

$$\Gamma_r(\tau) = \overline{\ddot{W}_r(t)\ \ddot{W}_r(t+\tau)}$$

$$= \int_0^\infty (2\pi f)^2 h_{nr}(\tau_1) \int_0^\infty (2\pi f)^2 h_{nr}(\tau_2)\ \overline{F_n(t-\tau_1)F_n(t+\tau-\tau_2)}\ d\tau_2\, d\tau_1$$

For stationary processes, a change in the origin of t will make no change in the meaned quantity. Therefore

$$\Gamma_r(\tau) = (2\pi f)^4 \int_0^\infty h_{nr}(\tau_1) \int_0^\infty h_{nr}(\tau_2)\ \Gamma_n(\tau_1 - \tau_2 + \tau)\ d\tau_2\, d\tau_1 \qquad (44)$$

This relationship between the autocorrelation $\Gamma_r(\tau)$ of the response and the autocorrelation $\Gamma_n(\tau)$ of the force is not a simple one. However, the difficult relationship above will result in a simple relation between the spectral density $S_r(f)$ of the response and the spectral density $S_n(f)$ of the input force by using the Fourier transform relation of Equation (33).

$$S_r(f) = 2 \int_{-\infty}^{\infty} \Gamma_r(\tau)\, e^{-i2\pi f\tau}\ d\tau$$

$$2 \int_{-\infty}^{\infty} \left[\int_0^\infty (2\pi f)^2 h_{nr}(\tau_1) \int_0^\infty (2\pi f)^2 h_{nr}(\tau_2)\ \Gamma_n(\tau_1 - \tau_2 + \tau)\ d\tau_2\, d\tau_1 \right] e^{-i2\pi f\tau}\ d$$

Rearranging this integral gives

$$S_r(f) = \int_0^\infty (2\pi f)^2 h_{nr}(\tau_1) e^{i2\pi f\tau_1} d\tau_1 \int_0^\infty (2\pi f)^2 h_{nr}(\tau_2) e^{-i2\pi f\tau_2} d\tau_2 \cdot$$

$$\cdot 2 \int_{-\infty}^{\infty} I_n(\tau_1 - \tau_2 + \tau) e^{-i2\pi f(\tau_1 - \tau_2 + \tau)} d(\tau_1 - \tau_2 + \tau) ,$$

and, finally, from Equations (35) and (33), this expression reduces to

$$S_r(f) = a_{nr}^*(f)\, a_{nr}(f)\, S_n(f)$$

or

$$S_r(f) = \left|a_{nr}(f)\right|^2 S_n(f) \tag{45}$$

B. Response of Single Degree-of-Freedom System

Consider now the single degree of freedom system shown in Figure 2 and assume that the applied force is random. In order to maintain the same notation as that used above, the spectral density of the acceleration response of the mass is denoted by $\ddot{W}_r(f)$ and the spectral density of the applied force is denoted by $S_n(f)$. Substituting Equation (9) into Equation (45) gives the following relationship between the spectral densities of response and excitation

$$S_r(f) = \frac{(2\pi f)^4 S_n(f) / k^2}{\left[1 - \left(\frac{f}{f_o}\right)^2\right]^2 + \frac{1}{Q^2}\left(\frac{f}{f_o}\right)^2} \tag{46}$$

where f_o is the resonant frequency and k the spring constant for the single degree-of-freedom system.

The mean-square value of the response $\ddot{W}_r(t)$ can be obtained by integrating Equation (46) over all frequencies,

$$\overline{\ddot{W}_r^2(t)} = \int_0^\infty S_r(f)\, df \quad . \tag{47}$$

Now, if the excitation force $F_n(t)$ is white noise, then the spectral density $S_r(f)$ can be replaced by the constant S; and for this case, Equation (46)

$$S_r(f) = \frac{(2\pi f)^4 \, S/k^2}{\left[1 - \left(\frac{f}{f_0}\right)^2\right]^2 + \frac{1}{Q^2}\left(\frac{f}{f_0}\right)^2} \tag{48}$$

And, hence, the mean-square acceleration response for the single degree-of-freedom system is given by the equation,

$$\overline{\ddot{W}_r^2(t)} = \frac{S}{k^2} \int_0^\infty \frac{(2\pi f)^4}{\left[1 - \left(\frac{f}{f_0}\right)^2\right]^2 + \frac{1}{Q^2}\left(\frac{f}{f_0}\right)^2} \, df$$

which upon using residue theory gives

$$\overline{\ddot{W}_r^2(t)} = \frac{SQ}{4\, m^2 (2\pi f_0)^3} \tag{49}$$

C. Crosscorrelation and Cross-Spectral Density of Excitation and Response

The crosscorrelation $\Gamma_{nr}(\tau)$ of the single input force $F_n(t)$ and the response $\ddot{W}_1(t)$ can be obtained by substituting Equation (34)

$$\Gamma_{nr}(\tau) = \overline{F_n(t)\,\ddot{W}_r(t+\tau)}$$

$$= \overline{F_n(t) \int_0^{\omega} -(2\pi f)^2\, h_{nr}(\tau_1)\, F_n(t+\tau-\tau_1)\, d\tau_1}$$

$$= -(2\pi f)^2 \int_0^{\infty} h_{nr}(\tau_1)\, \overline{F_n(t)\, F_n(t+\tau-\tau_1)}\, d\tau_1$$

$$\Gamma_{nr}(\tau) = -(2\pi f)^2 \int_0^{\infty} h_{nr}(\tau_1)\, \Gamma_n(\tau-\tau_1)\, d\tau_1 \qquad (50)$$

which gives the crosscorrelation $\Gamma_{nr}(\tau)$ in terms of the unit-impulse response function $h_{nr}(t)$ and the autocorrelation $\Gamma_n(\tau)$ of the input force $F_n(t)$.

The cross-spectral density $S_{nr}(f)$ of the input force $F_n(t)$ and the response $\ddot{W}_r(t)$ is defined, as in Equation (39), as

$$S_{nr}(f) = 2 \int_{-\infty}^{\infty} \Gamma_{nr}(\tau)\, e^{-i2\pi f\tau}\, d\tau$$

and, from Equation (50)

$$S_{nr}(f) = 2 \int_{-\infty}^{\infty} \left[(2\pi f)^2 \int_0^{\infty} h_{nr}(\tau_1)\, \Gamma_n(\tau - \tau_1)\, d\tau_1 \right] e^{-i2\pi f\tau}\, d\tau$$

$$= (2\pi f)^2 \int_0^{\infty} h_{nr}(\tau_1)\, e^{-i2\pi f\tau_1}\, d\tau_1 \cdot$$

$$\cdot\ 2 \int_{-\infty}^{\infty} \Gamma_n(\tau - \tau_1)\, e^{-i2\pi f(\tau - \tau_1)}\, d(\tau - \tau_1)$$

$$S_{nr}(f) = a_{nr}(f)\ S_n(f) \tag{51}$$

The cross-spectral density $S_{nr}(f)$ of the input force $F_n(t)$ and the response $\ddot{W}_r(t)$ is simply the product of the transfer function $a_{nr}(f)$ and the spectral density $S_n(f)$ of the input force $F_n(t)$.

The cross-spectral density $S_{nr}(f)$ in Equation (51) can also be written in terms of the spectral density $S_r(f)$ of the response $\ddot{W}_r(t)$. The complex conjugate of Equation (51) is

$$S^*_{nr}(f) = a^*_{nr}(f)\ S_n(f) \tag{52}$$

since $S_n(f)$ is a real quantity. Multiplying Equation (51) by $a^*_{nr}(f)$

$$a^*_{nr}(f)\, S_{nr}(f) = a^*_{nr}(f)\ a_{nr}(f)\ S_n(f)$$

$$= |a_{nr}(f)|^2\ S_n(f)$$

$$= S_r(f)$$

Hence,

$$S_{nr}(f) = \frac{1}{a^{*}_{nr}(f)} \; S_r(f) \tag{53}$$

The spectral density of white noise is a constant S. Thus, the cross-spectral density of the acceleration response $\ddot{W}_r(t)$ of a point $\vec{y_r}$ on a structure excited by white noise is from Equation (51)

$$S_{nr}(f) = a_{nr}(f) \; S \tag{54}$$

The cross-spectral density $S_{nr}(f)$ has the same form as the transfer function $a_{nr}(f)$.

The crosscorrelation function $\Gamma_{nr}(\tau)$ of the white noise excitation and the response $W_r(t)$, using the definition of the autocorrelation $\Gamma_n(\tau)$ of white noise given by Equation (A.10) Appendix A , as

$$\Gamma_n(\tau) = \frac{1}{2} \; S\delta(\tau),$$

is written as

$$\Gamma_{nr}(\tau) = (2\pi f)^2 \int_0^{\infty} h_{nr}(\tau_1) \; \Gamma_n(\tau - \tau_1) \; d\tau_1$$

$$= \frac{(2\pi f)^2}{2} \int_0^{\infty} h_{nr}(\tau_1) \; S\,\delta(\tau - \tau_1) \; d\tau_1$$

$$\Gamma_{nr}(\tau) = 2\pi^2 f^2 \; S \; h_{nr}(\tau). \tag{55}$$

For white noise excitation, therefore, the crosscorrelation of excitation and response has the form of the unit impulse response function $h_{nr}(\tau)$.

The above result has application as a good experimental method for determining the vibration transfer characteristics of structures.

Response of Multiple Points Due to Multiple Loadings

A. Autocorrelation and Spectral Density of the Response to Multiple Loadings

The autocorrelation $\Gamma_n(\tau)$ of the acceleration response $\ddot{W}_r(t)$ at a single point $\vec{y}_r$ on a structure subjected to three forces $F_1(t)$, $F_2(t)$ and $F_3(t)$ which are applied at points $\vec{x}_1$, $\vec{x}_2$ and $\vec{x}_3$, respectively, is expanded from Equation (32) by substituting from Equation (34)

$$\Gamma_r(\tau) = \overline{\ddot{W}_r(t)\,\ddot{W}_r(t+\tau)}$$

$$= (2\pi f)^4 \overline{\int_0^\infty \left[h_{1r}(\tau_1)\,F_1(t-\tau_1) + h_{2r}(\tau_1)\,F_2(t-\tau_1) + h_{3r}(\tau_1)\,F_3(t-\tau_1)\right] d\tau}$$

$$\cdot \overline{\int_0^\infty \left[h_{1r}(\tau_2)\,F_1(t-\tau_2+\tau) + h_{2r}(\tau_2)\,F_2(t-\tau_2+\tau) + h_{3r}(\tau_2)\,F_3(t-\tau\right.}$$

and multiplying and rearranging,

$$\Gamma_r(\tau) = (2\pi f)^4 \sum_{m=1}^{3} \sum_{n=1}^{3} \int_0^\infty h_{mr}(\tau_1) \left[\int_0^\infty h_{nr}(\tau_2)\,\overline{F_m(t)\,F_n(t+\tau_1-\tau_2+\tau)}\,d\tau_2\right.$$

And, since

$$\Gamma_{mn}(\tau_1 - \tau_2 + \tau) = F_m(t)\, F_n(t + \tau_1 - \tau_2 + \tau)$$

then,

$$\Gamma_r(\tau) = (2\pi f)^4 \sum_{m=1}^{3} \sum_{n=1}^{3} \int_0^\infty h_{mr}(\tau_1) \left[\int_0^\infty h_{nr}(\tau_2)\, \Gamma_{mn}(\tau_1 - \tau_2 + \tau)\, d\tau_2 \right] d\tau_1 \qquad (56)$$

The autocorrelation function $\Gamma_r(\tau)$ of the response to three input random forces is now written in terms of the three autocorrelation functions $\Gamma_n(\tau)$ and the six crosscorrelation functions $\Gamma_{mn}(\tau)$ of the applied forces $F_m(t)$ and $F_n(t)$ and the appropriate unit-impulse response functions $h_{mr}(\tau)$.

The spectral density $S_r(f)$ of the response $W_r(t)$ is determined from the Fourier transform relation

$$S_r(f) = 2 \int_{-\infty}^{\infty} \Gamma_r(\tau)\, e^{-i2\pi f\tau}\, d\tau$$

$$2(2\pi f)^4 \sum_{m=1}^{3} \sum_{n=1}^{3} \int_{-\infty}^{\infty} \left[\int_0^\infty h_{mr}(\tau_1) \int_0^\infty h_{nr}(\tau_2)\, \Gamma_{mn}(\tau_1 - \tau_2 + \tau)\, d\tau_2\, d\tau_1 \right] e^{-i2\pi f\tau}\, d\tau$$

$$(2\pi f)^4 \sum_{m=1}^{3} \sum_{n=1}^{3} \int_{-\infty}^{\infty} h_{mr}(\tau_1) e^{i2\pi f\tau_1}\, d\tau_1 \int_0^\infty h_{nr}(\tau_2)\, e^{-i2\pi f\tau_2}\, d\tau_2 \cdot$$

$$\cdot\, 2 \int_{-\infty}^{\infty} \Gamma_{mn}(\tau_1 - \tau_2 + \tau)\, e^{-i2\pi f(\tau_1 - \tau_2 + \tau)}\, d(\tau_1 - \tau_2 + \tau)$$

$$S_r(f) = \sum_{m=1}^{3} \sum_{n=1}^{3} a^*_{mr}(f)\, a_{nr}(f)\, S_{mn}(f), \qquad (57)$$

where

$$S_{mn}(f) = 2 \int_{-\infty}^{\infty} \Gamma_{mn}(\tau) e^{-i2\pi f\tau}\, d\tau$$

is the cross-spectral density of the applied forces $F_m(t)$ and $F_n(t)$.

Now, in general the autocorrelation $\Gamma_n(\tau)$ and spectral density $S_r(f)$ of $W_r(t)$ to N applied forces $F_n(t)$ are, respectively,

$$\Gamma_r(\tau) = (2\pi f)^4 \sum_{m=1}^{N} \sum_{n=1}^{N} \int_0^{\infty} h_{mr}(\tau_1) \int_0^{\infty} h_{nr}(\tau_2)\, \Gamma_{mn}(\tau_1 - \tau_2 + \tau)\, d\tau_2\, d\tau_1 \qquad (58)$$

and

$$S_r(f) = \sum_{m=1}^{N} \sum_{n=1}^{N} a^*_{mr}(f)\, a_{nr}(f)\, S_{mn}(f)\,. \qquad (59)$$

To illustrate the effect of crosscorrelation on the response of a point in a structure, consider the previous case of the three forces, where (1) the three forces are independe and no crosscorrelations exist between the forces, and (2) the three forces are perfectly correlated and have identical spectral densities. In the first case, the spectral density the response is

$$S_r(f) = \sum_{m=1}^{3} \left| a_{mr}(f) \right|^2 S_m(f)\,. \qquad (60)$$

Now, let $S_1(f) = S_2(f) = S_3(f) = S$, and the spectral density of the response in the second case becomes

$$S_r(f) = \sum_{m=1}^{3} \sum_{n=1}^{3} a^*_{mr}(f)\, a_{nr}(f) \cdot S$$

$$= \left[\sum_{m=1}^{3} a^*_{mr}(f)\right]\left[\cdot \sum_{n=1}^{3} a_{nr}(f)\right] \cdot S$$

$$= \left|\sum_{m=1}^{3} a_{mr}(f)\right|^2 \cdot S$$

$$S_r(f) = \sum_{m=1}^{3} \left|a_{mr}(f)\right|^2 \cdot S + \sum_{m=1}^{3} \sum_{n=1}^{3} \left|a_{mr}(f)\right| \left|a_{nr}(f)\right| \cos\theta_{mn} \cdot S \qquad (61)$$

where θ_{mn} are the relative phase angles between each pair of transfer functions at the particular frequency f.

Therefore, it is seen that when there is correlation between the applied forces the spectral density of the response at any frequency depends upon the relative phase angles between the transfer functions of the structural paths. And, when no correlation exists, the relative phase angles have no effect on the response magnitude.

B. Crosscorrelation and Cross-Spectral Density of Two Responses to Multiple Loadings

Consider the responses $\ddot{W}_r(t)$ and $\ddot{W}_s(t)$ at points $\vec{y}_r$ and $\vec{y}_s$ to three input random forces $F_1(t)$, $F_2(t)$ and $F_3(t)$ applied at points $\vec{x}_1$, $\vec{x}_2$ and $\vec{x}_3$, respectively. The crosscorrelation function $\Gamma_{rs}(\tau)$ of the responses $\ddot{W}_r(t)$ and $\ddot{W}_s(t)$ can be obtained by expanding the responses as before from Equation (34)

$$\Gamma_{rs}(\tau) = \overline{\ddot{W}_r(t)\ \ddot{W}_s(t+\tau)}$$

$$= (2\pi f)^4 \int_0^\infty h_{1r}(\tau_1) F_1(t-\tau_1) + h_{2r}(\tau_1) F_2(t-\tau_1) + h_{3r}(\tau_1) F_3(t-\tau_1)\ d\tau_1 \cdot$$

$$\cdot \int_0^\infty h_{1s}(\tau_2) F_1(t-\tau_2+\tau) + h_{2s}(\tau_2) F_2(t-\tau_2+\tau) + h_{3s}(\tau_2) F_3(t-\tau_2+\tau)\ d\tau_2$$

multiplying and rearranging, gives

$$\Gamma_{rs}(\tau) = (2\pi f)^4 \sum_{m=1}^{3} \sum_{n=1}^{3} \int_0^\infty h_{mr}(\tau_1) \int_0^\infty h_{ns}(\tau_2)\ \Gamma_{mn}(\tau_1 - \tau_2 + \tau)\ d\tau_2\, d\tau_1 \qquad (62)$$

Similarly, the cross-spectral density $S_{rs}(f)$ is

$$S_{rs}(f) = \sum_{m=1}^{3} \sum_{n=1}^{3} a^*_{mr}(f)\ a_{ns}(f)\ S_{mn}(f) \qquad (63)$$

Obviously the extension of Equations (62) and (63) to the case of N random loadings yields

$$\Gamma_{rs}(\tau) = (2\pi f)^4 \sum_{m=1}^{N} \sum_{n=1}^{N} \int_0^\infty h_{mr}(\tau_1) \int_0^\infty h_{ns}(\tau_2)\ \Gamma_{mn}(\tau_1 - \tau_2 + \tau) d\tau_2\, d\tau_1 \qquad (64)$$

and

$$S_{rs}(f) = \sum_{m=1}^{N} \sum_{n=1}^{N} a^*_{mr}(f)\ a_{ns}(f)\ S_{mn}(f), \qquad (65)$$

This completes the general theory describing the response of multiple structural points excited by multiple random loadings applied at other structural points. A description of the responses at many internal points of a st.uctural segment, such as, a compartment, etc., relating each response $\ddot{W}_r(t)$ to each response $\ddot{W}_s(t)$, and to each input force $F_m(t)$ as well, can be obtained.

C. Crosscorrelation and Cross-Spectral Density of Beam Responses

Consider the uniform beam of length L, shown in Figure 5 with normal modes $\phi_q(\vec{y})$ and natural frequencies f_q. The generalized mass M_q in each mode is

$$M_q = \int_0^L \phi_q^2(\vec{y})\, m\, d\vec{y}$$

where m is the mass per unit length of the beam. The cross-spectral density of the acceleration responses $\ddot{W}_r(t)$ and $\ddot{W}_s(t)$ at $\vec{y}_r$ and $\vec{y}_s$ due to an input random force $F_n(t)$ at $\vec{y}_n$ is,

$$S_{rs}(f) \quad a_{nr}^*(f)\; a_{ns}(f)\; S_n(f).$$

Writing the transfer function in complex form

$$a_{mr}(f) \quad \sum_q \frac{\phi_q(\vec{y}_m)\;\phi_q(\vec{y}_r)}{M_q} \quad \frac{f^2}{f_q^2 - f^2 + \frac{icf}{2\pi M_q}}$$

$$\sum_q \frac{\phi_q(\vec{y}_m)\,\phi_q(\vec{y}_r)}{M_q} \quad \left\{ \frac{\left(\frac{f}{f_q}\right)^2}{1 - \left(\frac{f}{f_q}\right)^2 + \frac{ic}{2\pi M_q f_q}\left(\frac{f}{f_q}\right)} \right\}$$

$$a_{mr}(f) = \sum_q \frac{\phi_q(\vec{y}_m)\,\phi_q(\vec{y}_r)}{M_q} \left\{ \frac{\left(\frac{f}{f_q}\right)^2 - \left(\frac{f}{f_q}\right)^4 - \frac{i}{Q}\left(\frac{f}{f_q}\right)^3}{\left[1 - \left(\frac{f}{f_q}\right)^2\right]^2 + \frac{1}{Q^2}\left(\frac{f}{f_q}\right)^2} \right\} \quad (66)$$

$$a_{mr}(f) = \sum_q \left(R_{mrq}\left(\frac{f}{f_q}\right) - i\,X_{mrq}\left(\frac{f}{f_q}\right) \right) \quad (67)$$

where

$$R_{mrq}\left(\frac{f}{f_q}\right) = \frac{\phi_q(\vec{y}_m)\,\phi_q(\vec{y}_r)}{M_q} \cdot \frac{\left(\frac{f}{f_q}\right)^2 \left[1 - \left(\frac{f}{f_q}\right)^2\right]}{\left[1 - \left(\frac{f}{f_q}\right)^2\right]^2 + \frac{1}{Q^2}\left(\frac{f}{f_q}\right)^2} \quad (68)$$

$$X_{mrq}\left(\frac{f}{f_q}\right) = -\frac{\phi_q(\vec{y}_m)\,\phi_q(\vec{y}_r)}{M_q} \cdot \frac{\frac{1}{Q}\left(\frac{f}{f_q}\right)^3}{\left[1 - \left(\frac{f}{f_q}\right)^2\right]^2 + \frac{1}{Q^2}\left(\frac{f}{f_q}\right)^2} \quad (69)$$

and substituting

$$S_{rs}(f) = \left[\sum_q \left(R_{mrq} + i\,X_{mrq}\right)\right]\left[\sum_j \left(R_{mrj} - i\,X_{mrj}\right)\right] S_{in}(f) \quad (70)$$

expanding and rearranging

$$S_{rs}(f) = \left[\sum_q R_{mrq} \sum_j R_{msj} + \sum_q X_{mrq} \sum_j X_{msj} \right.$$

$$\left. - i \left(\sum_q R_{mrq} \sum_j X_{msj} - \sum_q X_{mrq} \sum_j R_{msj} \right) \right] S_m(f) \quad (71)$$

which is in general complex and cannot be simplified any further because of the product terms.

Simplifications result, however, from the assumptions that the structural damping is small and that the response peaks are well separated. Then the product terms where $q = j$ predominate over those where $q \neq j$, and, therefore, the latter can be neglected. Hence,

$$S_{rs}(f) \approx \left[\sum_q R_{mrq} R_{msq} + \sum_q X_{mrq} X_{msq} \right.$$

$$\left. - i \left(\sum_q R_{mrq} X_{msq} - \sum_q X_{mrq} R_{msq} \right) \right] S_m(f) \quad . \quad (72)$$

D. Response at Two Points Due to Two Input Forces

Now, consider the problem of computing the crosscorrelation of two acceleration responses $\ddot{W}_r(t)$ and $\ddot{W}_s(t)$ at points $\vec{y}_r$ and $\vec{y}_s$ on a structure excited by two input forces $F_m(t)$ and $F_n(t)$ applied at points $\vec{x}_m$ and $\vec{x}_n$. The unit-impulse response functions $h_{mr}(t)$, $h_{ms}(t)$, $h_{nr}(t)$ and $h_{ns}(t)$ describe the dynamic characteristics of the structure between the points $\vec{y}_r$, $\vec{y}_s$ and $\vec{x}_m$, $\vec{x}_n$. Figure 6 schematically illustrates the problem.

From Equation (64) the form of the crosscorrelation function $\Gamma_{rs}(\tau)$ is

$$\Gamma_{rs}(\tau) = (2\pi f)^4 \sum_{m}^{2}{}_1 \sum_{n}^{2}{}_1 \int_{-\infty}^{\infty} h_{mr}(\tau_1) \int_{-\infty}^{\infty} h_{ns}(\tau_2) \Gamma_{mn}(\tau_1 - \tau_2 + \tau)\, d\tau_2\, d\tau_1$$

Hence,

$$\begin{aligned}\Gamma_{rs}(\tau) = (2\pi f)^4 \Bigg[& \int_{-\infty}^{\infty} h_{mr}(\tau_1) \int_{-\infty}^{\infty} h_{ms}(\tau_2) \Gamma_{mn}(\tau_1 - \tau_2 + \tau)\, d\tau_2\, d\tau_1 \\ & + \int_{-\infty}^{\infty} h_{mr}(\tau_1) \int_{-\infty}^{\infty} h_{ns}(\tau_2) \Gamma_{mn}(\tau_1 - \tau_2 + \tau)\, d\tau_2\, d\tau_1 \\ & + \int_{-\infty}^{\infty} h_{nr}(\tau_1) \int_{-\infty}^{\infty} h_{ms}(\tau_2) \Gamma_{nm}(\tau_1 - \tau_2 + \tau)\, d\tau_2\, d\tau_1 \\ & + \int_{-\infty}^{\infty} h_{nr}(\tau_1) \int_{-\infty}^{\infty} h_{ns}(\tau_2) \Gamma_{nn}(\tau_1 - \tau_2 + \tau)\, d\tau_2\, d\tau_1 \Bigg] \end{aligned} \quad (73)$$

Now, let $\tau_2 = \tau_1$ in Equation (73)

$$\Gamma_{rs}(\tau) = (2\pi f)^4 \left[\int_{-\infty}^{\infty} \int_{-\infty}^{\infty} h_{mr}(\tau_1)\, h_{ms}(t+\tau_1)\, d\tau_1 \;\; \Gamma_{mm}(\tau - t)\, dt \right.$$

$$+ \int_{-\infty}^{\infty} \int_{-\infty}^{\infty} h_{mr}(\tau_1)\, h_{ns}(t+\tau_1)\, d\tau_1 \;\; \Gamma_{mn}(\tau - t)\, dt$$

$$+ \int_{-\infty}^{\infty} \int_{-\infty}^{\infty} h_{nr}(\tau_1)\, h_{ms}(t+\tau_1)\, d\tau_1 \;\; \Gamma_{nm}(\tau - t)\, dt$$

$$\left. + \int_{-\infty}^{\infty} \int_{-\infty}^{\infty} h_{nr}(\tau_1)\, h_{ns}(t+\tau_1)\, d\tau_1 \;\; \Gamma_{nn}(\tau - t)\, dt \right] \qquad (74)$$

The crosscorrelation function $\Gamma_{mr,ms}(t)$ of the unit-impulse response functions $h_{nr}(\tau_1)$ and $h_{ms}(t+\tau_1)$ is defined as

$$\Gamma_{mr,ms}(t) = (2\pi f)^4 \int_{-\infty}^{\infty} h_{mr}(\tau_1)\, h_{ms}(t+\tau_1)\, d\tau_1 \qquad (75)$$

Thus, Equation (74) becomes

$$\Gamma_{rs}(\tau) \int_{-\infty}^{\infty} \Gamma_{mr,ms}(t)\, \Gamma_{mm}(\tau - t)\, dt + \int_{-\infty}^{\infty} \Gamma_{mr,ns}(t)\, \Gamma_{mn}(\tau - t)\, dt$$

$$+ \int_{-\infty}^{\infty} \Gamma_{nr,ms}(t)\, \Gamma_{nm}(\tau - t)\, dt + \int_{-\infty}^{\infty} \Gamma_{nr,ns}(t)\, \Gamma_{nn}(\tau - t)\, dt. \qquad (76)$$

E. Responses of Two Single Degree-of-Freedom Systems to Impulse Excitation

Consider two linear mechanical systems each of which represents a single degree of freedom system. As shown schematically in Figure 7, an impulse input F_m is applied to the first system at time $t = 0$ and the resulting response at $\vec{y}_r$ is $h_{mr}(t)$; while the impulse F_m is applied to the second system at time $t = \tau$ and the resulting response at $\vec{y}_s$ is $h_{ms}(t + \tau)$.

From Equation (13), it is seen that the above impulse responses are written

$$h_{mr}(t) \quad \begin{cases} \dfrac{F_m}{M_r 2\pi\sigma_r} e^{-\zeta_r 2\pi f_r t} \sin 2\pi\sigma_r(t), & t \geq 0 \\ 0, & t \leq 0 \end{cases} \qquad (77)$$

$$h_{ms}(t + \tau) \quad \begin{cases} \dfrac{F_m}{M_s 2\pi\sigma_s} e^{-\zeta_s 2\pi f_s (t + \tau)} \sin 2\pi\sigma_s(t + \tau), & t \geq -\tau \\ 0, & t \leq -\tau \end{cases} \qquad (78)$$

The crosscorrelation $\Gamma_{mr,ms}(\tau)$ of the two responses is, from Equation (75).

$$\Gamma_{mr,ms}(\tau) = \int_{-\infty}^{\infty} h_{mr}(t)\, h_{ms}(t+\tau)\, dt \tag{79}$$

If $\tau \geq 0$, then from Equations (77) and (78) the above integrand equals zero in the range $-\infty \leq t \leq 0$ so that Equation (79) reduces to

$$\Gamma_{mr,ms}(\tau) = \int_{0}^{\infty} h_{mr}(t)\, h_{ms}(t+\tau)\, dt, \quad t \geq 0 \tag{80}$$

When $\tau < 0$, then Equation (79) is written

$$\Gamma_{mr,ms}(-|\tau|) = \int_{-\infty}^{\infty} h_{mr}(t)\, h_{ms}(t-|\tau|)\, dt, \quad t \leq 0 \tag{31}$$

where, from Equations (77) and (78) it is seen that the integrand above is zero in the range $-\infty < t < |\tau|$ so that Equation (81) reduces to

$$\Gamma_{mr,ms}(-|\tau|) = \int_{\tau}^{\infty} h_{mr}(t)\, h_{ms}(t-|\tau|)\, dt, \quad \tau < 0$$

And, letting $t = t + |\tau|$, gives

$$\Gamma_{mr,ms}(-|\tau|) \quad \int_0^\infty h_{mr}(t+|\tau|)\, h_{ms}(t)\, dt \quad , \tau \leq 0. \tag{82}$$

Equations (80) and (82) are used to compute the crosscorrelation $\Gamma_{mr,ms}(\tau)$ of the responses $h_{mr}(t)$, $h_{ms}(t)$ of two single degree of freedom systems to the impulse excitation F_m.

Substituting Equations (77) and (78) into Equation (80)

$$\Gamma_{mr,ms}(\tau) \quad \frac{F_m^2 \, e^{-\zeta_s 2\pi f_s \tau}}{M_r M_s 4\pi^2 \sigma_r \sigma_s} \int_0^\infty e^{-2\pi(\zeta_r f_r + \zeta_s f_s)}$$

$$\cdot \quad \sin 2\pi \sigma_r t \, \sin 2\pi \sigma_s (t+\tau)\, dt, \quad t \geq 0$$

and expanding by using a trigonometric identity,

$$\Gamma_{mr,ms}(\tau) \quad \frac{F_m^2 \, e^{-\zeta_s 2\pi f_s \tau}}{M_r M_s 4\pi^2 \sigma_r \sigma_s} \left[\cos 2\pi \sigma_s \tau \int_0^\infty e^{-2\pi(\zeta_r f_r + \zeta_s f_s)} \cdot \right.$$

$$\cdot \quad \sin 2\pi \sigma_r t \, \sin 2\pi \sigma_s t \, dt$$

$$\left. + \sin 2\pi \sigma_s \tau \int_0^\infty e^{-2\pi(\zeta_r f_r + \zeta_s f_s)} \sin 2\pi \sigma_r t \, \cos 2\pi \sigma_s t \quad dt \right] , \quad t \geq 0$$

Integ ating and collecting terms

$$\Gamma_{mr,ms}(\tau) = e^{-\zeta_s 2\pi f_s \tau}\left[a\cos 2\pi\sigma_s\tau + b\sin 2\pi\sigma_s\tau\right], \quad \tau \geq 0 \tag{83}$$

where

$$a = \frac{2\pi\gamma F_m^2}{32\pi^4 M_r M_s \sigma_r \sigma_s}\left[\frac{1}{\gamma^2 + (\sigma_r - \sigma_s)^2} - \frac{1}{\gamma^2 + (\sigma_r + \sigma_s)^2}\right]$$

$$b = \frac{F_m^2}{32\pi^4 M_r M_s \sigma_r \sigma_s}\left[\frac{\sigma_r - \sigma_s}{\gamma^2 + (\sigma_r - \sigma_s)^2} + \frac{\sigma_r + \sigma_s}{\gamma^2 + (\sigma_r + \sigma_s)^2}\right]$$

$$\gamma = \zeta_r f_r + \zeta_s f_s$$

Equation (82) shows that the corresponding expression for negative values of τ can be obtained by interchanging the σ_r and σ_s in Equation (83) and replacing τ with $|\tau|$. The obvious result is

$$\Gamma_{mr,ms}(-|\tau|) = e^{-\zeta_r 2\pi f_r |\tau|}\left[c\cos 2\pi\sigma_r|\tau| + d\sin 2\pi\sigma_r|\tau|\right], \quad \tau \leq 0 \tag{84}$$

where

$$c = \frac{2\pi\gamma F_m^2}{32\pi^4 M_r M_s \sigma_r \sigma_s}\left[\frac{1}{\gamma^2 + (\sigma_s - \sigma_r)^2} - \frac{1}{\gamma^2 + (\sigma_s + \sigma_r)^2}\right]$$

$$d = \frac{F_m^2}{32\pi^4 M_r M_s \sigma_r \sigma_s}\left[\frac{\sigma_s - \sigma_r}{\gamma^2 + (\sigma_s - \sigma_r)^2} + \frac{\sigma_s + \sigma_r}{\gamma^2 + (\sigma_s + \sigma_r)^2}\right]$$

$$\gamma = \zeta_r f_r + \zeta_s f_s$$

The crosscorrelation as a function of τ is seen to be continuous, in magnitude, everywhere including $\tau = 0$. At $\tau = 0$, both Equations (83) and (84) reduce to

$$\Gamma_{mr,ms}(0) = \frac{2\pi\gamma F_m^2}{32\pi^4 M_r M_s \sigma_r \sigma_s}\left[\frac{1}{\gamma^2 + (\sigma_r - \sigma_s)^2} - \frac{1}{\gamma^2 + (\sigma_r + \sigma_s)^2}\right] \tag{85}$$

Several interesting special cases can be obtained from Equation (85). If both mechanical systems are undamped, then $\gamma = 0$ and

$$\Gamma_{mr,ms}(0)\Big]_{\zeta_r = \zeta_s = 0} = 0, \quad \sigma_r \neq \sigma_s \tag{86}$$

If $\sigma_r = \sigma_s$, then

$$\Gamma_{mr,ms}(0)\Big]_{\sigma_r = \sigma_s = \sigma} = \frac{2\pi\gamma F_m^2}{32\pi^4 M_r M_s \sigma_r \sigma_s}\left[\frac{1}{\gamma^2} - \frac{1}{\gamma^2 + 4\sigma^2}\right] \tag{87}$$

Thus, if $\sigma_r = \sigma_s$ and $\gamma = 0$, then

$$\Gamma_{mr,ms}(0)\Big]_{\substack{\sigma_r = \sigma_s \\ \zeta_r = \zeta_s = 0}} = \infty \tag{88}$$

Equations (86) and (88) can be combined to give a more general form, namely

$$\Gamma_{mr,ms}(0)\Big]_{\zeta_r = \zeta_s = 0} = \delta(\sigma_r - \sigma_s)\begin{cases} 0, & \sigma_r \neq \sigma_s \\ \infty, & \sigma_r = \sigma_s \end{cases} \tag{89}$$

The quantities $\zeta_r f_r$ and $\zeta_s f_s$ are the bandwidths of the two systems and γ is the sum of the bandwidths. If the frequency separation $|\sigma_r - \sigma_s|$ is much larger than γ, the quantity a above will be much smaller than the quantity b above; and the quantity c above will be much smaller than the quantity d above. Further, both of the quantities b and d can be simplified by neglecting γ^2 so that

$$b \approx \frac{F_m^2}{16\pi^4 M_r M_s \sigma_s (\sigma_r^2 - \sigma_s^2)}$$

$$d \approx \frac{F_m^2}{16\pi^4 M_r M_s \sigma_r (\sigma_s^2 - \sigma_r^2)}$$

In this case, Equations (83) and (84) are approximately

$$\Gamma_{mr,ms}(\tau) \approx \frac{2\pi F_m^2}{16\pi^4 M_r M_s (\sigma_r^2 - \sigma_s^2)} \tau e^{-\zeta_s 2\pi f_s \tau} \cdot \frac{\sin 2\pi \sigma_s \tau}{2\pi \sigma_s \tau} \qquad (90)$$

$$\Gamma_{mr,ms}(-|\tau|) \approx \frac{2\pi F_m^2}{16\pi^4 M_r M_s (\sigma_s^2 - \sigma_r^2)} |\tau| e^{-\zeta_r 2\pi f_r |\tau|} \cdot \frac{\sin 2\pi \sigma_r |\tau|}{2\pi \sigma_r |\tau|} \qquad (91)$$

where $\zeta_r f_r + \zeta_s f_s \quad \gamma \ll |\sigma_r - \sigma_s|$ (bandwidths do not overlap)

$a \ll b$

$c \ll d$.

Note that the larger the frequency separation $|\sigma_r - \sigma_s|$, the smaller the crosscorrelation $\Gamma_{mr,ms}(\tau)$ becomes. Equations (90) and (91) will generally be sufficiently accurate

for two lightly damped systems whose bandwidths do not overlap. When the bandwidths do overlap, that is, when $|\sigma_r - \sigma_s| < \gamma$, the dampings of the two systems control the crosscorrelation $\Gamma_{mr,ms}(\tau)$ of their responses to impulse excitations. In this case, the more general Equations (83) and (84) must be used. However, when $|\sigma_r - \sigma_s| << \gamma << (\sigma_r + \sigma_s)$, these general expressions reduce to the following:

$$\Gamma_{mr,ms}(\tau) \approx \frac{2\pi F_m^2}{32\pi^4 \gamma M_r M_s \sigma_r \sigma_s} e^{-\zeta_s 2\pi f_s \tau} \cos 2\pi \sigma_s \tau \qquad (92)$$

$$\Gamma_{mr,ms}(-|\tau|) \approx \frac{2\pi F_m^2}{32\pi^4 \gamma M_r M_s \sigma_r \sigma_s} e^{-\zeta_r 2\pi f_r |\tau|} \cos 2\pi \sigma_r |\tau| \qquad (93)$$

where,

$|\sigma_r - \sigma_s| << \gamma << (\sigma_r + \sigma_s)$, (bandwidths overlap)

$b << a$

$d << c$

$\gamma = \zeta_r f_r + \zeta_s f_s$

Finally, it is to be noted that the slope of the crosscorrelation $\Gamma_{mr,ms}(\tau)$ is discontinuous, in general, at $\tau = 0$. Also, since for $\tau \geq 0$, the frequency of the function $\Gamma_{mr,ms}(\tau)$ is σ_s, and $\tau \leq 0$ the frequency of the function $\Gamma_{mr,ms}(-|\tau|)$ is σ_r, the two crosscorrelation functions may be quite different in character. These characteristics of the crosscorrelation function are shown in Figure 8 .

F. Crosscorrelation of the Responses of Two Single Degree-of-Freedom Systems to Bandwidth Limited White Noise

Now, consider that the same two independent mechanical single degree of freedom systems as above (Figure 7), are excited by bandwidth limited white noise. Then, as shown in Figure 9 , the force $F_m(t)$, input to the first system results in an acceleration response $\ddot{W}_r(t)$. The same force $F_m(t + \tau_1)$, input to the second system, with time delay τ_1, results in an acceleration response $\ddot{W}_s(t)$. The unit-impulse response functions for the two systems are $h_{mr}(t)$ and $h_{ms}(t)$ respectively.

If the first input force $F_m(t)$, is deterministic, then the second input force $F_m(t + \tau_1)$ is also deterministic and has the same functional form as $F_m(t)$. For example, if $F_m(t) = A \sin 2\pi ft$, then $F_m(t) = A \sin 2\pi f(t + \tau_1)$. However, if $F_m(t)$ represents a random signal which contains a continuous band of frequencies over a finite bandwidth, then the composite signal $F_m(t + \tau_1)$ over all frequencies in the band can appear quite different from $F_m(t)$. To obtain $F_m(t + \tau_1)$ from $F_m(t)$, each frequency component in $F_m(t)$ is advanced in time by a constant τ_1 which changes the phase of that frequency component.

The amount of phase change $2\pi f\tau_1$ depends upon the frequency and because there are an infinity of frequency components in $F_m(t)$, each of which experiences a different phase shift, the summation of all of these phase-shifted frequency components will, in general, produce a much different signal than the original signal $F_m(t)$. For small values of τ_1, the phase shift at low frequencies will be small, whereas at high frequencies the shift will be large. Also, the larger the time interval τ_1 the larger the phase change for all frequencies except those having periods approximately equal to τ_1. Thus, the crosscorrelation

$\Gamma_{mm}(\tau_1 + \tau)$ between $F_m(t)$ and $F_m(t + \tau_1)$ which is equivalent to the auto-correlation of $F_m(t)$ with time delay τ_1 over some frequency band, is greater when the band contains only low frequencies than when the band contains only high frequencies, and is greater for small values of τ_1 than for large values of τ_1. Also, this crosscorrelation is dependent upon the bandwidth so that for a given τ_1, and a given center frequency of the band, the magnitude of the correlation is greater for narrow bands than for broad bands.

The similarities of the responses of the two systems in Figure 9 reflect the similarities of the input. Thus the crosscorrelation $\Gamma_{rs}(\tau)$ of the responses $\ddot{W}_r(t)$ and $\ddot{W}_s(t)$ is greatest when the crosscorrelation $\Gamma_{mm}(\tau_1 + \tau)$ of $F_m(t)$ and $F_m(t + \tau_1)$ is greatest. However, the crosscorrelation $\Gamma_{rs}(\tau)$ is also governed by similarities, or dissimilarities, of the response characteristics of the two systems, these response characteristics being the resonant frequencies f_r, f_s and the dampings ζ_r, ζ_s. It is expected that the response crosscorrelation $\Gamma_{rs}(\tau)$ is greater when the two resonant frequencies f_r and f_s are nearly equal than when these frequencies are widely separated. The effect of damping on the response crosscorrelation is more complex; however, in general, the response correlation decreases as the damping decreases, since, in this case, the two systems become more like pure tone oscillators with zero bandwidth, for which the crosscorrelation is zero if the two resonant frequencies are different.

Equation (76), the general expression for the system shown in Figure 6, can be applied to the system being considered here by using only the first term which is the crosscorrelation of two single degree of freedom systems to the same input force $F_m(t)$, hence

$$\Gamma_{rs}(\tau) = (2\pi f)^4 \int_{-\infty}^{\infty} \Gamma_{mr,ms}(\tau_2)\, \Gamma_m(\tau_1 + \tau - \tau_2)\, d\tau_2 \qquad (94)$$

where the crosscorrelation $\Gamma_{mr,ms}(\tau_2)$ of the unit-impulse response functions $h_{mr}(t)$ and $h_{ms}(t + \tau_2)$ is given by Equations (83) and (84) for positive and negative values of τ_2, respectively. An expression for the autocorrelation function $\Gamma_m(\tau_1 + \tau - \tau_2)$ of a bandwidth limited white noise is derived in Equation (B.1), Appendix B, and is written as

$$\Gamma_m(\tau_1 + \tau - \tau_2) \quad S_m \left[\frac{\sin 2\pi f_u(\tau_1 + \tau - \tau_2) - \sin 2\pi f_L(\tau_1 + \tau - \tau_2)}{\tau_1 + \tau - \tau_2} \right] \tag{95}$$

where

$$S_m \begin{cases} \text{constant spectral density of } F_m(t) \text{ for } f_L \leq f \leq f_u \\ 0, \text{otherwise} \end{cases}$$

f_L lower band limit frequency

f_u upper band limit frequency

In the present analysis, the crosscorrelation between the responses of the two systems shown in Figure 7 is to be taken with no time delay so that $\tau = 0$. Hence, Equations (94) and (95) reduce to

$$\Gamma_{rs}(0) \quad (2\pi f)^4 \int_{-\infty}^{\infty} \Gamma_{mr,ms}(\tau_2)\, \Gamma_m(\tau_1 - \tau_2)\, d\tau_2 \tag{96}$$

$$\Gamma_m(\tau_1 - \tau_2) \quad S \left[\frac{\sin 2\pi f_u(\tau_1 - \tau_2) - \sin 2\pi f_L(\tau_1 - \tau_2)}{\tau_1 - \tau_2} \right] \tag{97}$$

The crosscorrelation $\Gamma_{mr,ms}(\tau_2)$ of the unit impulse response functions is obtained from Equations (83) and (34) by setting $F_m = 1$,

$$\Gamma_{mr,ms}(\tau_2) = e^{-\zeta_s 2\pi f_s \tau_2}\left[a \cos 2\pi\sigma_s\tau_2 + b \sin 2\pi\sigma_s\tau_2\right], \tau_2 \geq 0 \quad (98)$$

$$\Gamma_{mr,ms}(-|\tau_2|) = e^{-\zeta_r 2\pi f_r \tau_2}\left[c \cos 2\pi\sigma_r|\tau_2| + d \sin 2\pi\sigma_r|\tau_2|\right], \tau_2 \leq 0 \quad (99)$$

where a, b, c, and d are as defined for Equations (83) and (34) with $F_m = 1$.

Substituting Equations (97), (98) and (99) into Equations (96) gives

$$\begin{aligned}\Gamma_{rs}(\tau) = (2\pi f)^4 \Bigg[& a \cdot S_m \int_0^\infty e^{-\zeta_s 2\pi f_s \tau_2} \cos 2\pi\sigma_s\tau_2 \frac{\sin 2\pi f_u(\tau_1-\tau_2) - \sin 2\pi f_L(\tau_1-\tau_2)}{(\tau_1-\tau_2)} d\tau_2 \\ & + b S_m \int_0^\infty e^{-\zeta_s 2\pi f_s \tau_2} \sin 2\pi\sigma_s\tau_2 \frac{\sin 2\pi f_u(\tau_1-\tau_2) - \sin 2\pi f_L(\tau_1-\tau_2)}{(\tau_1-\tau_2)} d\tau_2 \\ & + c S_m \int_0^\infty e^{-\zeta_r 2\pi f_r|\tau_2|} \cos 2\pi\sigma_r|\tau_2| \frac{\sin 2\pi f_u(\tau_1-\tau_2) - \sin 2\pi f_L(\tau_1-\tau_2)}{(\tau_1-\tau_2)} d\tau_2 \\ & + d S_m \int_0^\infty e^{-\zeta_r 2\pi f_r \tau_2} \sin 2\pi\sigma_r|\tau_2| \frac{\sin 2\pi f_u(\tau_1-\tau_2) - \sin 2\pi f_L(\tau_1-\tau_2)}{(\tau_1-\tau_2)} d\tau_2 \Bigg], \end{aligned} \quad (100)$$

Spectral Density of Response Differences

A convenient means for presenting the frequency response transfer relationships existing between two acceleration responses $\ddot{W}_r(t)$ and $\ddot{W}_s(t)$ at points $\bar{y}_r$ and $\bar{y}_s$ on a complex structure is found by computing the spectral density $S_{(r-s)}(f)$ of the difference between $\ddot{W}_r(t)$ and $\ddot{W}_s(t)$. Equations (42) and (43) define the autocorrelation $\Gamma_{(r-s)}(\tau)$ and the spectral density $S_{(r-s)}(f)$ of the response difference $\ddot{W}_r(t) - \ddot{W}_s(t)$. Expand Equation (42) and obtain the autocorrelation

$$\Gamma_{(r-s)}(\tau) = \overline{\left[\ddot{W}_r(t) - \ddot{W}_s(t)\right]\left[\ddot{W}_r(t+\tau) - \ddot{W}_s(t+\tau)\right]}$$

$$= \overline{\ddot{W}_r(t)\ddot{W}_r(t+\tau)} - \overline{\ddot{W}_r(t)\ddot{W}_s(t+\tau)} - \overline{\ddot{W}_s(t)\ddot{W}_r(t+\tau)} + \overline{\ddot{W}_s(t)\ddot{W}_s(t+\tau)}$$

$$\Gamma_{(r-s)}(\tau) = \Gamma_r(\tau) - \Gamma_{rs}(\tau) - \Gamma_{sr}(\tau) + \Gamma_s(\tau) . \qquad (101)$$

The spectral density $S_{(r-s)}(f)$ of the response difference, by inspection, is written as

$$S_{(r-s)}(f) = \int_{-\infty}^{\infty} \Gamma_{(r-s)}(\tau)\, e^{-i2\pi f\tau}\, d\tau$$

$$S_{(r-s)}(f) = S_r(f) - S_{rs}(f) - S_{sr}(f) + S_s(f) \qquad (102)$$

Close examination of Equation (102) reveals a useful tool for presenting measured response data.

For example, consider two independent, but identical systems. When two independent random input forces $F_1(t)$ and $F_2(t)$ are applied to the systems, their acceleration responses $\ddot{W}_r(t)$ and $\ddot{W}_s(t)$ are uncorrelated. For this case, the spectral density $S_{(r-s)}(f)$ of the response difference $\ddot{W}_r(t) - \ddot{W}_s(t)$ becomes simply the sum of the separate spectral densities

$$S_{(r-s)}(f) = S_r(f) + S_s(f), \text{ (uncorrelated)}, \tag{103}$$

which is what would be expected, since uncorrelated responses are independent of their relative phase, and hence, the sign of their combination; that is

$$S_{(r+s)}(f) = S_r(f) + S_s(f), \text{ (uncorrelated)}.$$

For the case of perfectly correlated input forces with identical input spectral densities $S_1(f) = S_2(f) = S(f)$, the cross-spectral densities $S_{rs}(f)$ and $S_{sr}(f)$ and the spectral densities $S_r(f)$ and $S_s(f)$ are equal, hence the spectral density $S_{(r-s)}(f)$ of the response difference is zero,

$$S_{(r-s)}(f) = S_r(f) - S_{rs}(f) - S_{sr}(f) - S_s(f)$$

$$S_{(r-s)} = 0, \text{ (correlated)} \tag{104}$$

The response difference spectral density $S_{(r-s)}$ is sensitive to the relative correlation existing between the frequency spectra of the two responses $\ddot{W}_r(t)$ and $\ddot{W}_s(t)$. When $S_{(r-s)}(f)$ is large at some frequency f, there is a lack of correlation or, rather, "transmission loss" of that particular frequency component between the points $\vec{y}_r$ and $\vec{y}_s$. The distribution of various frequency components of vibration can be traced throughout a complex structure via this method, which would result in the location and identification of excitation sources from data measured at selected points on a structure. Figure 10 schematically illustrates the utility of this method.

The spectral density $S_{(r-s)}(f)$ of the response difference $\ddot{W}_r(t) - \ddot{W}_s(t)$ is indicative of the "transmission loss" of the structural segment between the response points $\vec{y}_r$ and $\vec{y}_s$. Dividing Equation (102) by Equation (103), which is the maximum value of $S_{(r-s)}(f)$, yields a nondimensional coefficient $TL_{(r-s)}$

$$TL_{(r-s)} \qquad \frac{S_{(r-s)}(f)}{S_r(f) + S_s(f)} \tag{105}$$

which evaluates the "transmission loss" between the points $\vec{y}_r$ and $\vec{y}_s$.

DISTRIBUTED PRESSURE EXCITATION AT DISCRETE FREQUENCIES

Consider now the case of a distributed pressure loading which has a discrete frequency spectrum and let $P_k(\vec{x},t)$ denote the component of the pressure applied at the point $\vec{x}$ at frequency f_k. An expression for the acceleration response $\ddot{W}_r(t)$ at a point $\vec{y}_r$ can be obtained from equation (4) by replacing the point force $F_{nk}(t)$ by its equivalent $P_k(\vec{x}, t) \cdot dA(\vec{x})$, where $dA(\vec{x})$ denotes an incremental area over which the pressure acts, and by replacing the summation over n by an integration over area, giving

$$\ddot{W}_r(t) = \sum_k \int_A a(\vec{x}, \vec{y}_r ; f_k) \cdot P_k(\vec{x}, t) \cdot dA(\vec{x}) \quad (106)$$

In Equation (106), the area A denotes the entire area of the vehicle over which the fluctuating pressures act. For purposes of developing empirical correlation techniques, it is convenient to break up this surface area into zones or area segments A_n as shown in Figure 11. The choice of the size of these zones will generally depend upon the surface pressure correlation lengths, crosscorrelations of the responses along different structural transmission paths, excitation frequency and bandwidth. Discussions on these points are presented in Section IV. The integral over the vehicle area A can be written as a summation of integrals over each of the area segments A_n, and thus the expression for the acceleration response $\ddot{W}_r(t)$ in Equation (106) can be written in the form

$$\ddot{W}_r(t) = \sum_k \sum_n \int_{A_n} a(\vec{x}, \vec{y}_r ; f_k) P_k(\vec{x}, t) \cdot dA(\vec{x}) \quad (107)$$

The pressure $P_k(\vec{x}, t)$ can be written in complex form in a manner similar to that used for the complex force $F_{nk}(t)$ given in Equation (19),

$$P_k(\vec{x}, t) = \left|P_k(\vec{x})\right| \cdot e^{i\phi_k(\vec{x})} \, e^{2\pi i f_k t} \tag{108}$$

Also, the complex form of $a(\vec{x}, \vec{y}_r ; f_k)$ can be written in a form similar to that given by Equation (7), namely

$$a(\vec{x}, \vec{y}_r ; f_k) = \left|a(\vec{x}, \vec{y}_r ; f_k)\right| e^{i\theta(\vec{x}, \vec{y}_r ; f_k)} \tag{109}$$

Substituting Equation (108) and (109) into Equation (107) gives the following expression for the acceleration $\ddot{W}_r(t)$,

$$\ddot{W}_r(t) = \sum_k \sum_n \int_{A_n} \left|a(\vec{x}, \vec{y}_r ; f_k)\right| \cdot \left|P_k(\vec{x})\right| \cdot e^{i\theta(\vec{x}, \vec{y}_r ; f_k)} \cdot e^{i\phi_k(\vec{x})} \cdot e^{2\pi i f_k t} \cdot dA(\vec{x}) \tag{110}$$

Equation (110) is seen to have the same form as Equation (20) and thus the expression for the mean-square acceleration response $\overline{\ddot{W}_r^2(t)}$ is similar to that given by Equation (22). Thus for the case of a distributed pressure loading,

$$\overline{\ddot{W}_r^2(t)} = \frac{1}{2} \sum_k \sum_n \int_{A_n} \int_{A_n} Q(\vec{x}, \vec{x}', \vec{y}_r ; f_k) \, dA(\vec{x}) \, dA(\vec{x}') + \frac{1}{2} \sum_k \sum_{\substack{n \\ (n \neq m)}} \sum_m \int_{A_n} \int_{A_m} Q(\vec{x}, \vec{x}', \vec{y}_r ; f_k) \, dA(\vec{x}) \, dA(\vec{x}') \tag{111}$$

where

$$Q(\vec{x}, \vec{x}', \vec{y}_r ; f_k) \left|a(\vec{x}, \vec{y}_r ; f_k)\right| \cdot \left|a(\vec{x}', \vec{y}_r ; f_k)\right| \cdot \left|P_k(\vec{x})\right| \cdot \left|P_k(\vec{x}')\right| \cdot$$

$$\cdot \cos\left[\theta(\vec{x}, \vec{y}_r ; f_k) - \theta(\vec{x}', \vec{y}_r ; f_k) + \phi_k(\vec{x}) - \phi_k(\vec{x}')\right] \qquad (112)$$

Similarly, the crosscorrelation $\Gamma_{rs}(\tau)$ of the acceleration responses $\ddot{W}_r(t)$, $\ddot{W}_s(t)$ at $\vec{y}_r$, $\vec{y}_s$ respectively has the same form as Equation (29) and is

$$\Gamma_{rs}(\tau) = \frac{1}{2} \sum_k \sum_n \sum_m \int_{A_n} \int_{A_m} Q(\vec{x}, \vec{x}', \vec{y}_r, \vec{y}_s ; f_k)\, dA(\vec{x})\, dA(\vec{x}') \qquad (113)$$

where

$$Q(\vec{x}, \vec{x}', \vec{y}_r, \vec{y}_s ; f_k) = \left|a(\vec{x}, \vec{y}_r ; f_k)\right| \cdot \left|a(\vec{x}', \vec{y}_s ; f_k)\right| \cdot$$

$$\cdot \left|P_k(\vec{x})\right| \cdot \left|P_k(\vec{x}')\right| \cdot$$

$$\cdot \cos\left[\theta(\vec{x}, \vec{y}_r ; f_k) - \theta(\vec{x}', \vec{y}_s ; f_k) + \phi_k(\vec{x}) - \phi_k(\vec{x}')\right] \qquad (114)$$

It is to be noted that Equation (113) and (114) reduce to Equation (111) and (112) when $\vec{y}_s = \vec{y}_r$. Considering the generality of Equations (110) - (114) for the mean-square response and crosscorrelation of response, these expressions are quite compact; and being expressed in real form, they are easily interpreted.

Normal Mode Representation of Spectral Density and Crosscorrelation

When equations of this type are presented in the literature, they are usually presented in terms of normal modes of the structure. To show how these equations can be written

in terms of normal modes, it is convenient to write the expression (114) for $Q(\vec{x}, \vec{x}', \vec{y}_r, \vec{y}_s; f_k)$ in an alternate form. In order to shorten the notation, let a_r, a'_s, θ_r, θ'_s be used to denote $a(\vec{x}, \vec{y}_r; f_k)$, $a(\vec{x}', \vec{y}_s; f_k)$, $\theta(\vec{x}, \vec{y}_r; f_k)$, and $\theta(\vec{x}', \vec{y}_s; f_k)$ respectively. Note first that the real and imaginary forms of a_r and a'_s are

$$\left.\begin{aligned} \mathcal{R}\{a_r\} &= |a_r| \cos\theta_r \\ \mathcal{I}\{a_r\} &= |a_r| \sin\theta_r \\ \mathcal{R}\{a'_s\} &= |a'_s| \cos\theta'_s \\ \mathcal{I}\{a'_s\} &= |a'_s| \sin\theta'_s \end{aligned}\right\} \tag{115}$$

Expanding the cosine function in Equation (114) and using Equation (115) to simplify the resulting expression, gives

$$\begin{aligned} &Q(\vec{x}, \vec{x}', \vec{y}_r, \vec{y}_s; f_k) \\ &\left[\mathcal{R}\{a_r\}\mathcal{R}\{a'_s\} + \mathcal{I}\{a_r\}\mathcal{I}\{a'_s\}\right] \cdot \left|P_k(\vec{x})\right| \cdot \left|P_k(\vec{x}')\right| \cos\left[\phi_k(\vec{x}) - \phi_k(\vec{x}')\right] \\ &\left[\mathcal{R}\{a_r\}\mathcal{I}\{a'_s\} - \mathcal{I}\{a_r\}\mathcal{R}\{a'_s\}\right] \left|P_k(\vec{x})\right| \cdot \left|P_k(\vec{x}')\right| \sin\left[\phi_k(\vec{x}) - \phi_k(\vec{x}')\right] \end{aligned} \tag{}$$

As shown in a previous example for a uniform beam, the form of the transfer function, when expanded in terms of normal modes of the structure, is that given by Equation (13). Thus, for a general structure, a_r can be written as follows

$$a_r = -(2\pi f_k)^2 \sum_{\nu=1}^{\infty} \frac{H_\nu(f_k)}{k_\nu} \phi_\nu(\vec{x}) \phi_\nu(\vec{y}_s) \tag{117}$$

and the comparable equation for a_s' is

$$a_s' = -(2\pi f_k)^2 \sum_{\mu=1}^{\infty} \frac{H_\mu(f_k)}{k_\mu} \phi_\mu(\vec{x}') \phi_\mu(\vec{y}_s) \tag{113}$$

The subscripts ν and μ denote the mode number, k_ν and k_μ the generalized modal stiffnesses, $\phi_\nu(\vec{x})$ and $\phi_\mu(\vec{x})$ the mode shapes. The complex function $H_\nu(f)$ is defined by Equation (10), and the real and imaginary parts of $H_\nu(f_k)$ are

$$\left.\begin{aligned} \mathcal{R}\{H_\nu(f_k)\} &= \left[1 - \left(\frac{f_k}{f_\nu}\right)^2\right] |H_\nu(f_k)|^2 \\ \mathcal{I}\{H_\nu(f_k)\} &= -\frac{1}{Q}\left(\frac{f_k}{f_\nu}\right) |H_\nu(f_k)|^2 \end{aligned}\right\} \tag{119}$$

where the function $|H_\nu(f)|$ is defined by Equation (11). Similarly for the function $H_\mu(f_k)$. Substituting Equations (117) - (119) into Equation (116) gives expansion of $Q(\vec{x}, \vec{x}', \vec{y}_r, \vec{y}_s; f_k)$ in terms of normal modes of the structure

$$Q(\vec{x}, \vec{x}', \vec{y}_r, \vec{y}_s; f_k) = (2\pi f_k)^4 \sum_{\nu=1}^{\infty} \sum_{\mu=1}^{\infty} \chi_{\nu\mu}^{(1)} \chi_{\nu\mu}^{(2)} \cdot$$

$$\cdot |P_k(\vec{x})| \cdot |P_k(\vec{x}')| \tag{120}$$

where the functions $\chi_{\nu\mu}^{(1)}$ and $\chi_{\nu\mu}^{(2)}$ are defined as follows:

$$\chi_{\nu\mu}^{(1)} = \frac{1}{k_\nu k_\mu} \cdot |H_\nu(f_k)|^2 \cdot |H_\mu(f_k)|^2 \cdot \phi_\nu(\vec{x}) \phi_\nu(\vec{y}_r) \phi_\mu(\vec{x}') \phi_\mu(\vec{y}_s) \tag{121}$$

$$\chi^{(2)}_{\nu\mu} \quad \mathcal{R}\left[H_\nu(f_k)\ H^*_\mu(f_k)\right] \cos\left[\phi_k(\vec{x}) - \phi_k(\vec{x}')\right]$$

$$+ \mathcal{I}\left[H^*_\nu(f_k)\ H_\mu(f_k)\right] \sin\left[\phi_k(\vec{x}) - \phi_k(\vec{x}')\right] \tag{122}$$

It is to be noted that when $\nu = \mu$, the second term in Equation 122 is equal to zero. By using Equations (119) - (122), Equations (111) and (113), the mean-square response at a point on the structure and the crosscorrelation of responses between two points on the structure, can be expressed in terms of normal modes of the structure.

DISTRIBUTED RANDOM EXCITATION

The analysis developed above for distributed pressures at discrete frequencies can be extended to the case of distributed randomly varying pressures acting over the whole surface area A of a complex structure. The preceding section on point force random excitation contains all of the necessary development for determining the important quantities and parameters necessary for describing the response of a structure to distributed loadings. To accomplish this transition, replace the point random forces $F_n(t)$ which are applied at the points x^*_n by their equivalent pressures $P(x^*, t)\, dA(\vec{x})$, where $dA(x^*)$ denotes an incremental area over which the pressure acts. The surface area A is represented by zones or area segment A_n. Thus, the equation for the acceleration response $\ddot{W}_r(t)$ at a point $\vec{y}_r$ can be obtained from a form of Equation (34) by an integration over each area segment A_n and, then, a summation over the N area segments,

$$\ddot{W}_r(t) \quad = \sum_{n=1}^{N} (2\pi f)^2 \int_{A_n} \int_0^\infty h(x^*, y^*_r; \tau)\ P(x^*, t-\tau)\, d\tau\ dA(x^*). \tag{123}$$

The autocorrelation function $\Gamma_r(\tau)$ of the response $\ddot{W}_r(t)$ can be defined in a manner similar to the development of Equation (58), hence, the equation

$$\Gamma_r(\tau) = \overline{\ddot{W}_r(t)\ \ddot{W}_r(t+\tau)}$$

$$\Gamma_r(\tau) = \sum_{m=1}^{N}\sum_{n=1}^{N}(2\pi f)^4 \int_{A_n}\int_{A_m}\int_{0}^{\infty} h(\dot{x},\dot{y}_r;\tau_1)\int_{0}^{\infty} h(\dot{x}^{-1},\dot{y}_r;\tau_2)$$

$$\cdot P(\dot{x},t)\,P(\dot{x}^{-1},t+\tau_1-\tau_2+\tau)\,d\tau_2 d\tau_1 dA(\dot{x})dA(\dot{x}^{-1}). \qquad (124)$$

And, the spectral density $S_r(f)$ of $\ddot{W}_r(t)$ is defined, from Equation (33), as the equation

$$S_r(f) = 2\int_{-\infty}^{\infty}\Gamma_r(\tau)\,e^{-i2\pi f\tau}\,d\tau$$

$$= \sum_{m=1}^{N}\sum_{n=1}^{N}\int_{A_n}\int_{A_m}(2\pi f)^4\int_{0}^{\infty} h(\vec{x},\vec{y}_r;\tau)e^{i2\pi f\tau_1}\,d\tau_1$$

$$\cdot\int_{0}^{\infty} h(\vec{x}',\vec{y}_r;\tau_2)\,e^{-i2\pi f\tau_2}\,d\tau_2 \cdot$$

$$\cdot 2\int_{-\infty}^{\infty} P(\vec{x},t)\,P(\vec{x}',t+\tau_1-\tau_2+\tau)\,e^{-i2\pi f(\tau_1-\tau_2+\tau)}\,d(\tau_1-\tau_2+\tau)\cdot$$

$$\cdot\, dA(\vec{x})\,dA(\vec{x}')$$

$$S_r(f) = \sum_{m=1}^{N} \sum_{n=1}^{N} \int_{A_n} \int_{A_m} a^*(\vec{x}, \vec{y}_r; f)\, a(\vec{x}', \vec{y}_r; f) \cdot S(\vec{x}, \vec{x}', f)\, dA(\vec{x})\, dA(\vec{x}') \qquad (125)$$

Thus, the mean-square acceleration response becomes

$$\overline{\dot{W}_r^2(t)} = \int_0^{\infty} S_r(f)\, df \qquad (126)$$

Equations (124) and (125) are general expressions for the autocorrelation $\Gamma_r(\tau)$ and spectral density $S_r(f)$ of the response $\ddot{W}_r(t)$ of a point $\vec{y}_r$ due to N distributed loadings over the area segments A_n.

Equation (125) can be written in terms of the normal mode shapes $\phi_q(\vec{x})$ of the entire complex structure. In this case the transfer function $a(\vec{x}, \vec{y}_r; f)$ can be written as

$$a(\vec{x}, \vec{y}_r; f) = \sum_{q=1}^{\infty} a_{qr}(f)\, \phi_q(\vec{y}_r)\, \phi_q(\vec{x}),$$

where $a_{qr}(f)$ is the generalized transfer function of the q-th mode, $\phi_q(\vec{y}_r)$ is the q-th modal deflection of $\vec{y}_r$ and $\phi_q(\vec{x})$ is the q-th normal mode of the structure. Hence, Equation (125) becomes

$$S_r(f) = \sum_{q=1}^{\infty} \sum_{j=1}^{\infty} \sum_{m=1}^{N} \sum_{n=1}^{N} a^*_{qr}(f)\, a_{jr}(f) \cdot$$

$$\cdot \phi_q(\vec{y}_r)\, \phi_j(\vec{y}_r) \int_{A_n} \int_{A_m} S(\vec{x}, \vec{x}'; f)\, \phi_q(\vec{x})\, \phi_j(\vec{x}') \cdot$$

$$\cdot dA(\vec{x})\, dA(\vec{x}') \,. \qquad (127)$$

Note that the integrations in Equation (127) are only over the area segments A_n, which are in the q-th mode of the entire complex structure. The integrations are then summed over the N area segments for each of the q normal modes and then the q modes are summed.

Now, the crosscorrelation $\Gamma_{rs}(\tau)$ of the responses $\ddot{W}_r(t)$ and $\ddot{W}_s(t)$ at $\vec{y}_r$ and $\vec{y}_s$ is obviously, from Equation (124)

$$\Gamma_{rs}(\tau) = \overline{\ddot{W}_r(t)\,\ddot{W}_s(t+\tau)}$$

$$\Gamma_{rs}(\tau) = \sum_{m=1}^{N}\sum_{n=1}^{N} (2\pi f)^4 \int_{A_n}\int_{A_m} \int_0^\infty h(\vec{x},\vec{y}_r;\tau_1) \int_0^\infty h(\vec{x}',\vec{y}_s;\tau_2) \cdot$$

$$\cdot P(\vec{x},t)\,P(\vec{x}',t+\tau_1-\tau_2+\tau)\,d\tau_2\,d\tau_1\,dA(\vec{x})dA(\vec{x}'), \qquad (128)$$

and, also, the cross-spectral density $S_{rs}(f)$ is defined, from Equation (125), as

$$S_{rs}(f) = 2\int_{-\infty}^{\infty} \Gamma_{rs}(\tau)\,e^{-i2\pi f\tau}\,d\tau$$

$$\sum_{m=1}^{N}\sum_{n=1}^{N} \int_{A_n}\int_{A_m} a^*(\vec{x},\vec{y}_r;f)\;a(\vec{x}',\vec{y}_s;f)\cdot$$

$$\cdot S(\vec{x},\vec{x}';f)\;dA(\vec{x})\;dA(\vec{x}')\,. \qquad (129)$$

Equation (129) can also be written in terms of the normal mode shapes $\phi_q(x)$ as the equation

$$S_{rs}(f) = \sum_{q=1}^{\infty} \sum_{j=1}^{\infty} \sum_{m=1}^{N} \sum_{n=1}^{N} a^*_{qr}(f)\, a_{js}(f) \cdot$$

$$\cdot \phi_q(\vec{y}_r)\, \phi_j(\vec{y}_s) \int_{A_n} \int_{A_m} S(\vec{x}, \vec{x}'; f)\, \phi_q(\vec{x})\, \phi_j(\vec{x}')\ dA(x)\, dA(x') \quad (130)$$

Response of a Beam to Distributed Loading

Consider a uniform beam of length L, excited by a distributed pressure loading of intensity $P(\vec{x},t)$ per unit length. The acceleration response $\ddot{W}_1(t)$ at a point $\vec{x}$ on the beam, which is in its first normal mode $\phi_1(\vec{x})$ only, subject to the distributed loading $P(x,t)\, dL(x)$, is written

$$\ddot{W}_1(t) = \int_0^L -(2\pi f)^2 \int_0^{\infty} h(\vec{x}, \vec{x}_1; \tau)\, P(\vec{x},\ t-\tau)\, d\tau\ dL(x) \quad (131)$$

The spectral density $S_1(f)$ of the response in the first mode from Equation (127), is

$$S_1(f) = \left|a_{11}(f)\right|^2 \phi_1{}^2(\vec{x}_1) \int_0^L \int_0^L S(x, \vec{x}'; f)\ \phi_1(\vec{x})\, \phi_1(\vec{x}')\, dL(\vec{x})\, dL(\vec{x}') \quad (132)$$

where $S(\vec{x}, \vec{x}'; f)$ is the cross-spectral density of the pressures at $\vec{x}$ and $\vec{x}'$, $a_{11}(f)$ is the generalized transfer function of the first mode, $\phi_1(\vec{x}_1)$ is the modal deflection at $\vec{x}_1$ and $\phi_1(x)$ is the first normal mode shape of the beam.

Now, the double integral over the length L of the beam from Reference 2 is of the form

$$S_p(f)L^2 j_{11}^2(f) = \int_0^L \int_0^L S(\vec{x},\vec{x}';f)\,\phi_1(\vec{x})\,\phi_1(\vec{x}')\,dL(\vec{x})\,dL(\vec{x}') \qquad (133)$$

where $S_p(f)$ is the spectral density of the pressures and $j_{11}^2(f)$ is the "joint acceptance squared" of the first beam mode $\phi_1(\vec{x})$ subjected to the distributed pressures $P(\vec{x},t)$. Therefore, substitution of Equation (133) into Equation (132) gives

$$S_1(f) = \phi_1^2(\vec{x}_1)\left|a_1(f)\right|^2 L^2 S_p(f)\, j_{11}^2(f) \cdot \qquad (134)$$

SECTION IV

GENERAL METHODS FOR EMPIRICAL CORRELATIONS

BACKGROUND

The process of empirical correlation of vibration or other data generally begins with the comparison of the data found for specified conditions on one or more flight vehicles. If these data show any degree of similarity, or can be normalized to show similarities, the engineer is encouraged to utilize them as a predictive tool for a future vehicle. Correlations of this type have been made throughout engineering history, and though a rational basis for their use is not always easily found, they have often been extremely useful and surprisingly accurate. As a result, one might question the real reasons behind the applicability of the empirical correlation technique to many diverse vehicles.

In the examination of data from single engine fighter aircraft, multi-engine bombers, and launch vehicles for space flight, Reference 3 , one can find many similarities despite the gross apparent differences in the structural types. The existence of these similarities suggests that many structural types, even though radically different in geometry and other apparent design factors, do possess certain properties which have statistical similarity. Perhaps the most readily identifiable of these properties is the high-frequency input impedance of complex structures which tends to be purely resistive as the structure begins to behave as a transmission line. Preliminary investigations suggest that the application of the model scale laws, modified by consideration of the volumetric density, will enable direct comparison of data over a wide range of vehicle types. In fact, comparison of the input impedances of a submarine and Snark fuselage appear to correlate well when adjusted for these deterministic parameters.

It is important to recognize that the validity of an empirical correlation, particularly when the correlation is to be utilized as a predictive tool for a future vehicle, is entirely dependent on the statistical similarity of those structural properties which are

significant to vehicle vibration. Therefore, any correlation of structural vibration which accounts for the gross structural parameters, at least in terms of the model scale laws, volumetric density and dynamic magnification factor, is applicable to other vehicles as long as their structures actually exhibit similar properties. Thus, empirical correlations may often be applied to a great variety of geometrical configurations.

The next subsections will review two of the simpler correlations which have been made in the past and are followed by the development of a general method for empirical correlation.

Direct Correlation of Noise and Adjacent Structural Vibration in Aircraft. *

One approach to the correlation of vibration response of aircraft with external noise has been suggested previously by Convair in References 4 - 6 . This correlation was obtained by direct comparison of the external sound pressure level on the B-58 resulting from jet engine noise with the vibratory response of adjacent internal structure. Thus, vibration measurements in the nose of the aircraft were compared directly to sound pressure levels measured on the external skin of the nose section, and vibration measurements in the aft end of the aircraft were compared to sound pressure levels measured on the external skin of the aft section, etc. Since the external noise environment on the B-58 and other types of jet aircraft varies considerably from the relatively low noise levels forward to the very high levels toward the aft end, a comparison of this type includes a range of external noise levels of the order of approximately 30 db.

A similar comparison of external noise and internal vibration from Snark data in References 7 and 8 is given for two frequency bands in Figure 12 . The lower pressure levels and their associated vibration data are obtained at forward fuselage

* Taken from Reference 3.

stations, and the higher sound pressure levels and the associated vibration data are obtained at aft fuselage stations adjacent to the rocket booster exhaust. It should be noted that the small variations in sound pressure level at one microphone position result from data of repeated firings and that the acceleration data include some from transducers attached to airplane structure and oriented in various directions.

As might be expected, the data exhibit considerable scatter, so that it is possible only to estimate a trend through the points; however, more significant than the scatter, is the slope of the trend line. Note that if the acceleration amplitude increases by a factor of 10 for an increase of 20 db spl, a direct linear relationship exists between the internal structural vibration amplitude and the adjacent external sound pressure amplitude. In this event, the trend line through the data gives a constant of proportionality between external sound and internal vibration. However, if the trend line has a slope of less than unity, as is the case of the low-frequency data of Figure 12, a direct linear relationship between internal vibration and adjacent external sound pressure cannot be proved by the correlation.

Several factors might, individually or collectively, be responsible for slopes less than unity. These factors include:

1. Structure borne transmission of vibration from high external noise level areas to those of lower external noise level;
2. Nonuniform structure throughout the fuselage (which undoubtedly contributes to scatter);
3. Non linear response of the structure;
4. Unfortunate selection of transducer location with respect to model response.

Before considering any of these factors in more detail, it is helpful to examine the slopes of the trend curves as a function of frequency. Figure 13 summarizes the results of this type of direct correlation for four aircraft type structures, including

the B-66 of Reference 9 , together with Snark, B-58 and B-52. The upper portion of the figure gives the slopes of the trend curves and the lower portion gives the average rms acceleration for each octave band when the adjacent external octave band spl is 150 db. It is clear from Figure 13 that some correlation between adjacent external noise may exist above 150 cps for the Snark and at the higher frequencies for the other aircraft where the slopes of the trend curves approach unity. Since a large number of randomly selected transducer locations are included in the various surveys, it is doubtful that the accidental location of transducers with respect to the various vibration modes accounts for the lower slopes at the lower frequencies. Similarly, since several experiments give the same general conclusion with regard to the trend curves, it is not felt that structural nonuniformity is a particular factor in the determination of the slope of the trend curve, although it undoubtedly is a most significant factor in the scatter of the individual data.

The role of nonlinear behavior in the structure cannot be evaluated with respect to the trend curves from the available data; however, it is considered to be less important than the fact that the response at any general position in the structure is given by the sum of the noise energy transmitted directly to adjacent structure, plus the noise energy received at more remote locations and transmitted as vibratory energy through the structure to the position as illustrated in Equation (146) . Thus, at higher frequencies better correlation would be expected between adjacent acoustical excitation and response because the vibrational energy transmitted through the structure from remote locations has been significantly attenuated and makes only a minor contribution Conversely, at low frequencies the vibrational energy transmitted from the areas which have the highest external noise levels would be expected to exceed the local excitation. This general result might be anticipated since the attenuation of vibratory energy transmitted by bending waves along the fuselage is essentially constant per wave-length. Thus, the high-frequency energy suffers considerably more attenuation than does low-frequency energy when both are transmitted for the same distance through the fuselage.

Correlation of Ballistic Missile Launch Noise and Response *

The vibration data given in Reference 3 for structure located in the forward region of ballistic missiles during both launch and maximum dynamic pressure flight, consistently showed that the vibration environment of the large and heavy missiles was significantly less than the vibration of the smaller and lighter missiles. This suggests that the next generation of space vehicle launch platforms, which are anticipated to be considerably larger than the present ICBMs, might have even less severe vibration. On the other hand, changes in launch configuration, engine parameters, or maximum q could result in increases. It is, therefore, desirable to determine an empirical relationship between the response in forward structure and the forcing function, appropriately modified by the vehicle's structural parameters.

It is believed that an empirical correlation can be found by equating the available power of the forcing function with the mechanical energy stored in the vibratory system and power dissipated through damping. It is fundamental that these quantities are related since all of the incident acoustical power which is absorbed by the vehicle must result in vibration and be dissipated through damping.

For this special case, an alternative approach to the correlation of the launch acoustical forcing function with vehicle response appears to give encouraging results. It is well known that complicated (and even simple) structure has many resonances, distributed throughout the frequency range, which occur at frequencies above the fundamental resonant frequency. Consequently, the response of a structure to a random forcing function, which has energy approximately equally distributed over a broad frequency range, exhibits many resonant peaks. Similarly, the majority of the missile launch data in Figure 14 are representative of the vibration amplitudes associated with one or more of the many resonances which occur in the missile.

---

* Taken from Reference 3.

It is well known that the natural vibration characteristics of many complex structures can be approximated by individual consideration of each resonance or mode of vibration, assuming it to be essentially unaffected by, or decoupled from, any other mode. The response of the vehicle in any one of these modes can be obtained from expressions similar to those developed for the single degree of freedom if an appropriate definition can be obtained for the amount of the total mass which is involved in actual vibratory motion, and for the effective or "generalized force" on the vehicle. Viewed in this perspective, the total response of the vehicle at any location is simply the sum of the contributions from all of the vehicle's vibratory modes.

The mean square displacement response of a single degree of freedom system to a continuous random forcing function is given by:

$$\overline{x^2} = \frac{Q\,\omega_n\,\overline{F(f)^2}}{4k^2}$$

where

$\overline{x^2}$ is the mean square displacement

Q is one divided by twice the damping ratio

ω_n is the natural frequency in radians/second

$\overline{F(f)^2}$ is the mean square force per cycle/second

and

k is the stiffness of the system.

The mean square acceleration ratio $(a/g)^2$ associated with this response can be easily obtained from the Equation above:

$$\overline{\left(\frac{a}{g}\right)^2} = \frac{\omega_n Q \overline{F(f)^2}}{4W^2}$$

where

W is the weight of the mass.

In order to apply this simple concept of the single degree of freedom system to the empirical correlation of multimode missile vibration, it is necessary to consider the relationship between the generalized force and generalized mass of the vehicle with the single forcing function and single mass in the single degree of freedom solution. For example, the generalized force on a panel in a space vehicle resulting from acoustic excitation depends, in addition to the actual magnitude of the sound pressure, primarily upon the spatial correlation of the sound pressure, or the distances over which the pressure is in phase, in relationship to the distance between modes in the panel's bending response. It is also known that when acoustic phenomena are similar, except for a scale factor, their spatial correlations are similar when compared on a wave number basis. Here, the wave number (kr) is equal to the number of radians per unit distance ($\omega/c = k$) times a distance which is chosen to be characteristic of the size of the object or missile. For the purpose of this correlation, r is defined as the radius of the vehicle, and it is assumed that the spatial correlation is essentially similar at launch for geometrically similar vehicles and similar launch configurations when compared at equal values of kr.

Now, the natural frequency of any mode of two geometrically similar panels varies inversely with the ratio of the panel dimensions (or the scale factor). Consequently, since the distance between nodes on the panel varies directly with the scale factor, the relationship between the scaled spatial correlation of the sound pressure and the

scaled shape of the bending panel remains unaltered when compared on a constant kr basis. It can also be shown that the generalized mass of the scaled panel would be the same proportion of the total mass for the same mode of vibration. Hence, it would be expected that any empirical correlation for geometrically similar structures would be a function of kr and that for this purpose the previous equation should be written

$$\overline{\left(\frac{a}{g}\right)^2} = \frac{\beta^2 \omega_n Q \overline{F(f)^2}}{4 W^2}$$

where

β represents the constant of proportionality and is assumed to be a function of kr.

It is clear that both the damping in the structure and the type of structure will affect any correlation of response with forcing function, as both additional damping or additional stiffness in a specific vehicle will reduce the response for a fixed forcing function. Therefore, in absence of sufficient data describing these two factors for the data of various missiles in Reference 3, a constant Q of 15 was assumed for all missiles and all natural frequencies. The missile weight (W) was taken as the gross launch weight, but the stiffness variable remains in the correlation as an additional unknown.

The forcing functions were calculated for surface launch of each of the eight missiles represented in Figure 14 using Figures 8 and 13 from Reference 3 together with the appropriate engine parameters, to define the external noise environment. The estimated value of mean square force per cps was obtained by determining the space average of the predicted mean square pressure per cps on the vehicle and multiplying this result by the square of the vehicle's surface area.

Thus

$$\overline{F(f)^2} = A_t \int_{A_t} \overline{p^2}\, dA$$

where A_t is the total surface area. It is obvious that this quantity cannot represent the true generalized force on the vehicle, but it should be proportional to the genera force for constant values of kr.

A value of β was determined for each of the (a/g) data points in Figure (14). The results are given as a function of kr in Figure 15 . β appears to be almost constant, slowly decreasing with increasing wave number. The standard deviation of 20 log β is approximately 6 db, which indicates that 68 percent of the values of β are between 0.5 and 2.0, as seen in the histogram of Figure 16 . Although it would be desirable to effect a reduction in the scatter of the values for β, it is actually somewhat surprising that the scatter is so small when all the assumptions are considered. Several comments are pertinent, including:

- First it is improbable that all of these missiles are dynamically similar, since a wide variety of structural design concepts are represented.

- Second, the forcing functions have been estimated through necessity, as insufficient measured launch noise data has been made available. While it might be thought that the use of an estimator rather than measured data would help to insure consistency, the estimation did not consider minor and largely unknown variations in rocket deflectors and other configuration details.

- Third, the assumption of constant C for all missiles and all frequencies adds to the deviation.

- Fourth, it is well known that the launch noise environment has a relatively short duration and that the response cannot be considered stationary from the

statistical viewpoint. Consequently, variation in response can be expected at the same location for different launches or short duration engine runups.

- Fifth, the scatter at various transducer locations and various flights of one missile is seen to be almost as great as the total scatter in the figure.

When these and other factors are considered, the results of this correlation are encouraging. Perhaps the most startling result is the fact that the mean value of β is approximately one, as in the single degree of freedom case. This indicates that the ratio of force to total vehicle mass remains constant with wave number and that the method of obtaining the forcing function used for the correlation fortuitiously gives the ratio exactly equivalent to the single degree of freedom case.

It would be highly desirable to test this empirical correlation with additional data and, wherever possible, to use measured launch noise data in the comparison. It would be desirable also to test an extension of these concepts to the maximum dynamic pressure portion of flight; however, the necessary flight parameters were not available for such an extension. In lieu of this test, it appears that the value of β in Figure 16 could be used at a desired confidence level, together with the boundary layer pressure fluctuation forcing function in Section 3, Part I of Reference 3 to estimate this response.

ENGINEERING MODEL FOR EMPIRICAL CORRELATIONS

For a linear structure, the mean-square acceleration response at a point can be determined exactly from Equations (125)and (126) for any distribution of random pressures. In order to evaluate these expressions, it is necessary to know the cross-spectral density $S(\vec{x}, \vec{x}'; f)$ of the pressures between any two points $\vec{x}, \vec{x}'$ where fluctuating pressures are applied, and to know the force-to-acceleration transfer function $\alpha(\vec{x}, \vec{y}_r'; f)$ between each point $\vec{x}$ where pressure is applied and the point $\vec{y}_r$ where vibration response is being considered. Alternatively, the pressure crosscorrelation $r(\vec{x}, \vec{x}'; \tau)$ and the unit impulse response $h(\vec{x}, \vec{y}_r; \tau)$ can be known and the pressure cross-spectral density and the transfer function can be obtained by use of the Fourier transform integrals of Equations (39) and (35).

The transfer functions are readily obtained in terms of normal modes of the structure when the structure is elementary, such as a uniform beam; and in such cases, Equation (125) can be readily evaluated when the pressure field is known, or can be determined, in terms of the pressure cross-spectral densities. However, for complex flight vehicle structures, the transfer functions are not known as continuous functions of frequency or as continuous functions of position $\vec{x}$ on the skin for any other point $\vec{y}_r$ on the structure. Furthermore, the cross-spectral densities of pressure are not known accurately for all pairs of points on the skin. Thus, in its exact form, Equation (125) is not a practical engineering tool for predicting the vibration response of a complex structure, nor is it practical to use for empirical correlation. Equation (125) can be useful, however, if approximations are introduced based on certain knowledge of the pressure field and of the acceptance and transmission characteristics of flight vehicle structures.

Vehicle Surface Area Segmentation

In developing Equation (125), the spatial integrations of the pressure spectral densities and transfer functions were taken over area segments as shown in Figure 11 . A typical term in this equation for which $m = n$ involves integration over a single area segment A_n; and this term is equal to the component of mean-square acceleration response at $\vec{y}_r$ due to pressure excitation over the area A_n. If there are N such area segments, then there are N components of mean square response at $\vec{y}_r$ due to excitation over each of the segments; and as seen in Equation (125), the mean-square response components are summed linearly. In addition there are $N^2 - N$ terms for which $m \neq n$; and a typical term is equal to the crosscorrelation of the two response components at $\vec{y}_r$ due to excitation over the area segments A_m and A_n. The integrations were performed in this manner in order to account more easily for pressure gradients over the skin, and to take advantage of possible small crosscorrelations of the excitations over different areas and small crosscorrelations of the response of different structural transmission paths.

The significant sources of excitation for flight vehicles are the noise emanating from the engine exhaust and aerodynamic pressure fluctuations due to boundary layer turbulence, separated flow and oscillating shocks. The amplitudes of these pressures have significant gradients over the vehicle surface; and the regions of high amplitude pressures depend upon the locations of the engines and locations of aerodynamic discontinuities. For example, in long slender vehicles having engines at the aft end, the sound pressure levels may be significantly lower at the nose of the vehicle than at the aft portions. For aircraft with wing mounted engines, the regions of highest excitations occur on those portions of the fuselage nearest the exhaust stream. In the case of aerospace vehicles, localized excitation can occur at the nose due to turbulence and at aerodynamic discontinuities, where two stages are joined, due to separated flow and oscillating shocks. If the sizes

of the surface area segments are properly chosen, the pressure level gradient can, in some cases, be neglected over a given area segment. In other cases, such as oscillating shocks, the area segments may be chosen as those areas over which the shocks produce significant pressure fluctuations.

Segment Size Based on Pressure Correlation Length

Exhaust noise and aerodynamic pressure fluctuations are known to be random phenomena having limited spatial correlation, where the crosscorrelation of the pressures at two points decreases as the distance between the two points increases. Thus if two points are sufficiently separated, the random pressures at the two points will be almost statistically independent which results in effectively no crosscorrelation and a very small cross-spectral density. From this standpoint, if the areas are chosen large enough, the effective pressure correlation lengths will be of the order of or less than the dimensions of the area segments. With such a choice, the pressures over different area segments could be considered uncorrelated so that all cross-spectral densities between pressures on different area segments could be neglected. The result would be that all crosscorrelation terms, for which $m \neq n$, in Equation (125) would be negligibly small; and the net response at point $\dot{y}_r$ would be the summation of the mean square responses due to excitation over each of the area segments A_n.

If the surface area is to be segmented on the basis of correlation lengths, then the size of the areas will depend upon the type of excitation, frequency of the excitation, and bandwidth. Measured data show that acoustic correlation lengths are dependent upon wave-length in the sense that there is a certain loss of cross-correlation of pressures at two points for each wavelength of separation of the points. Acoustic wave lengths at low frequencies can be of the order of the length of a flight vehicle, so that in narrow bandwidths at low frequencies the

acoustic pressures are well correlated over large surface areas of the vehicle. At these frequencies, the above correlation criteria for segmenting the surface might lead to only a few area segments. At higher frequencies however, the shorter wave lengths are associated with shorter correlation lengths and hence, smaller correlation areas. Thus the higher the frequency, the smaller these area segments can become, and the larger the number of area segments which have zero crosscorrelation of pressures. Correlation lengths also shorten as the bandwidth increases since the pressure signals tend more toward white noise signals. This is shown in Appendix B where the autocorrelation of bandwidth limited white noise is discussed. The delay time τ in the autocorrelation function is equal to the distance of separation of two points divided by the speed of propagation of the sound waves when the points lie along a line parallel to the direction of propagation. In the limit, if all frequencies were considered simultaneously, it would be found that the correlation lengths would become variably small. Correlation lengths for aerodynamic pressure fluctuations are very short compared with acoustic correlation lengths, since they are of the order of the scale of the turbulent eddies in the turbulent boundary layer and separated flows. Thus for all except the very low frequency acoustic excitations the surface area of the vehicle can logically be subdivided into zones over each of which the pressure amplitudes can be considered constant, and between which these fluctuating pressures can be considered uncorrelated so as to have zero valued cross-spectral densities.

Segment Size Based on Structural Correlation Length

Pressure correlation length and pressure gradient are not the only bases for choosing the sizes of the area segments. Vibrating energy transmitted along a complex structural path experiences filtering and phase shifting which varies with frequency; and two structure transmission paths within the structure can have quite different dynamical characteristics. Random excitation supplied at two different points on the structure will follow two different transmission paths in arriving at a

single point within the structure. If the two paths have quite different detailed dynamical characteristics, then the two response components at the single point could be partially correlated, or nearly uncorrelated, even though the two applied excitations are well correlated. The dynamical similarity of two transmission paths which slant to two different points and end at a common point depends in general upon the spatial separation of the two starting points, and the frequency and bandwidth of the excitation. Generally, this similarity decreases with increasing distance between the starting points, with increasing frequency and with increasing bandwidth. In this sense, the crosscorrelations of responses along two structural transmission paths have characteristics which are similar to the crosscorrelations of the applied random pressures.

Regular structures respond primarily in well defined modes of vibration, and the correlations of responses at a point due to inputs at two different points may be well correlated if the inputs are correlated. In a complex structure, the response paths are much more complex; however, the lack of crosscorrelation between responses along two paths represents a significant simplification. Thus the surface area segments can also be chosen on the basis of structural correlation lengths so that the crosscorrelation response terms in Equation (125) can be neglected. It is to be noted that the structural correlation lengths may be shorter than the pressure correlation lengths, such as in the case of a stiffened cylinder or stiffened panel excited by acoustic waves where the distances between stiffeners is much less than the wave length of the sound waves.

Response Spectral Density with Crosscorrelation Terms Neglected

Based on the above comments, it is reasonable to assume that Equation (125) for the response spectral density can be written in the simpler form

$$S_r(f) \quad \sum_{n=1}^{N} \int_{A_n} \int_{A_n} a^*(\vec{x}, \vec{y}_r; f)\ a(\vec{x}', \vec{y}_r; f)\ S(\vec{x}, \vec{x}'; f)\, dA(\vec{x})\, dA(\vec{x}') \qquad (135)$$

The two integrations in Equation (135) are taken over a common area segment A_n shown in Figure (11); and the resulting term in Equation (135) is equal to the acceleration response spectral density at $\vec{y}_r$ due to fluctuating pressure excitation over the area A_n. The net spectral density of response at $\vec{y}_r$ is then the summation of such response spectral density components over all N area segments.

Before proceeding, it should be noted that for a given frequency and bandwidth, the area segments chosen will in general be different for different types of excitation; and hence, separate analyses should be conducted for exhaust noise and for aerodynamic pressure fluctuations.

It is assumed now that the area segments have been so chosen that the pressure spectral density at a given frequency is constant over each area segment. Denoting the pressure spectral density over A_n as $S_n(f)$, Equation (135) can be written in the form

$$S_r(f) \quad \sum_{n=1}^{N} S_n(f) \int_{A_n} \int_{A_n} a^*(\vec{x}, \vec{y}_r; f)\ a(\vec{x}', \vec{y}_r; f)\ C(\vec{x}, \vec{x}'; f)\, dA(\vec{x})\, dA(\vec{x}') \qquad (136)$$

where $C(\vec{x}, \vec{x}'; f)$ is a spatial correlation coefficient of the applied pressures which has a maximum absolute value of unity. This correlation coefficient which

is defined by the equation

$$C(\vec{x}, \vec{x}';f) \qquad \frac{S(\vec{x}, \vec{x}';f)}{S_n(f)} \tag{137}$$

is equal to unity where $\vec{x} = \vec{x}'$ and is approximately equal to zero when $\left| \vec{x} - \vec{x}' \right|$ is large. A typical variation of $C(\vec{x}, \vec{x}';f)$ with separation distance $\left| \vec{x} - \vec{x}' \right|$ for a homogeneous pressure field is given by the exponentially damped cosine function,

$$C(\vec{x}, \vec{x}';f) = e^{-\left| \vec{x} - \vec{x}' \right| \cdot d(f)} \cos k(f) \cdot \left| \vec{x} - \vec{x}' \right| \tag{138}$$

where the constants $d(f)$ and $k(f)$ are frequency dependent. For a plane wave acoustic field at frequency f, the constant $d(f)$ is equal to zero and $k(f)$ where c is the velocity of propagation of the waves in the direction of the vect $\vec{x} - \vec{x}'$.

The double area integral in Equation (135) is of the form of the square of an average force-to-acceleration transfer function between the area A_n and the point $\vec{y}_r$. This can be seen by noting that $S_n(f)\, dA(\vec{x})\, dA(\vec{x}')$ has the units of $(\text{force})^2/\text{cps}$, $S_r(f)$ has the units of $(\text{acceleration})^2/\text{cps}$, and by comparing Equation (135) with the definition of the transfer function given in Equation (Thus if $\overline{a_n(\vec{y}_r;f)}$ denotes this average transfer function at frequency f, then th acceleration response spectral density becomes

$$S_r(f) = \sum_{n=1}^{N} A_n^2 \, \overline{a_n^2(\vec{y}_r;f)} \, S_n(f) \tag{139}$$

where

$$a_n^2(y_r;f) \quad \frac{1}{A_n^2} \int_{A_n} \int_{A_n} a^*(\vec{x},\vec{y}_r;f)\, a(\vec{x}',\vec{y}_r;f)\, C(\vec{x},\vec{x}';f)\, dA(\vec{x})\, dA(\vec{x}') \qquad (140)$$

The Average Transfer Function in Terms of Frequency Bands

For elementary structures having pressure fields which can be defined in terms of the correlation coefficient $C(\vec{x},\vec{x}';f)$, the average transfer function $\overline{a_n(\vec{y}_r;f)}$ can be determined in terms of normal modes of the structure. For coupled structure this average transfer function can only be determined experimentally. Average transfer functions of this type were determined experimentally for the Snark missile as reported in Reference (12). Measured vibration data are usually taken in frequency bands, such as 1 3 - octave bands, and it is of interest to develop an expression for the mean-square acceleration response in such frequency bands. Let $\overline{\ddot{W}_r^2(\vec{y}_r;f_c,\Delta f)}$ denote the mean-square acceleration response at the point $\vec{y}_r$ in the frequency band Δf centered on the frequency f_c. The mean-square response is given by the equation

$$\overline{\ddot{W}_r^2(\vec{y}_r;f_c,\Delta f)} \quad \int_{f_L}^{f_U} S_r(f) \cdot df \qquad (141)$$

where f_L and f_U denotes the lower and upper frequency limits of the band ($\Delta f \quad f_U - f_L$). If the pressure spectral density $S_n(f)$ is reasonably constant over the frequency band Δf, and if $S_n(f_c,\Delta f)$ denotes the average value of $S_n(f)$ in this band, then substitution of Equation (139) into (141) gives

$$\overline{\ddot{W}_r^2(y_r;f_c,\Delta f)} \quad (\Delta f) \sum_{n\ 1}^{N} A_n^2\, \overline{\overline{a_n^2(y_r;f_c,\Delta f)}} \cdot S_n(f_c,\Delta f) \qquad (142)$$

where the quantity $\overline{\overline{a_n^2(\vec{y}_r; f_c, \Delta f)}}$ is the space average and frequency average value of the transfer function between the area A_n and the point $\vec{y}_r$; and this quantity is defined by the equation

$$\overline{\overline{a_n(\vec{y}_r; f_c, \Delta f)}} \quad \frac{1}{\Delta f} \int_{f_L}^{f_U} \overline{a_n^2(\vec{y}_r; f)}\, df \tag{143}$$

Equation (142) has a more useful form for practical engineering application than its exact counterpart given by the expression immediately following Equation (126). The only assumptions that have been made in developing Equation (142) are that the pressure spectral densities are constant over each of the surface area segments A_n, and that the sizes of the area segments were so chosen (for the frequency band Δf centered on frequency f_c) that either pressures acting on the surface are uncorrelated between different segments A_m and A_n $(m \neq n)$ or the responses at $\vec{y}_r$ due to excitations over different area segments are uncorrelated.

Approximation Formula for the Average Transfer Function

At the present state-of-the-art, however, it is necessary to approximate the average transfer function $\overline{\overline{a_n^2(\vec{y}_r; f_c, \Delta f)}}$. To shorten the notation let this average transfer function be denoted by the symbol $\overline{\overline{a_n^2}}$. In order to arrive at a reasonable engineering model for representing $\overline{\overline{a_n^2}}$ the structural transmission path will be assumed to be made up of three series of elements as shown in Figure (12). The first element represents the acceptance by the structure of the incidence surface pressures and if a mean square force $\overline{F_n^2(t)}$, having a constant spectral density, is applied over the area A_n, then the mean-square acceleration response of the surface structure will be denoted by the quantity

$$\overline{\overline{\beta_n^2(f_c, \Delta f)}} \cdot \overline{F_n^2(t)}$$

where $\overline{\overline{\beta_n^2}}$ is a space average and frequency average transfer function of the surface structure over A_n. The quantity $\overline{\overline{\beta_n^2}}$ contains the effect of joint-acceptance of skin panels at the surface of the vehicle. The second element in the series denotes the transmission of this vibratory motion from the area A_n to the region of the point $\vec{y}_r$; and the output of this element is denoted by

$$\overline{\gamma_{nr}^2(f_c, \Delta f)} \cdot \overline{\overline{\beta_n^2}}(f_c, \Delta f) \cdot \overline{F_n^2(t)}$$

Thus the acceleration-to-acceleration transfer function $\overline{\gamma_{nr}^2}$ gives the ratio of the mean-square response "in the neighborhood" of $\vec{y}_r$ to the mean-square acceleration response "in-the-neighborhood" of A_n. Experiments on the fuselage of the Snark missile, as reported in Reference (12) show that $\overline{\gamma_{nr}^2}$ can be approximated by an exponential decay function with distance along the structure as the argument of the function. Thus

$$\overline{\gamma_{nr}^2(f_c, \Delta f)} \approx e^{-\left| \vec{x}_n - \vec{y}_r \right| \delta(f_c, \Delta f)} \qquad (141)$$

where $\vec{x}_n$ in this equation denotes a position of a representative point within the area A_n. The quantity $\delta(f_c, \Delta f)$ is a constant which depends upon bandwidth and frequency. The final element shown in Figure (17) denotes the acceptance of structurally transmitted energy by a "receiving" element which may be a structural component or a piece of equipment. Letting $\overline{\psi_r^2}(f, \Delta f_c)$ denote the acceleration-to-acceleration transfer function at the "receiver", the mean-square acceleration response of the receiver is

$$\overline{\psi_r^2(f_c; \Delta f)} \cdot \overline{\gamma_{nr}^2(f_c, \Delta f)} \cdot \overline{\overline{\beta_n^2}}(f_c, \Delta f) \cdot \overline{F_n^2(t)}$$

It follows that the average transfer function $\overline{\overline{a_n(\vec{y}_r; f_c, \Delta f)}}$ can be approximated by the product

$$\overline{\overline{a_n(\vec{y}_r; f_c, \Delta f)}} \equiv \overline{\overline{\beta_n^2(f_c, \Delta f)}} \cdot \overline{\gamma_{nr}^2(f_c, \Delta f)} \cdot \overline{\psi_r^2(f_c, \Delta f)} \qquad (145)$$

$\overline{\overline{\beta_n^2(f_c, \Delta f)}}$ — space average, frequency average force-to-acceleration acceptance function

$\overline{\gamma_{nr}^2(f_c, \Delta f)}$ — frequency average, acceleration-to-acceleration transmission function

$\overline{\psi_n^2(f_c, \Delta f)}$ — frequency average acceleration-to-acceleration receiver function

where $\overline{\gamma_{nr}(f_c, \Delta f)}$ is given approximately by Equation (144).

Substituting Equations (145) into (142) gives the final approximate expression for the mean-square response in a given frequency band in terms of the acceptance, transmission and receiver functions:

$$\overline{\ddot{W}_r^2} = \sum_{n=1}^{N} \overline{\overline{\beta_n^2}} \; \overline{\gamma_{nr}^2} \; \overline{\psi_r^2} \; \overline{\overline{F_n^2}} \qquad (146)$$

where

$$\overline{\ddot{W}_r^2} = \overline{\ddot{W}^2(y_r; f_c, \Delta_f)}$$

$$\overline{\overline{F_n^2}} = A_n^2 \cdot \Delta_f \cdot S_n(f_c, \Delta_f)$$

The quantity $\overline{\overline{F_n^2}}$ is the approximate mean-square force acting on the area segment A_n. All quantities in Equation (146) are averaged over the frequency band Δ_f whic has a center frequency f_c. The index n refers to applied excitation on the n-th compartment.

Determination of Transmission, Receiver, and Acceptance Functions

The separation of the transmission function $\overline{\gamma_{nr}^2}$ and the "receiver" function ψ_r^2 is in order to account for local structural parameters, such as local mass and stiffness, of the "receiver". In this connection a useful concept is obtained by dividing the structure into bays, as shown in Figure (18), letting $\overline{\gamma_{nr}^2}$ account for the average axial decay in response level between the region A_n where excitation is applied and the bay which contains the point $\vec{y}_r$, and denoting $\overline{\beta_n^2 \cdot \gamma_{nr}^2 \cdot F_n^2(t)}$ as an average response of the structure in the bay in which $\vec{y}_r$ is located. The product of this average bay response and the receiver function ψ_r^2 then gives the response of the particular structural or equipment component located at $\vec{y}_r$. Also shown in Figure (18) is a set of acceleration response points for various structural components along the axis of the vehicle, and it is seen that the response data are scattered about the exponential decay. The differerence between the exponential decay curve and each of these response points is accounted for by the receiver function

Experimentally, the functions $\overline{\overline{\beta_n^2}}$, $\overline{\gamma_{nr}^2}$, $\overline{\psi_n^2}$ can be determined by providing localized acoustic excitation to the vehicle skin in a manner similar to that done for the Snark in Reference (12) . For convenience, the vehicle can be segmented along the axis into structural zones; and for compartmented vehicles having bulkheads or other material structural divisions, these zones can be chosen as the compartments. Acoustic excitation could be applied to a portion of the skin of a single compartment and acceleration response measurements made at a number of points within the same compartment and in each of the other compartments. By averaging the mean-square acceleration responses within each of these compartments, an average response of each compartment could be obtained. The larger the number of points within the compartment and the wider the range of structural components considered, the more representative this average response will be.

When these average compartment responses, in a given frequency band, are plotted against axial distance along the vehicle, it will be found that the average acceleration amplitudes will decrease with distance from the compartment directly excited by sound. By fitting an exponential curve of the form given by Equation (141), to these data points, the parameter $\delta(f_c, \Delta f)$ in Equation (141) can be determined, and from this the transmission function $\overline{\gamma_{nr}^2}$ will be known from the directly excited bay to any other bay. Reporting this process by directly exciting each of the individual compartments and determining average responses for all compartments, the complete set of $\overline{\gamma_{nr}^2}(f_c, \Delta f)$ functions between the n-th and and r-th compartments can be determined. Clearly by use of filtered response data, the functions $\overline{\gamma_{nr}^2}$ can be obtained for each frequency band of interest. It has been tacitly assumed that the functions $\overline{\gamma_{nr}^2}$ are equal to unity; and in this sense, $\overline{\gamma_{nr}^2}$ represents the axial decay of average response amplitude between two different compartments.

An average acceptance function $\overline{\overline{\beta_n^2}}(f_c, \Delta f)$ can also be obtained, for the n-th compartment, from these measured data, since $\overline{\overline{\beta_n^2}}$ can be defined as the ratio of the average mean-square acceleration response in the compartment to the total mean-square excitation force acting on the surface area of that compartment. Here also $\overline{\overline{\beta_n^2}}$ can be determined for each frequency band of interest. For most vehicles, it can be assumed that if the excitation is applied to only a portion of the surface area of a given compartment, then, if this portion of surface structure directly excited is representative of the entire surface structure of the compartment, the acceptance function $\overline{\overline{\beta_n^2}}$ will be representative of that obtained for any other portion or the whole of the surface of the compartment.

It should be noted that the above definitions of the acceptance function $\overline{\overline{\beta_n^2}}$ and the transmission function $\overline{\gamma_{nr}^2}$ differ slightly from the original definitions which linked these functions directly to surface structure rather than to the structural zone or compartment. At the present state-of-the-art, however, these are reasonable first approximations of their more exact counterparts. As additional impedance data and other measured vibration response data are obtained, these functions can naturally be given more refined treatments.

The Significance of Local Structural Parameters

The difference between the mean-square response of a structural element and the average mean-square response of the bay in which the element is located is equal to the receiver function $\overline{\psi_i^2}(f_c, \Delta f)$ for that element. This function, which depends primarily upon local mass, stiffness and damping properties of the element, should be approximately the same for direct excitation of the compartment containing the element and excitation of any other compartment. At present, there is very little known concerning the distribution of energy throughout a complex structure, particularly within a localized region such as a compartment where local structural details significantly affect response amplitudes. In order to study this aspect of the structural vibration problem, statistical analyses can be made in which the receiver function $\overline{\psi_i^2}$ is correlated with such local structural parameters as mass, stiffness, length, characteristic or effective thickness for flexural vibrations of structural component, ratio of mass of component to mass of neighboring components, (similarly for stiffness ratios), curvature of element as in the case of skin panels, orientation relative to the primary direction of compartment excitation, frequency, bandwidth, and number of responses in a frequency band. Other significant local parameters may also become evident during such a statistical study. It is felt that a knowledge of such correlations would be of significant value in the development of an empirically based vibration response prediction technique.

By obtaining measured vibration data on a number of flight vehicles of the same class and of a number of different classes of vehicles, statistical analyses could be conducted to study the acceptance and transmission functions $\overline{\beta_n^2}$, $\overline{\gamma_{ni}^2}$. The functions could be correlated with more gross vehicle parameters such as mass, length, radius and average surface density of a compartment, overall length and weight of a vehicle, frequency, bandwidth, average damping, spatial correlation lengths for surface pressures, percent structural weight of total vehicle weight, etc.

Much could be learned from such statistical analyses of complex structures including the scaling laws which govern the response levels of different size but geometrically and dynamically similar vehicle structures. Scaling laws for exactly similar structures can be obtained easily from fundamental dynamics concepts; however, because of the interplay of the host of overall and local vehicle parameters, the exact elementary scaling laws provide only a first order approximation of the true scaling laws for complex structures.

Limitations on the Use of Flight Data

In general, measured excitation and response data from flights cannot be used direc to obtain the acceptance, transmission and receiver functions in Equation (146) since there is insufficient data for the number of unknown constants to be determined. To show this, let the subscript m denote points within the m-th compartment at which responses have been measured. Then the response at the r-th point in the m-th compartment is given by the expression

$$\overline{\ddot{w}_{rm}^2} \qquad \sum_{n=1}^{N} \overline{\overline{\beta_n^2}}\ \overline{\gamma_{nm}^2}\ \overline{\psi_{rm}^2}\ \overline{F_n^2} \qquad (147)$$

The acceptance function $\overline{\overline{\beta_n^2}}$ is associated with excitation over the n-th compartment; $\overline{\gamma_{nm}^2}$ is the fractional loss of mean-square acceleration response between the n-th and m-th compartments; $\overline{\psi_{rm}^2}$ is the receiver function for the r-th point in the m-th compartment; and $\overline{F_n^2}$ is the mean-square force acting on the m-th compartment.

Since $\overline{\psi_{rm}^2}$ is independent of the excitation, Equation (147) can be written as

$$\overline{\ddot{W}_{rm}^2} = \overline{\psi_{rm}^2} \sum_{n=1}^{N} \overline{\overline{\beta_n^2}}\ \overline{\gamma_{nm}^2}\ \overline{F_n^2} \tag{148}$$

Assume now that there are R measured responses at R different points in each compartment. The summation of the mean-square responses in the m-th compartment is

$$\sum_{r=1}^{R} \overline{\ddot{W}_{rm}^2} = \left[\sum_{r=1}^{R} \overline{\psi_{rm}^2}\right]\left[\sum_{n=1}^{N} \overline{\overline{\beta_n^2}}\ \overline{\gamma_{nm}^2}\ \overline{F_n^2}\right] \tag{149}$$

In this manner, the summation of the R individual receiver functions $\overline{\psi_{rm}^2}$ can be replaced by a single quantity, say $R \cdot \Phi_m$. Replacing the summation of mean-square responses in (149) by R times the space average value, $\overline{\overline{\ddot{W}_{rm}^2}}$, of the mean-square responses in the m-th compartment gives

$$\overline{\overline{\ddot{W}_{rm}^2}} = \Phi_m \sum_{n=1}^{\infty} \overline{\overline{\beta_n^2}}\ \overline{\gamma_{nm}^2}\ \overline{F_n^2} \tag{150}$$

In order to further simplify Equation (150) replace the transmission functio $\overline{\gamma_{nm}^2}$ in this equation by the exponential form of this function given in Equation (144)

$$\overline{\overline{\ddot{W}_{rm}^2}} = \Phi_m \sum_{n=1}^{N} \overline{\overline{\beta_n^2}}\ e^{-\Delta_{nm}\delta}\ \overline{F_n^2} \tag{151}$$

where

$\Delta_{nm} = x_n - x_m$ — average distance between compartments

$\delta = \delta(f_c, \Delta_f)$ — constant to be determined.

There is one such equation for each compartment ($m = 1,2,3,\ldots,N$) so that there are N such equations. There are N values of Φ_m, N values of $\overline{\overline{\beta_n^2}}$ and one value of δ; and hence there are $2N + 1$ unknowns to be determined from N equations. Thus, even when the acceptance and transmission functions are referred to compartments, and the transmission function is approximated by the one parameter exponential function, there is insufficient data to determine the unknown quantities.

It is possible to obtain at least first order approximations of the unknowns appearing in Equation (151), if measured excitation and vibration response data are available for $N + 1$ different flight (or ground run - up or ground firing) conditions. When the distribution of applied pressures over the vehicle surface changes, then the mean-square forces $\overline{F_i^2}$ vary, and so do the space average responses $\overline{\overline{W_{rm}^2}}$. Thus, if there are the $N + 1$ different flight conditions there are $N + 1$ different pressure distributions over the surface, then there are $N + 1$ equations of the form (151) for each value m, and hence there are $2N + 1$ equations in the unknowns Φ_m, $\overline{\overline{\beta_n^2}}$, δ. It is assumed of course that the averaged acceptance functions $\overline{\overline{\beta_n^2}}$ are unchanged for the different force distributions. This appears to be a reasonable approximation for a given type of excitation in which the pressure space correlations at the vehicle surface remain approximately fixed. Once numerical values of the quantities $\overline{\overline{\beta_n^2}}$ and δ are known, the averaged receiver functions $\overline{\overline{\psi_{rm}^2}}$ can be determined for each structural component by use of Equation (118).

A final simplification of Equation (116) is now considered. The product $(\overline{\overline{\beta_n^2}} \cdot \overline{\overline{f_n^2}})$ is an approximation of the average mean-square acceleration response of the n-th

compartment, and as such, this product should be inversely proportional to the square of the total mass M_n of that compartment. Thus the quantity $(M_n^2 \overline{\overline{\beta_n^2}})$ should be nearly independent of the total mass of the compartment. Furthermore, if the surface structures of all, or most, of the vehicle compartments are similar, the average joint-acceptance (or acoustic structural coupling between the applied pressured and the vehicle skin) should be approximately the same for each compartment. Since the acceptance function $\overline{\overline{\beta_n^2}}$ is clearly proportional to joint-acceptance, the quantity $M_n^2 \overline{\overline{\beta_n^2}}$ might have approximately the same value for all compartments. With this assumption, Equation (151) can be written in the form

$$\overline{\overline{\ddot{W}_{rm}^2}} \quad D \Phi_m \sum_{n=1}^{N} e^{-\Delta_{nm}\delta} \overline{F_n^2} / M_n^2 \qquad (152)$$

where D is a constant to be determined along with the quantities Φ_m and δ. There are now N + 2 unknowns, so that in addition to measured data in each of the N compartments, it is necessary to have measured data in two compartments for a second flight condition having a different distribution of fluctuating pressures. Once D and δ are known, the receiver functions ψ_r^2 can be found from the equation

$$\overline{\ddot{W}_{rm}^2} \quad \overline{\psi_{rm}^2} \; D \sum_{n=1}^{N} e^{-\Delta_{nm}\delta} \overline{F_n^2} / M_n^2 \qquad (153)$$

In conclusion, Equations (148) and (151) (153) can be used to determine empirically the acceptance, transmission and local vibratory characteristics of complex structures if there is sufficient measured data to describe the excitation and the response. The vehicle can be segmented into compartments as described above, and it is necessary

to determine the average mean square force acting on the exterior of each compartment and to have available a representative sampling of vibration response data within each compartment. It is necessary that such measured data be available for a number of different flight conditions in which the mean-square forces over the segmented areas of the vehicle have different distributions. When data of this type is not available, flight data cannot be used to develop empirical correlation prediction methods; and in this case it is necessary that impedance measurements (or any equivalent measurements) be used to evaluate the acceptance, transmission, and local dynamic characteristics of vehicle structures.

APPENDIX A

AUTOCORRELATION FUNCTION FOR WHITE NOISE

Let x(t) be a signal resulting from a stationary and ergodic random process which generates white noise. The autocorrelation function, $\Gamma(\tau)$, of x(t) is defined as

$$\Gamma(\tau) = \lim_{T \to \infty} \frac{1}{T} \int_0^T x(t) \cdot x(t+\tau) \cdot dt \qquad (A.1)$$

When x(t) represents white noise containing all frequencies, the autocorrelation function $\Gamma(\tau)$ is proportional to the Dirac Delta function, $\delta(\tau)$, which is defined as

$$\int_{-\epsilon}^{\epsilon} \delta(\tau) \cdot d\tau = 1.0 \qquad \delta(\tau) \begin{cases} \infty, & \tau = 0 \\ 0, & \tau \neq 0 \end{cases} \qquad (A.2)$$

$$\int_{0}^{\epsilon} \delta(\tau) \cdot d\tau = \int_{-\epsilon}^{0} \delta(\tau) \cdot d\tau = 1/2 \qquad \epsilon > 0$$

for any $\epsilon > 0$ no matter how small. This fact is not directly obvious from (A.1). In order to prove this point, and in order to determine the constant of proportionality, it is necessary to use the constant power spectral density definition of white noise and the Wiener - Khinchin relations.

Let $S(\omega)$ denote the power spectral density of the signal x(t). Since x(t) is characterized by the properties of white noise, the function $S(\omega) =$ constant. From page 67 of Reference (10), the Wiener-Khinchin relations are

$$S(\omega) = \frac{2}{\pi} \int_0^{\infty} \Gamma(\tau) \cdot \cos \omega\tau \cdot d\tau \qquad (A.3)$$

$$\Gamma(\tau) = \int_0^{\infty} S(\omega) \cdot \cos \omega\tau \cdot d\omega \qquad (A.4)$$

The symmetric, or cosine, forms of these relations are used because the functions $S(\omega)$ and $\Gamma(\tau)$ are symmetric, that is

$$\begin{array}{cc} \Gamma(-\tau) & \Gamma(\tau) \\ S(\omega) & S(\omega) \end{array}$$

The latter relations are given by Equation (1-61), page 20, and Equation (2-15), page 3 of Reference (10).

For constant power spectra, (A.4) can be written as

$$\Gamma(\tau) = S(\omega) \cdot \int_0^{\infty} \cos \omega\tau \cdot d\omega$$

$$= S(\omega) \cdot \left. \frac{\sin \omega\tau}{\tau} \right]_{\omega = 0}^{\infty} \qquad (A.5)$$

At the upper limit, the function in (A.5) is indeterminate since the $\sin \omega\tau$ can lie anywhere in the range $-1 \leq \sin \omega\tau \leq 1$. Neglecting this indeterminate upper limit, $\Gamma(\tau)$ is seen to equal zero except when $\tau = 0$. In the latter case, the auto-correlation $\Gamma(\tau)$ is infinite, hence $\Gamma(\tau)$ can be represented in terms of the Dirac Delta function

$$\Gamma(\tau) = k \cdot S(\omega) \cdot \delta(\tau) \qquad (A.6)$$

where k is a constant of proportionality. To determine the value of k and to show that (A.6) is the correct functional form, substitute (A.6) into (A.3) and integrate:

$$S(\omega) = \frac{2}{\pi} k S(\omega) \cdot \int_0^{\infty} \delta(\tau) \cdot \cos \omega \tau \cdot d\tau$$

or

$$k = \frac{\pi/2}{\int_0^{\infty} \delta(\tau) \cdot \cos \omega\tau \cdot d\tau} \qquad (A.7)$$

The integral in the denominator of (A.7) can be simplified as follows:

$$\int_0^{\infty} \delta(\tau) \cdot \cos \omega\tau \cdot d\tau = \int_0^{\epsilon} \delta(\tau) \cdot d\tau = \frac{1}{2}$$

by use of (A.2)above. Thus (A.7) becomes

$$k = \pi$$

and hence the autocorrelation function, $\Gamma(\tau)$, for white noise is:

$$\Gamma(\tau) = \pi \cdot S(\omega) \cdot \delta(\tau) \qquad (A.3)$$

Note that

$$S(\omega) \qquad \frac{1}{2\pi} \quad S(f) \qquad (A.9)$$

where $S(\omega)$ has the units of $(psf)^2$ /(rad/sec) and S(f) has the units of $(psf)^2$/cps. Substituting (A.9) into (A.8) gives an alternate form for the autocorrelation function, namely,

$$\Gamma(\tau) = \frac{1}{2} \cdot S(f) \cdot \delta(\tau) \qquad \text{(A.10)}$$

The form (A.10) agrees with Equation (2-126), page 69 of Reference (10).

APPENDIX B

AUTOCORRELATION FUNCTION FOR BANDWIDTH LIMITED WHITE NOISE

Given a random process which is characterized by bandwidth limited white noise. The power spectral density (PSD) for such a process is denoted by $S(\omega)$; and as shown in Figure 19 $S(\omega)$ is defined as

$$\begin{aligned} S(\omega) &= S, \ \omega_L < \omega < \omega_U \\ &= S, \ -\omega_U < \omega < -\omega_L \\ &= 0 \quad \text{otherwise} \\ S &= \text{constant} \geq 0 \end{aligned}$$

From the Wiener-Kinchin relations (page 67 of Reference 10) the autocorrelation function, $\Gamma(\tau)$, for the random process is

$$\Gamma(\tau) = \int_0^\infty S(\omega) \cdot \cos \omega\tau \cdot d\omega$$

$$= S \int_{\omega_L}^{\omega_U} \cos \omega\tau \cdot d\omega$$

$$= \frac{S}{\tau} \left[\sin \omega_U \tau - \sin \omega_L \tau \right] \qquad (B.1)$$

$$= \frac{2S}{\tau} \cdot \sin \frac{\omega_U - \omega_L}{2} \tau \cdot \cos \frac{\omega_U + \omega_L}{2} \tau$$

or

$$\Gamma(\tau) = S \cdot (\omega_U - \omega_L) \cdot \left[\frac{\sin \frac{\omega_L - \omega_U}{2}\tau}{\frac{\omega_U - \omega_L}{2}\tau}\right] \cos \frac{\omega_U + \omega_L}{2}\tau \qquad (B.2)$$

A graph of $\Gamma(\tau)/S \cdot (\omega_U - \omega_L)$ is shown in Figure 20. The values of τ_1 and τ_2 shown in this graph are

$$\tau_1 = \frac{\pi}{\omega_U + \omega_L} \qquad \text{and} \qquad \tau_2 = \frac{2\pi}{\omega_U - \omega_L} .$$

The following properties of $\Gamma(\tau)$ are to be noted:

1. $\lim_{\tau \to \infty} \Gamma(\tau) = 0 \qquad \omega_L \neq \omega_U$

2. $\Gamma(0) = S \cdot (\omega_L - \omega_U)$

   = mean square value

3. $\Gamma(\tau) \approx \left[S \cdot (\omega_U - \omega_L)\right] \cdot \cos \omega\tau; \quad \omega_U \approx \omega_L = \omega$

   This is the form of the correlation function for a sinusoidal signal; and $[S \cdot (\omega_U - \omega_L)]$ is the mean square value of the amplitude of the signal.

4. From the above equation for τ_2:

   $\tau_2 \to \infty$ as $\omega_U \to \omega_L$ (narrow band)

   $\tau_2 \to 0$ as $(\omega_U - \omega_L) \to \infty$ (broad band)

Also for τ_1:

$$\tau_1 \longrightarrow 0 \quad \text{as} \quad (\omega_U - \omega_L) \rightarrow \infty \quad \text{(broad band)}$$

5. Using Equation (B.1) above, it is seen that when $\omega_L = 0$, the autocorrelation function $\Gamma(\tau)$ becomes

$$\Gamma(\tau) = S \cdot \omega_U \cdot \frac{\sin \omega_U \tau}{\omega_U \tau}$$

Figure 16 shows two graphs of $\Gamma(\tau) / S \cdot \omega_U$, one for a small value of ω_U and the other for a large value of ω_U. Negative values of τ are shown in order to emphasize the symmetry of $\Gamma(\tau)$. It is seen that as ω_U becomes large (large bandwidth), the correlation function decays rapidly with time delay τ.

For the case of theoretical white noise, in which $\omega_L = 0$ and $\omega_U \rightarrow \infty$, the autocorrelation function approaches the Dirac delta function, $\delta(\tau)$. This function is defined as follows: (Reference 11)

$$\delta(\tau) = \lim_{a \rightarrow \infty} \frac{a}{\pi} \cdot \frac{\sin a\tau}{a\tau}$$

Thus in the limit, $\Gamma(\tau)$ becomes

$$\boxed{\Gamma(\tau) = \pi S_\omega \cdot \delta(\tau) \qquad \omega_L = 0 \ , \ \omega_U \rightarrow \infty}$$

S_ω denotes S in units of $(\ )^2$ / rad / sec.

Note that

$$S(f) = 2\pi\, S(\omega)$$

or

$$S_f = 2\pi\, S_\omega$$

S_f denotes S in units of $(\ )^2$ / cps

Thus an alternate form for $\Gamma(\tau)$ is

$$\boxed{\Gamma(\tau) = \frac{1}{2} \cdot S_f \cdot \delta(\tau) \qquad \omega_L = 0,\ \omega_U \to \infty}$$

Note: An alternate expression for the Dirac delta function can be obtained directly from the above integral expression for $\Gamma(\tau)$:

$$\Gamma(\tau) = S_\omega \cdot \int_0^\infty \cos\ \omega\tau \cdot d\omega$$

$$= \pi \cdot S_\omega \cdot \delta(\tau)$$

$$\delta(\tau) = \frac{1}{\pi} \int_0^\infty \cos \omega\tau \cdot d\omega$$

or

$$\delta(\tau) = 2\int_0^\infty \cos 2\pi f\tau \cdot df$$

or

$$\delta(\tau) = \int_{-\infty}^{\infty} \cos 2\pi f\tau \cdot df.$$

Important properties of $\delta(\tau)$ are

$$\delta(\tau) = \infty \quad \text{at} \quad \tau = 0$$
$$= 0 \quad \text{if} \quad \tau \neq 0$$

$$\int_{-\infty}^{\infty} \delta(\tau) \cdot d\tau = \int_{-\epsilon}^{\epsilon} \delta(\tau) \cdot d\tau = 2 \int_{0}^{\epsilon} \delta(\tau) \cdot d\tau =$$

$$= 2 \int_{-\epsilon}^{0} \delta(\tau) \cdot d\tau = 1$$

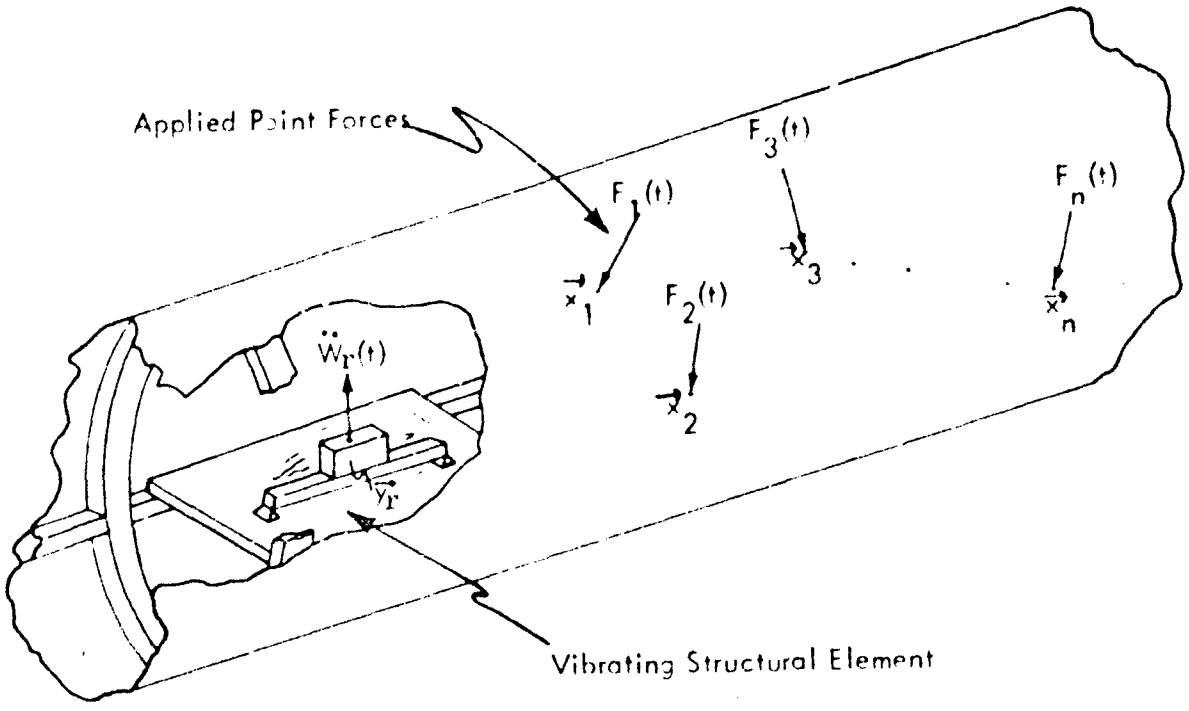

Figure 1: Arbitrary Structure with Forces, $F_n(t)$, Applied at Points $\vec{x}_n$, Showing Acceleration Response, $\ddot{W}_r(t)$, of an Element at Point $\vec{y}_r$.

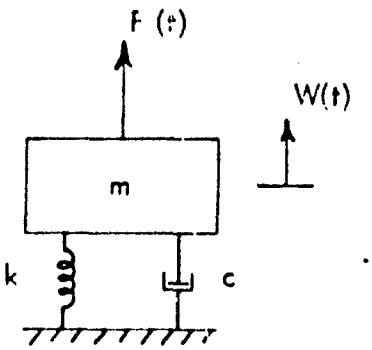

Figure 2: One-Degree-of-Freedom Spring-Mass System, with Spring Stiffness k, Damping Constant c, Mass m, Applied Force F(t) and Deflection W(t).

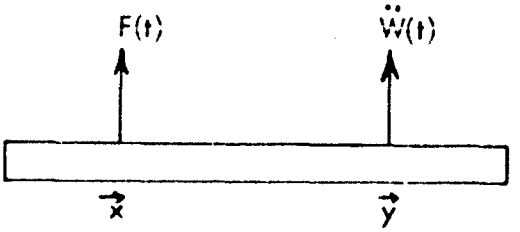

Figure 3: Uniform Beam with Point Force F(t) Applied at Point $\vec{x}$ and Acceleration Response $\ddot{W}(t)$ at $\vec{y}$.

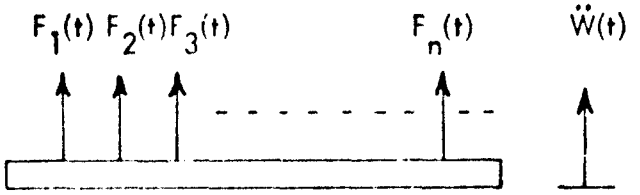

Figure 4: Rigid Bar Free to Translate, but Constrained in Pitch, and Having a Large Number of Applied Forces $F_n(t)$.

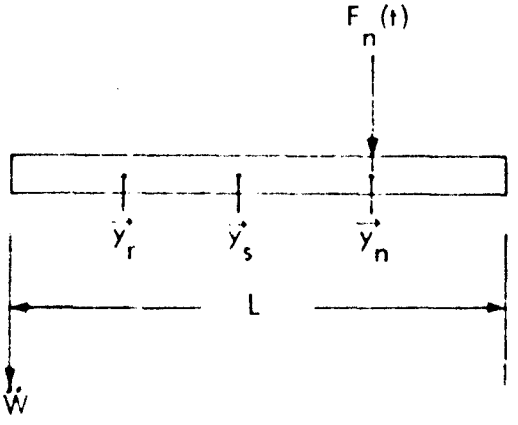

Figure 5: Uniform Beam Schematic for Response at $\vec{y}_r$ and $\vec{y}_s$ on A Excited By a Point Force $F_n(t)$ at $\vec{y}_n$.

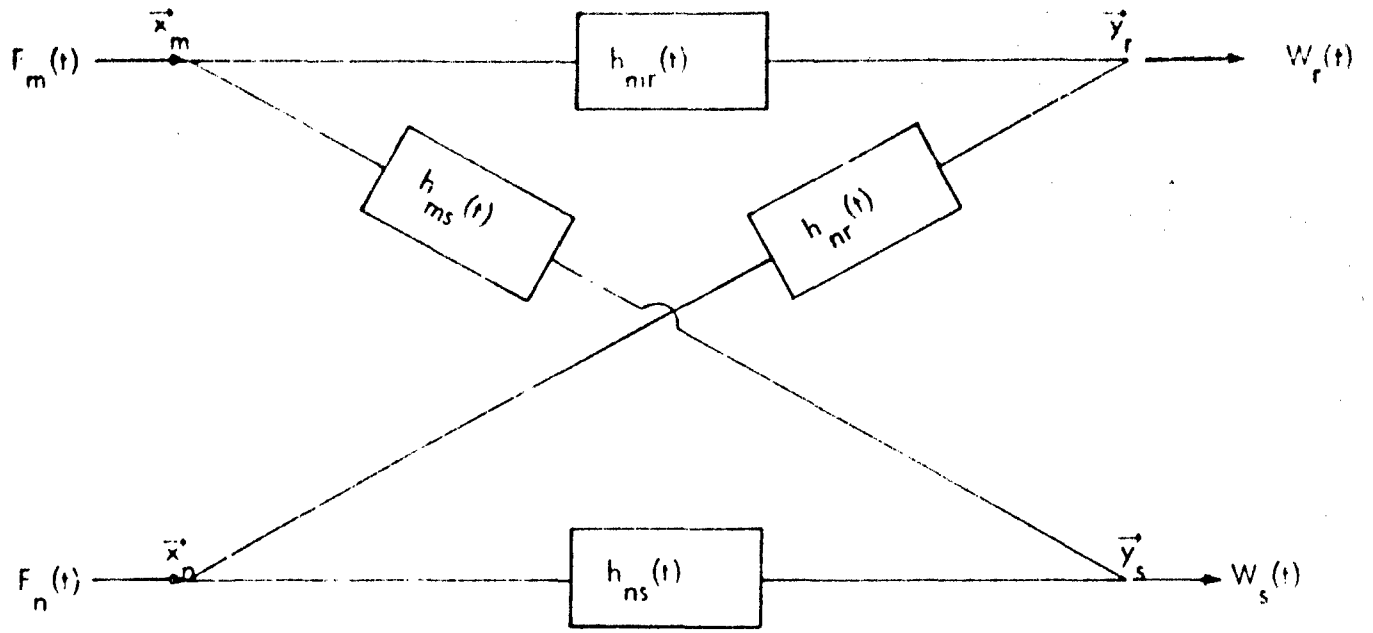

Figure 6: Two Points, $\vec{y}_r$ and $\vec{y}_s$, on a Structure Excited by Two Forces $F_m(t)$ and $F_n(t)$ at $\vec{x}_m$ and $\vec{x}_n$, Where $h_{mr}(t)$, $h_{ms}(t)$, $h_{nr}(t)$ and $h_{ns}(t)$ Represent Dynamic Transfer Characteristics of all Paths Between $\vec{y}_r$, $\vec{y}_s$ and $\vec{x}_m$, $\vec{x}_n$.

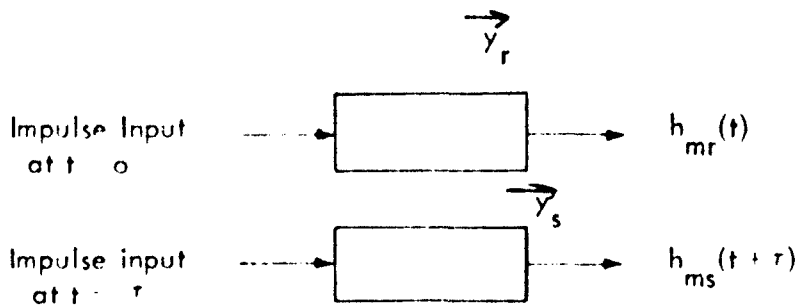

Figure 7. Two Single-degree- of Freedom Systems with Impulse Excitations

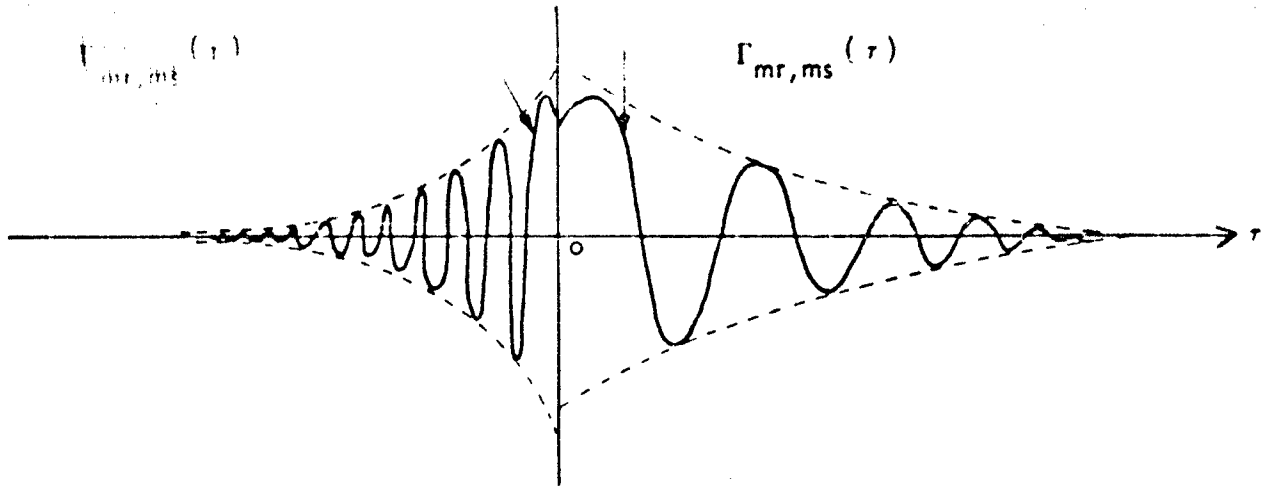

Figure 8: Graph of the Complete Crosscorrelation Function, Showing the Slope Discontinuity at $\tau = 0$, and Showing the Possible Different Forms of the Crosscorrelation for Positive and Negative Delay Times τ.

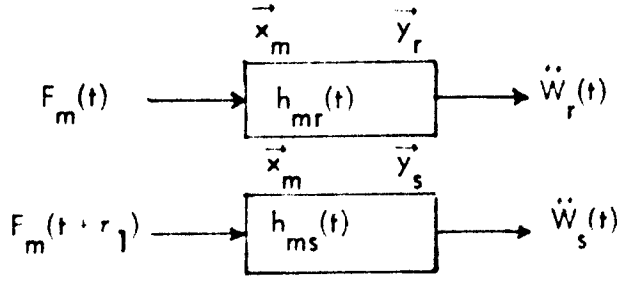

Figure 9: Inputs and Outputs For the Two Single Degree of Freedom Systems Subject to Bandwidth Limited White Noise.

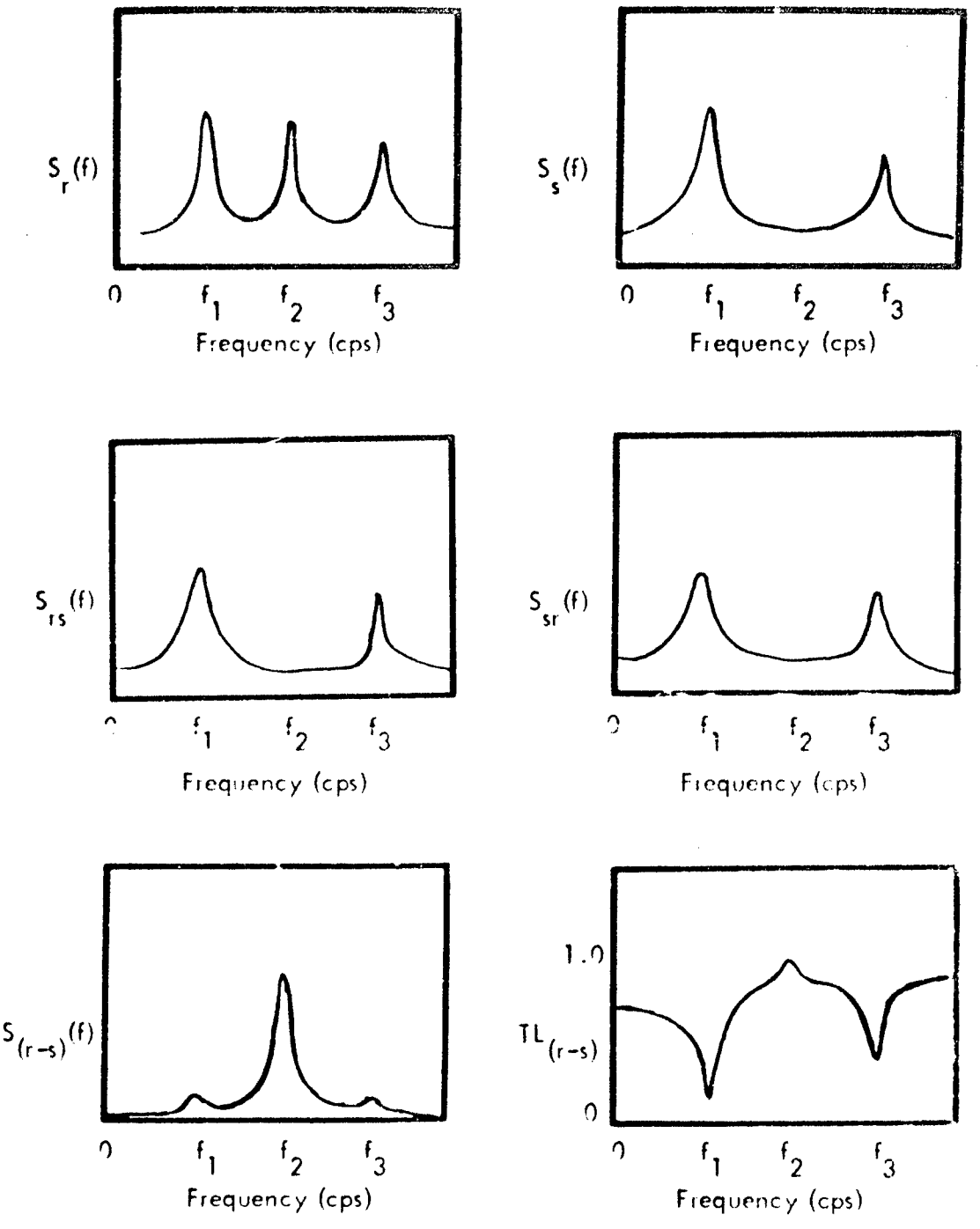

Figure 10: Illustrative Example of the Spectral Density $S_{(r-s)}(f)$ and Transmission Loss Coefficient $TL_{(r-s)}$ of the Difference Between Two Responses $\ddot{W}_r(t) - \ddot{W}_s(t)$.

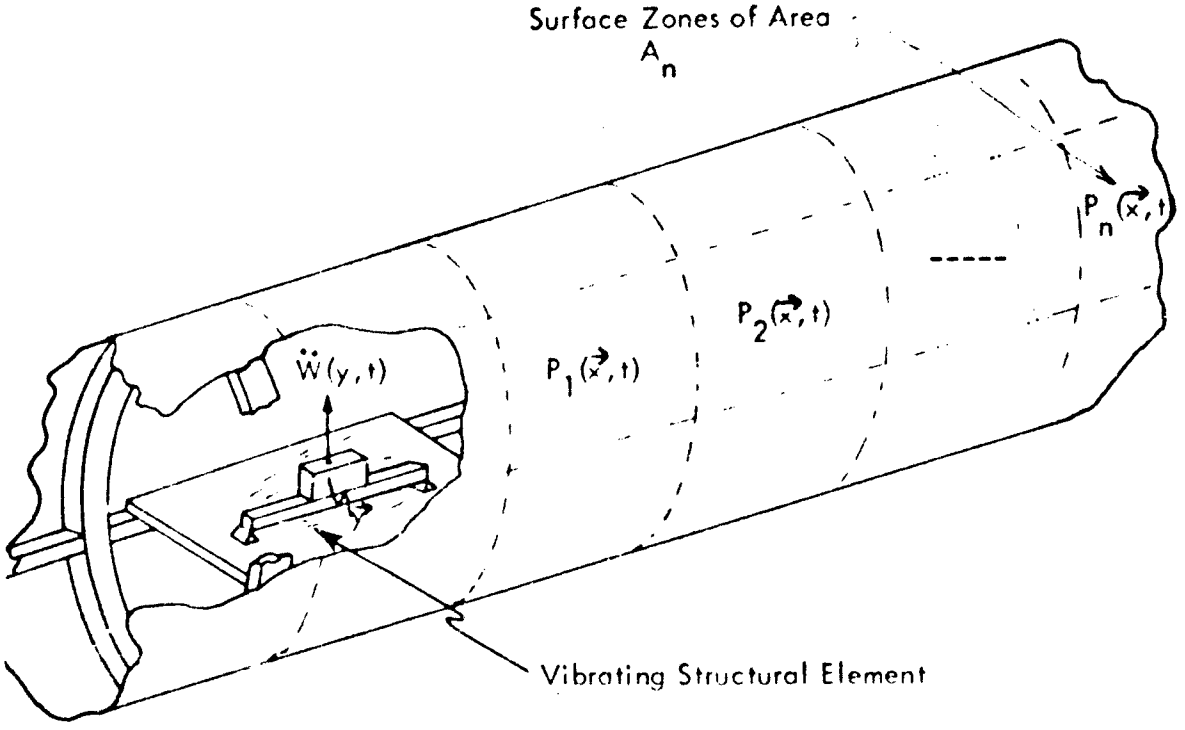

Figure 11 : Arbitrary Structure with Pressure, $P_n(\vec{x}, t)$, Applied over Surface Zones of Area, A_n, Showing Acceleration Response, $\ddot{W}(\vec{y}, t)$ of an Element at Point $\vec{y}$.

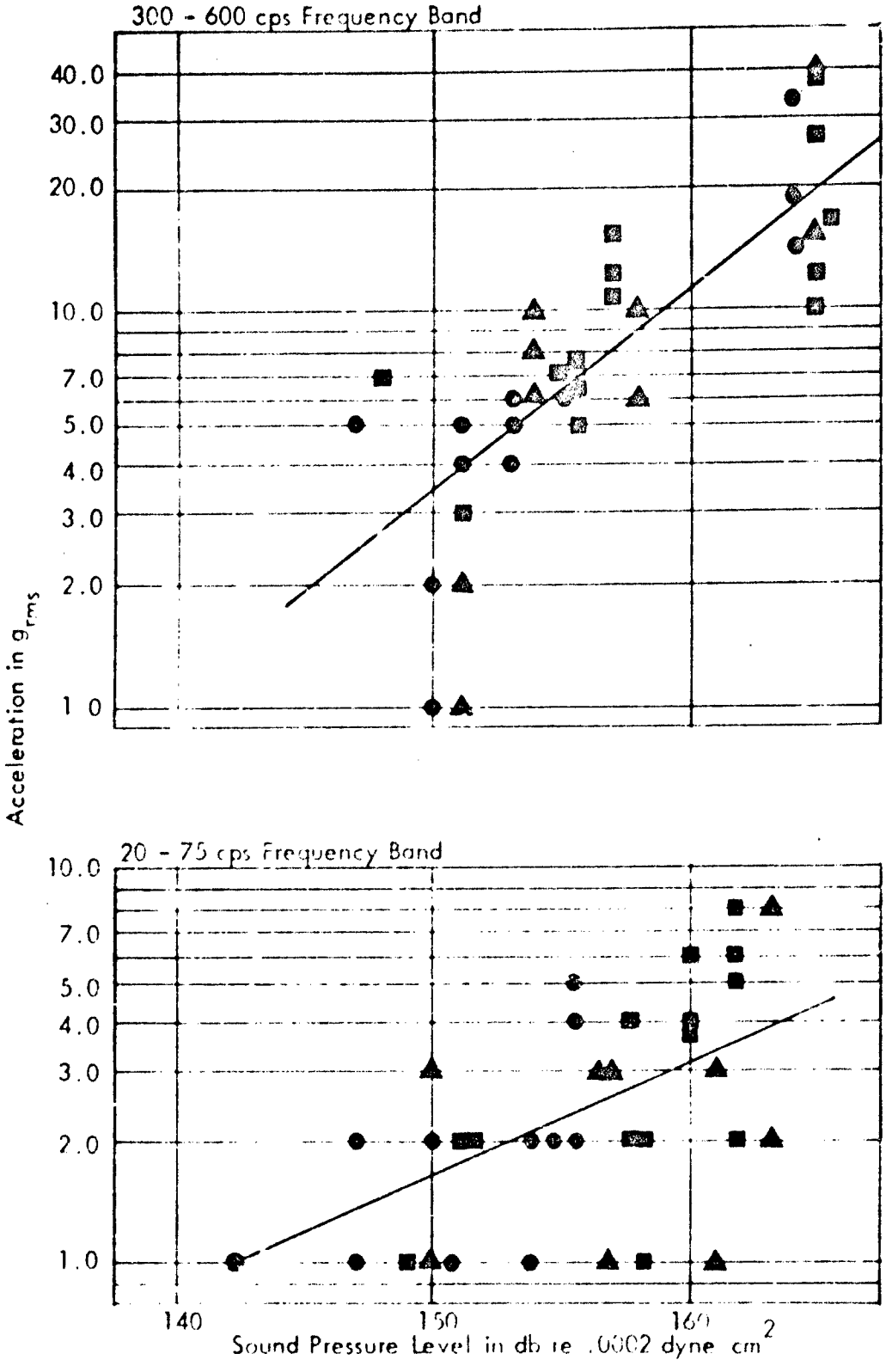

Figure 12. Comparison of Internal Vibration of Structure and Adjacent External Sound Pressure Level for Two Frequency Ranges.

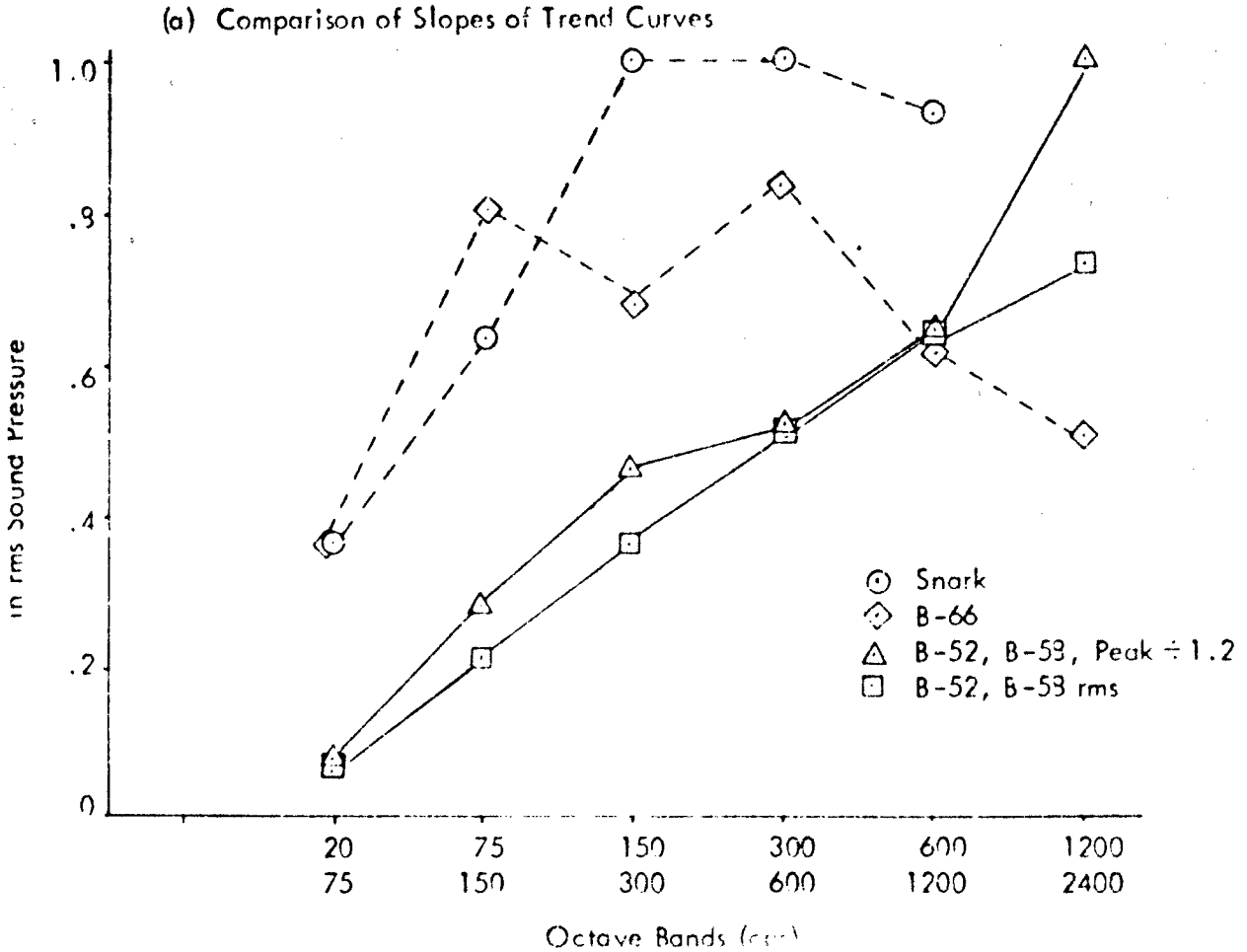

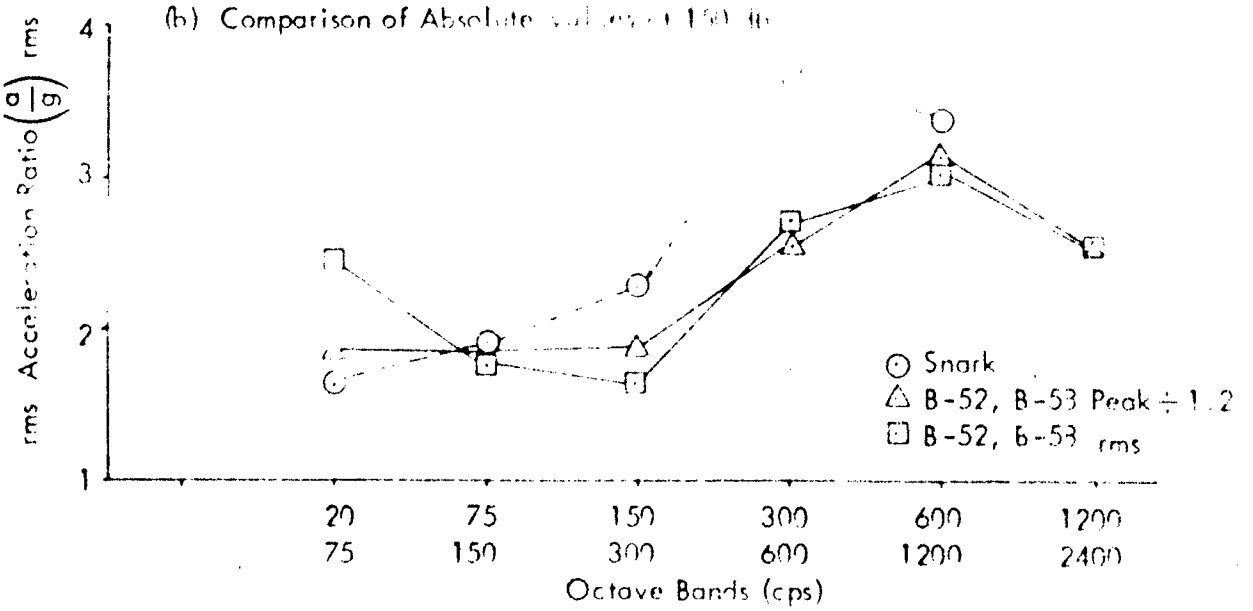

Figure 13: Summary of Aircraft Empirical Correlation of External Noise With Acceleration of Adjacent Structure.

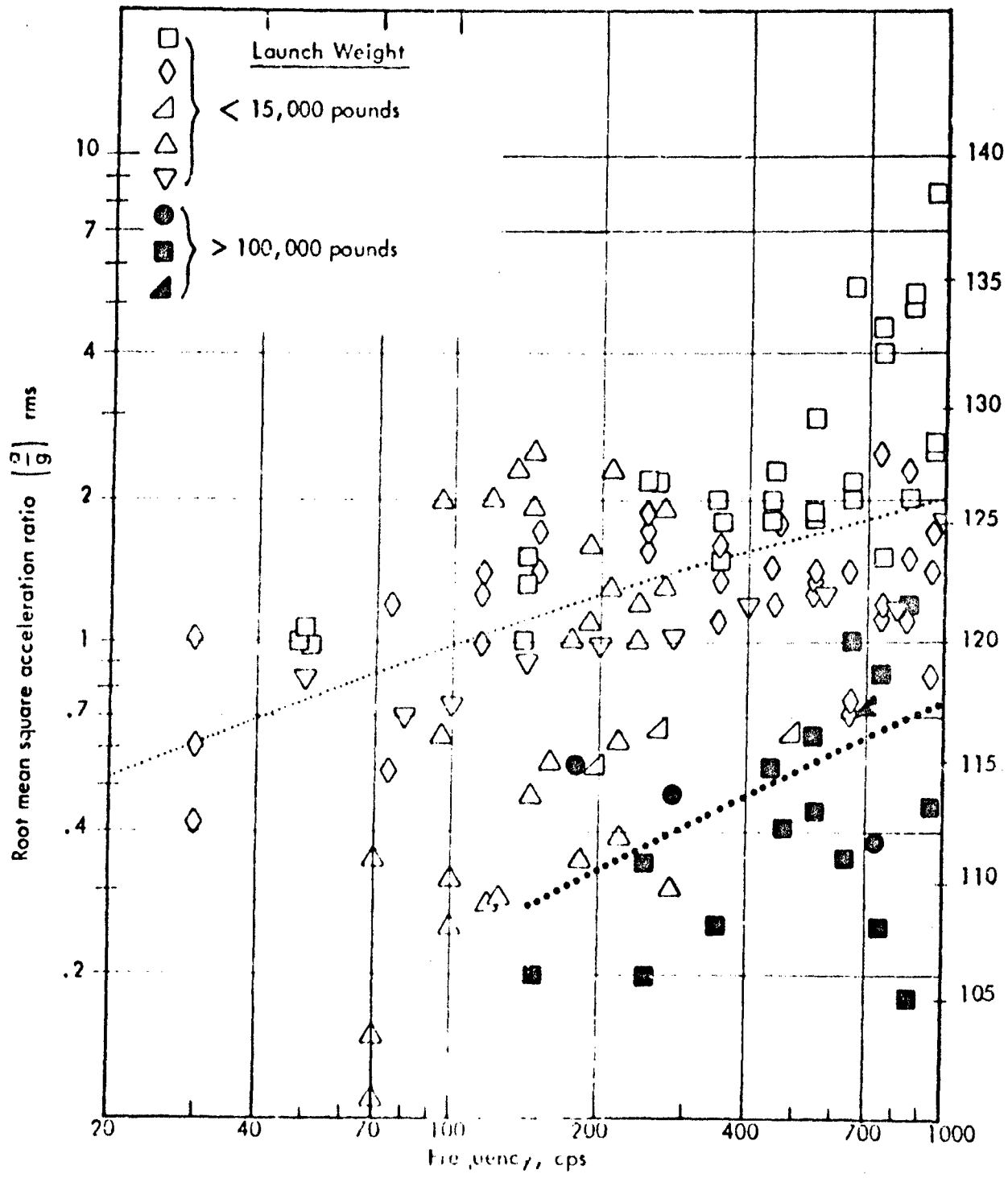

Figure 14 Missile Launch Accelerations Obtained on Structure in Forward Half of Vehicle.

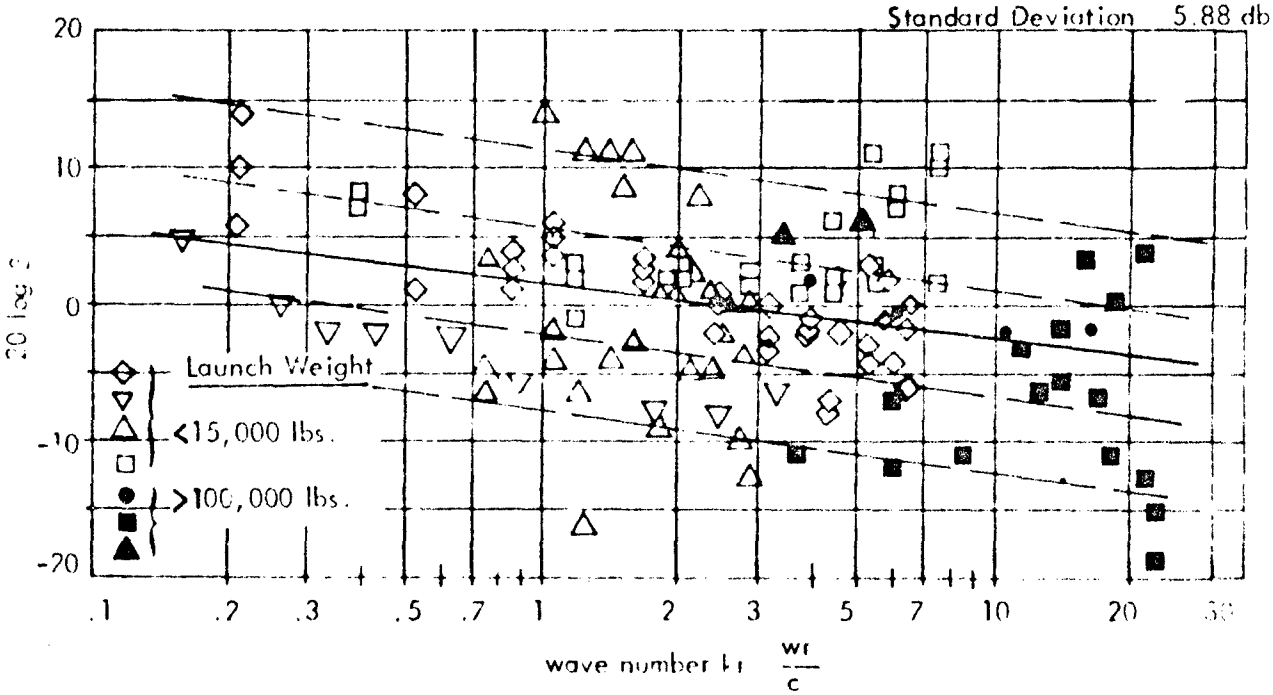

Figure 15 Variation of the Parameter β with kr for the Data of Figure 14 Where

$$\beta^2 \quad \left[\frac{4\left(\frac{a}{g}\right)^2 \quad W^2}{\omega_n \, Q \, F(f)^2}\right]$$

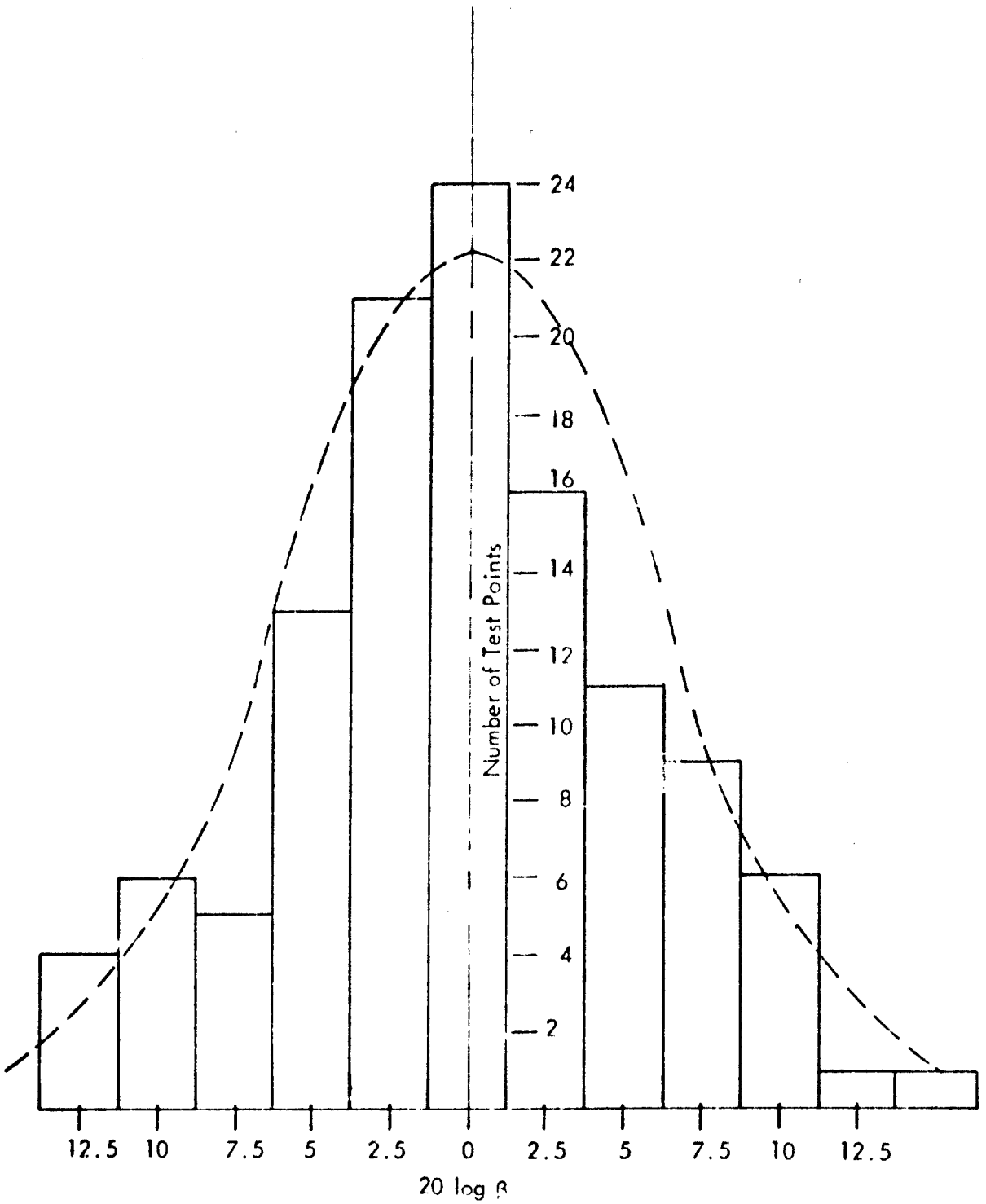

Figure 16. Histogram of β From Figure 15

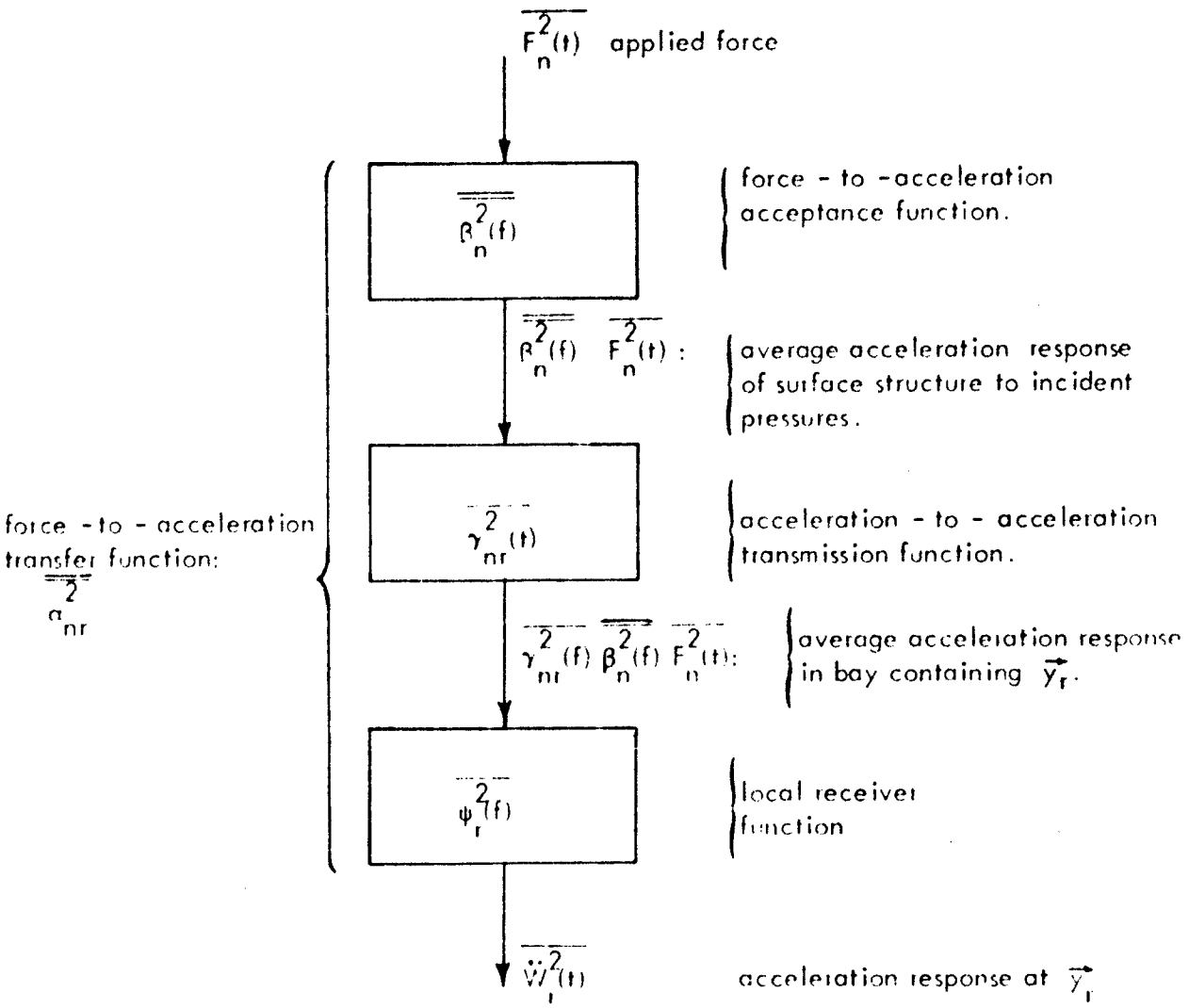

Figure 17: Diagram of Series Form of Force - to - Acceleration Transfer Function $\overline{\overline{a_{nr}^2}}$ in Terms of Acceptance, Transmission and Receiver Functions.

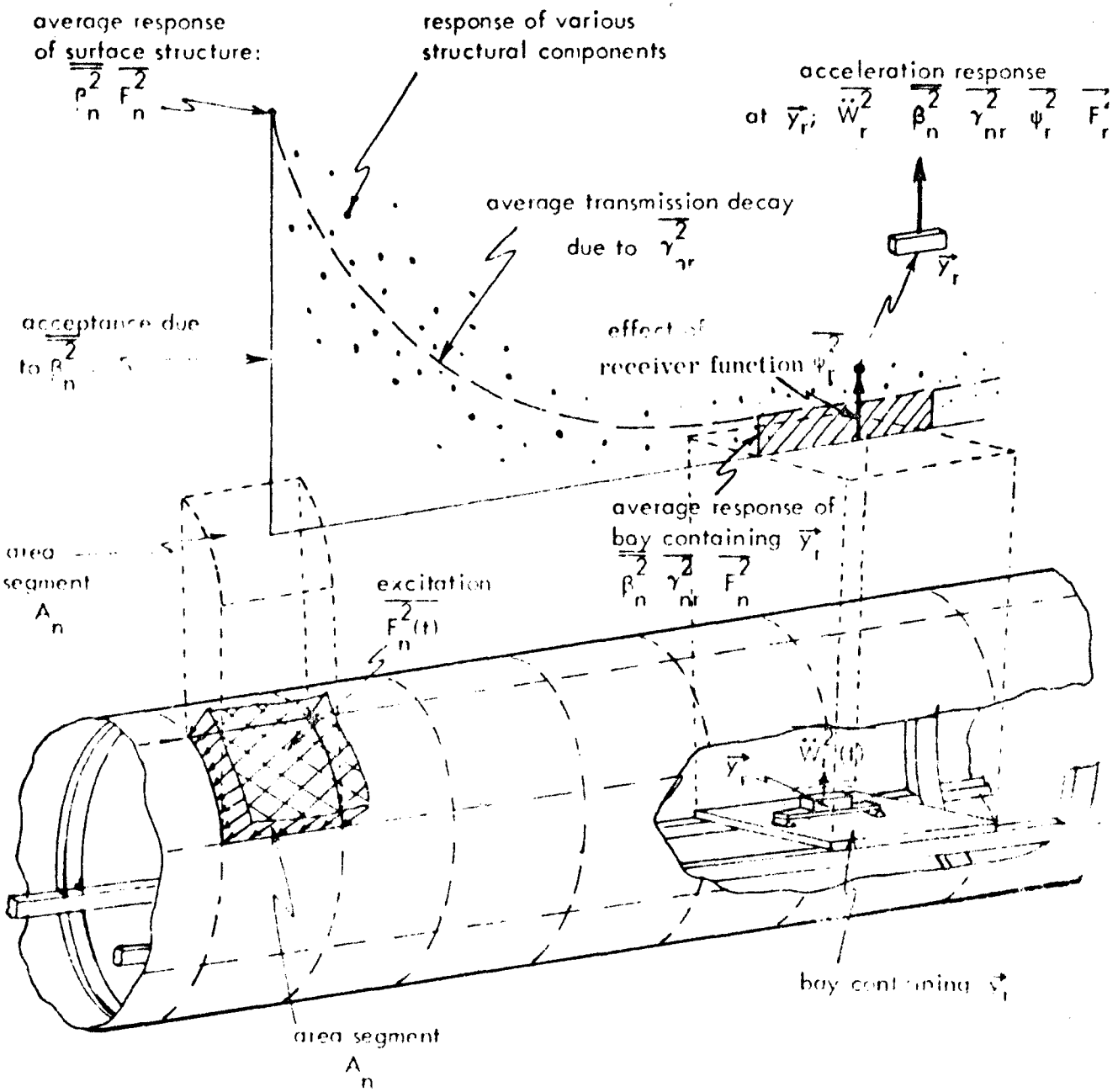

Figure 18. Diagram of Typical Vehicle Structure Showing Limited Excitation over Area Segment A_n, Average Response of Directly Excited Structure, Decay of Vibratory Energy Along Vehicle Axis, and Response of Typical Structural Component at y_r.

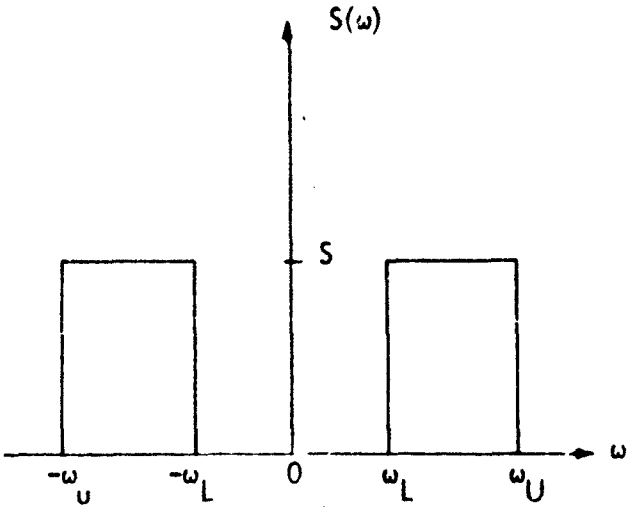

Figure 19: Plot of Bandwidth Limited White Noise PSD

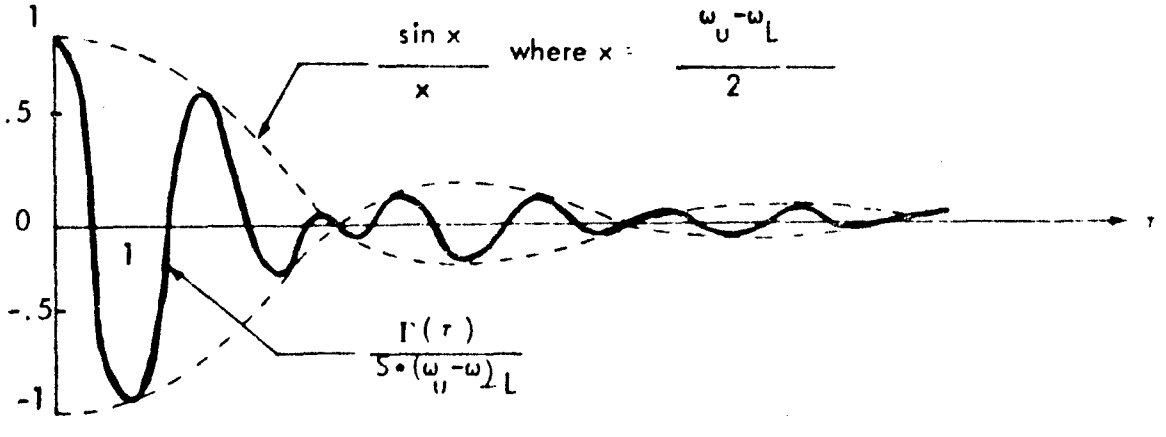

Figure 20: Graph of the Autocorrelation Function for Bandwidth Limited White Noise

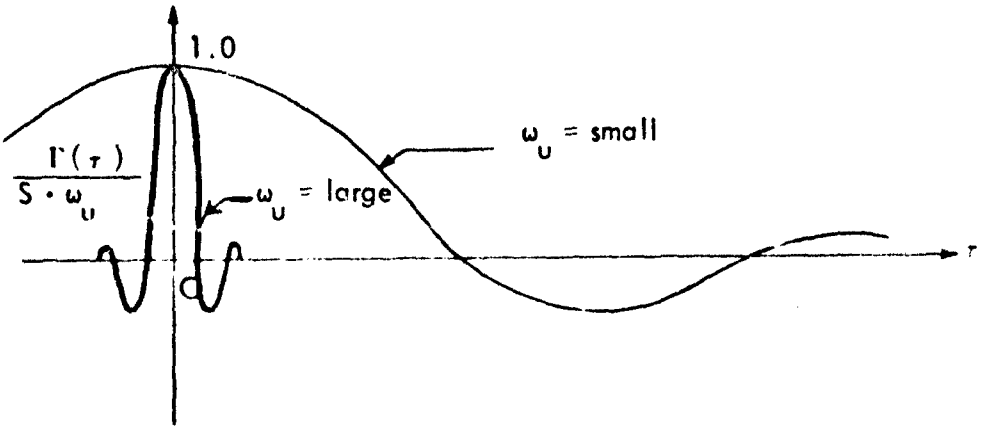

Figure 21: Graph of the Autocorrelation Function for Bandwidth Limited White Noise ($\omega_L = 0$).

REFERENCES

1. Crandall, S.H., Editor, Random Vibration, John Wiley and Sons, Inc., New York, N.Y., 1958.

2. Bozich, D.J., "Spatial Correlation in Acoustic-Structural Coupling," Journal of the Acoustical Society of America, Vol. 36, No. 1, pp. 52-58, January 1964.

3. Eldred, K.M., Roberts, Wm., and White, R.W., "Structural Vibrations in Space Vehicles," WADD-TR-61-62, Aeronautical Systems Div., Wright Patterson Air Force Base, Ohio, December 1961.

4. Smith, K.S., and Ballentine, J.R., "A Method for Predicting B/RB-58 Vibration Environment," Convair Report FZS-4-149, General Dynamics, Fort Worth, Texas, October 1957.

5. "B-58 Environmental Vibration Qualification Tests," Convair Report FZM-4-803, General Dynamics, Fort Worth, Texas, February 1958.

6. Smith, K.S., and Ballentine, J.R., "B-58 Predicted Vibration Environment and Vibration Range Curves for Environmental Test," Convair Report FZS-4-160, General Dynamics, Fort Worth, Texas, February 1958.

7. Egbert, D.T., and Harter, W.W., "Vibration and Acoustic Environment Measurements as Applied to Snark Missile Equipment," Shock and Vibration Bulletin, No. 24, U.S. Office of the Secy. of Defense (Research and Development), February 1957.

8. Mustain, R., and Vernier, B., "Snark Acoustic and Vibration Data Analysis," Northrop Report NAI-56-686, Vols. I and II, 1956, N69D Missile N3305, Nov. 1956; NAI-57-583, Nov. 1957; NAI-57-582, "Internal Acoustical Treatment," Jan. 1958; NAI-57-584, "Salted Grain Booster Bottles," July 1958; NAI-59-25, "Summary of Acoustic and Pressure Data Booster Blast Off Program," Dec. 1958; Northrop Corp., Hawthorne, Calif.

9. Kennard (Jr), D.C., "Some Vibration as Exemplified by the RB-66B Airplane," WADC-TR-59-158, Wright Air Development Center, Wright Patterson Air Force Base, Ohio, May 1959.

10. Bendat, J.S., Principles and Applications of Random Noise Theory, John Wiley and Sons, Inc., New York, N.Y., 1958.

11. Korn and Korn, Mathematical Handbook for Scientists and Engineers, McGraw-Hill Book Co., Inc., New York, N.Y., 1961.

12. White, R.W., Eldred, K.M., Roberts, W.H., "Investigation of a Method for the Prediction of Vibratory Response and Stress in Typical Flight Vehicle Structure," ASD-TDR-62-801, Aeronautical Systems Div., Wright-Patterson Air Force Base, Ohio, August 1963.

Security Classification

DOCUMENT CONTROL DATA - R&D

(Security classification of title, body of abstract and indexing annotation must be entered when the overall report is classified)

1 ORIGINATING ACTIVITY (Corporate author) Norair Division, Northrop Corporation	2a REPORT SECURITY CLASSIFICATION UNCLASSIFIED 2b GROUP

3 REPORT TITLE
Empirical Correlation of Excitation Environment and Structural Parameters with Flight Vehicle Vibration Response

4 DESCRIPTIVE NOTES (Type of report and inclusive dates)

5 AUTHOR(S) (Last name, first name, initial)
White, R. W., Bozich, D. J., Eldred, K. M.

6 REPORT DATE	7a TOTAL NO OF PAGES	7b NO OF REFS
December 1964	128	12

8a CONTRACT OR GRANT NO	9a ORIGINATOR'S REPORT NUMBER(S)
AF33(657)-8218 b PROJECT NO 1370 c Task No. 137005 d	AFFDL-TR-64-160 9b OTHER REPORT NO(S) (Any other numbers that may be assigned this report) NOR 64-226

10 AVAILABILITY/LIMITATION NOTICES

11 SUPPLEMENTARY NOTES	12 SPONSORING MILITARY ACTIVITY
	Air Force Flight Dynamics Laboratory

13 ABSTRACT

The design of fatigue resistant structures for high speed aircraft and aerospace vehicles depends largely on the prediction of realistic acoustic, fluctuating aerodynamic, and engine vibration environments and on the estimation of the attendant vibration levels of structural components and attached equipment. The practical engineering limitations on the mathematical and numerical analyses required to treat such structures rigorously by classical dynamics necessitate studies of alternate, approximate methods. In this report, a definitive statement is presented of the empirical approach for determining correlations between the excitation environment and the vibration response of typical flight vehicle structures by means of statistical analyses of measured vibration data. The various aspects of the vibration prediction problem and the general philosophy motivating research in the area of empirical correlation are discussed. Specific treatment is given to the effects of bandwidth, modal density, and surface pressure spacecorrelation on the crosscorrelation of energy transmitted along various structural transmission paths in complex linear structures. An engineering model for empirical correlation is developed and several examples are given to demonstrate the utility of the equations.

DD FORM 1 JAN 64 1473

UNCLASSIFIED

Security Classification

KEY WORDS	LINK A		LINK B		LINK C	
	ROLE	WT	ROLE	WT	ROLE	WT

INSTRUCTIONS

GINATING ACTIVITY: Enter the name and address ntractor, subcontractor, grantee, Department of De- tivity or other organization *(corporate author)* issuing rt.

PORT SECURITY CLASSIFICATION: Enter the over- rity classification of the report. Indicate whether ted Data" is included. Marking is to be in accord- h appropriate security regulations.

DUP: Automatic downgrading is specified in DoD Di- 200.10 and Armed Forces Industrial Manual. Enter p number. Also, when applicable, show that optional s have been used for Group 3 and Group 4 as author-

ORT TITLE: Enter the complete report title in all etters. Titles in all cases should be unclassified. ningful title cannot be selected without classifica- w title classification in all capitals in parenthesis iately following the title.

CRIPTIVE NOTES: If appropriate, enter the type of g., interim, progress, summary, annual, or final. inclusive dates when a specific reporting period is

HOR(S): Enter the name(s) of author(s) as shown on report. Enter last name, first name, middle initial. ry, show rank and branch of service. The name of cipal author is an absolute minimum requirement.

ORT DATE: Enter the date of the report as day, ear, or month, year. If more than one date appears eport, use date of publication.

TAL NUMBER OF PAGES: The total page count ollow normal pagination procedures, i.e., enter the f pages containing information.

MBER OF REFERENCES: Enter the total number of es cited in the report.

NTRACT OR GRANT NUMBER: If appropriate, enter icable number of the contract or grant under which rt was written.

8d. PROJECT NUMBER: Enter the appropriate department identification, such as project number, ct number, system numbers, task number, etc.

GINATOR'S REPORT NUMBER(S): Enter the offi- rt number by which the document will be identified rolled by the originating activity. This number must e to this report.

ER REPORT NUMBER(S): If the report has been l any other report numbers *(either by the originator sponsor)*, also enter this number(s).

ILABILITY/LIMITATION NOTICES: Enter any lim- on further dissemination of the report, other than those imposed by security classification, using standard statements such as:

(1) "Qualified requesters may obtain copies of this report from DDC."

(2) "Foreign announcement and dissemination of this report by DDC is not authorized."

(3) "U. S. Government agencies may obtain copies of this report directly from DDC. Other qualified DDC users shall request through

_____."

(4) "U. S. military agencies may obtain copies of this report directly from DDC. Other qualified users shall request through

_____."

(5) "All distribution of this report is controlled. Qualified DDC users shall request through

_____."

If the report has been furnished to the Office of Technical Services, Department of Commerce, for sale to the public, indicate this fact and enter the price, if known.

11. SUPPLEMENTARY NOTES: Use for additional explanatory notes.

12. SPONSORING MILITARY ACTIVITY: Enter the name of the departmental project office or laboratory sponsoring *(paying for)* the research and development. Include address.

13 ABSTRACT: Enter an abstract giving a brief and factual summary of the document indicative of the report, even though it may also appear elsewhere in the body of the technical report. If additional space is required, a continuation sheet shall be attached.

It is highly desirable that the abstract of classified reports be unclassified. Each paragraph of the abstract shall end with an indication of the military security classification of the information in the paragraph, represented as *(TS), (S), (C), or (U)*

There is no limitation on the length of the abstract. However, the suggested length is from 150 to 225 words.

14 KEY WORDS: Key words are technically meaningful terms or short phrases that characterize a report and may be used as index entries for cataloging the report. Key words must be selected so that no security classification is required. Identifiers, such as equipment model designation, trade name, military project code name, geographic location, may be used as key words but will be followed by an indication of technical context. The assignment of links, rules, and weights is optional.